AD NUMBER: ADB951585
LIMITATION CHANGES
TO: Approved for public release; distribution is unlimited.
FROM: Distribution authorized to US Government Agencies and Contractors; Administrative/Operational Use; 1 Mar 1953. Other requests shall be referred to Defense Nuclear Agency, Washington, DC 20301.
AUTHORITY
DNA ltr dtd 5 Mar 1980

AD B951585

UNCLASSIFIED

UNCLASSIFIED

WT-543

Copy No. A

Operation

TUMBLER-SNAPPER

NEVADA PROVING GROUNDS

April–June, 1952

Project [illegible].3

THERMAL RADIATION FROM A NUCLEAR DETONATION

Classification [illegible]
by Authority of [illegible]
by [illegible]

UNCLASSIFIED

RESTRICTED DATA

This document contains restricted data as defined in the Atomic Energy Act of 1946. Its transmittal or the disclosure of its contents in any manner to an unauthorized person is prohibited.

ARMED FORCES SPECIAL WEAPONS PROJECT
WASHINGTON, D.C.

SECRET
SECURITY INFORMATION

UNCLASSIFIED

PHOTOGRAPH THIS SHEET

AD B951585

DTIC ACCESSION NUMBER

LEVEL

UNANNOUNCED

INVENTORY

AEC

WT-543

DOCUMENT IDENTIFICATION

March 1953

None

DISTRIBUTION STATEMENT

ACCESSION FOR	
NTIS GRA&I	☐
DTIC TAB	☐
UNANNOUNCED	☒
JUSTIFICATION Release Ltr. on file	
BY	
DISTRIBUTION / AVAILABILITY CODES	
DIST: 2	AVAIL AND/OR SPECIAL

DISTRIBUTION STAMP

DTIC ELECTE S D MAR 27 1980 D

DATE ACCESSIONED

80 3 21 130

DATE RECEIVED IN DTIC

PHOTOGRAPH THIS SHEET AND RETURN TO DTIC-DDA-2

DTIC FORM OCT 79 70A

DOCUMENT PROCESSING SHEET

UNCLASSIFIED

[redacted]

THE - 43

CANCELED

This document contains information affecting the national defense of the United States within the meaning of the Espionage Laws, Title 18, U. S. C., Sections 793 and 794. The transmission or the revelation of its contents in any manner to an unauthorized person is prohibited by law.

Statement A
Approved for public release;
Distribution unlimited.

[redacted]

UNCLASSIFIED

TOW-2 23

UNCLASSIFIED

[redacted]

This document consists of 109 pages

No. 231 of 340 copies, Series A

OPERATION TUMBLER-SNAPPER

Project 8.3

THERMAL RADIATION FROM A NUCLEAR DETONATION

REPORT TO THE TEST DIRECTOR

by

A. Broido
C. P. Butler
R. P. Day
R. W. Hillendahl
S. B. Martin
A. B. Willoughby

March 1953

U. S. Naval Radiological Defense Laboratory
San Francisco 24, California

[redacted]

UNCLASSIFIED

Reproduced Direct from Manuscript Copy by
AEC Technical Information Service
Oak Ridge, Tennessee

Inquiries relative to this report may be made to

Chief, Armed Forces Special Weapons Project
P. O. Box 2610
Washington, D. C.

If this report is no longer needed, return to

AEC Technical Information Service
P. O. Box 401
Oak Ridge, Tennessee

UN[redacted]SIFIED

ABSTRACT

Measurements of thermal radiation from four nuclear detonations at Operation TUMBLER-SNAPPER are described. Data were obtained from stations along the thermal line from ground zero to 9000 ft, along the U. S. Forest Service (USFS) line from 11,000 to 20,000 ft, from certain stations where aircraft were parked, and from the drop aircraft. The instruments used were similar to those used in previous field operations, with the exception of a few new instruments for measuring directly the rate of delivery of the thermal energy. Instruments included disk calorimeters, passive receivers, photronic cells, radiometers, and sphere calorimeters.

In addition to measurements of the total thermal energy received as a function of distance, elevation, and field of view of the measuring device, measurements were made of the thermal pulse shape, the spectral distribution, and the energy reflected from the ground. The results show the relationship between weapon yield and such factors as total thermal energy at any distance, maximum intensity and duration of the thermal pulse, thermal efficiency of the weapons (ratio of thermal yield to total yield as determined by radiochemical analysis), and the amount of local obscuration caused by the thermal radiation and blast wave.

Although uncertainties are such that the range of weapon yields (1-30 KT) is not sufficiently great to allow accurate assessment of scaling laws, linear scaling of thermal efficiency and third power time scaling of the pulse do not seem to apply. The data reported here indicate a decrease in thermal efficiency with increasing weapon yield, ranging from about 44 per cent at 1 KT to about 34 per cent at 30 KT. The time to the second maximum of the thermal pulse ranges from approximately 100 msec for a 1 KT weapon to about 200 msec for a 30 KT detonation.

The spectral measurements indicate that the thermal radiation arriving at the measuring stations peaks in the visible region, with about 10 per cent of the energy in the wave length region below 3600 Å and about 25 per cent in wave lengths beyond 9500 Å. Total thermal radiation measurements made near ground level indicate that, even before the arrival of the shock wave, serious obscuration is produced by such effects of the radiation as "popcorning" of sand, and smoke produced by the burning of ground litter. The thermal energy received by aircraft flying above the detonation was appreciably greater than that received at equivalent distances along the ground. This increase is primarily due to reflection by the ground.

UN[redacted]SIFIED [redacted] UNCLASSIFIED

PREFACE

The U. S. Naval Radiological Defense Laboratory (USNRDL), participated in Projects 8.2 and 8.3 of Operation TUMBLER-SNAPPER.

The first of these projects concerned measurements of the temperatures produced in air near the earth's surface in the vicinity of a nuclear detonation. The other two each involved measurements of thermal radiation emitted in such a detonation. The work performed under Project 8.2 is reported elsewhere. However, no attempt was made to distinguish between measurements made for Projects 8.3 and 8.3a, and all thermal radiation measurements are included in this report.

This report includes results obtained from the analysis of data up to 15 August 1952. Also included for comparison purposes are results from similar measurements made during Operation BUSTER. It is expected that the results given are final. With a few minor exceptions, they include all data taken in these operations.

ACKNOWLEDGMENTS

Project 8.3 of Operation TUMBLER-SNAPPER was carried out under the direction of A. Guthrie, Project Officer. The successful completion of the project was due to the cooperation and unstinted efforts of many individuals at the USNRDL.

The assistance of R. L. Hopton, D. C. Gardenhire, CD2, USN, and J. R. Nichols, AFC, USN, in the laboratory phases of the project is gratefully acknowledged. In addition, J. R. Nichols contributed substantially to the field construction work in his capacity as Field Construction Chief at the Nevada Proving Grounds. A. L. Greig and F. I. Laughridge assisted in certain technical aspects of the project, both in the laboratory and in the field.

It is a pleasure to acknowledge the assistance and encouragement of P. C. Tompkins, Scientific Director, USNRDL. The assistance rendered by personnel of the Test Command contributed substantially to the success of the project.

CONTENTS

ILLUSTRATIONS

CHAPTER 2 INSTRUMENTATION

CHAPTER 3 CALIBRATION

CHAPTER 5 DISCUSSION OF RESULTS

TABLES

CHAPTER 2 INSTRUMENTATION

CHAPTER 3 CALIBRATION

CHAPTER 4 RESULTS

CHAPTER 5 DISCUSSION OF RESULTS

APPENDIX A MEASUREMENT OF THERMAL RADIATION INCIDENT UPON PARKED AIRCRAFT

UNCLASSIFIED

CHAPTER 1

INTRODUCTION

1.1 HISTORICAL

The thermal radiation produced during a nuclear detonation provides one of the principal methods for the dissipation of the tremendous quantities of energy released. Consequently, it constitutes one of the prime sources of damage produced by such a detonation. Therefore, in any consideration of the effects of a nuclear weapon certain characteristics of the thermal radiation emitted are of considerable interest.

Among the characteristics on which information is needed are the total thermal energy, the time variation of the energy, and the spectral quality of the energy, all expressed as functions of distance from the detonation. Some measurements of these characteristics were attempted at nearly all previous nuclear weapons tests. However, the detonations during most of the previous operations were from towers. The obscuring dust produced by detonations near the ground greatly complicated the results obtained during these operations and thus prevented the accumulation of sufficient data for accurate extrapolation and generalization of the thermal output of the nuclear weapon.

Operations CROSSROADS and BUSTER were the only previous operations during which extensive thermal measurements were made on air bursts. At Operation CROSSROADS very questionable results were obtained; for example, the thermal energy turned out to be greater than the total energy. Thus, at only one operation prior to the TUMBLER-SNAPPER tests have data been obtained which could be readily interpreted. It was important, therefore, to make additional thermal measurements under a variety of conditions and for several detonations in order to check existing theories, to permit the derivation of new theories, and, in general, to improve the chances of successful prediction of results of future detonations, particularly of very much larger weapons than have been detonated to date.

Even if one is able to eliminate the effect of the shock wave in producing obscuration of the thermal radiation, great care must be taken in the interpretation of thermal data obtained relatively close to ground zero. Measurements obtained at Operation GREENHOUSE by U.S. Naval Radiological Defense Laboratory (USNRDL) personnel[2] indicated the presence of obscuring material at times and distances such that it appeared questionable that the obscuration was produced by the blast wave. Photographs taken during Operation BUSTER[3] show that the incident thermal radiation, through the production of smoke and through "popcorning" of the sand, caused a high degree of local obscuration before the arrival of the blast

UNCLASSIFIED

[redacted]

ATOMIC ENERGY ACT

wave. Thus, in any field study of the effects of thermal radiation, it becomes advisable to make thermal measurements at stations at which these effects are being investigated.

When Project 8.3 was first approved (as Project 8.3 of Operation SNAPPER), it had as its immediate objective the measurement of the characteristics of thermal radiation at certain stations at which the effects of this radiation were being determined - primarily, on forest fuels, by U.S. Forest Service personnel, and on parked aircraft, by U.S. Air Force personnel. When Operation TUMBLER was first planned, USNRDL personnel were asked to make measurements of the air temperatures in the vicinity of the TUMBLER detonations (see Final Report[4], Operation TUMBLER, Project 8.2). At the same time Project 8.3 was approved to measure the incident thermal flux at the air temperature stations in order to permit the correlation of thermal with air temperature measurements.

The extensive instrumentation for the air temperature measurement program provided an excellent opportunity for the measurement of many parameters concerning the thermal radiation field not previously investigated. For example, the 55-ft steel towers erected for the temperature measurements provided an opportunity for the measurement of the incident thermal radiation as a function of the elevation of the measuring instrument. Later an extreme check on the importance of this parameter was afforded when Project 8.3 was invited to instrument one of the drop aircraft. Unfortunately, the short period of time available for preparation, and the utilization of much of the manpower of the Thermal Radiation Branch, USNRDL, in Project 8.2 work prevented the full utilization of the excellent opportunities afforded.

1.2 OBJECTIVES

The primary objective of Project 8.3 was to measure the total thermal radiation and the intensity-time relationship of the radiation as functions of distance from the detonation. More particularly, the objectives were:

1. To measure the total thermal flux and the time-intensity relationship as functions of distance from the detonations, as functions of the elevation of the measuring instruments, and as functions of the local obscuration caused by dust and smoke in support of Project 8.2 air temperature measurements.

2. To measure, in cooperation with Wright Air Development Center (WADC), the incident thermal flux at various locations where the effects of the nuclear detonations upon parked aircraft were being investigated.

3. To measure the incident thermal flux at various locations at which the effects of thermal radiation upon forest fuels were being studied.

4. To measure the incident thermal flux from the drop aircraft in support of the safety program for the dropping of nuclear weapons.

5. To obtain a rough indication of the spectral breakdown of the thermal radiation by the use of various Corning glass filters to split the energy into broad spectral regions.

6. To measure the effect of thermal radiation upon certain material indicators in order to obtain an indication of the effective thermal energy dose as distinguished from the actual thermal energy incident as measured by the calorimetric instruments.

7. To obtain additional data for purposes of checking proposed scaling laws for thermal radiation and for extrapolation to larger weapons.

8. To measure the thermal radiation received at various stations as a function of the field of view of the measuring device.

9. To obtain a very rough approximation of the amount of radiation absorbed and reflected by the ground by measuring both the incident and reflected radiation. Among other things, it was hoped that these measurements could give an indication of the amount of heating of the surface, and thus of the adjacent air.

CHAPTER 2

INSTRUMENTATION

2.1 MAKE-UP AND LOCATION OF STATIONS

During Operation TUMBLER-SNAPPER measurements of thermal radiation were attempted with several types of instruments. Prime reliance was placed on the disk calorimeter which had proven successful during Operations GREENHOUSE and BUSTER. Weston photronic cells were again used to measure the initial appearance of the thermal radiation.

Since there are several advantages to recording directly the intensity-vs-time pulse obtained during a nuclear detonation, the opportunity was taken to test certain instruments, which, it was hoped, would have a time constant short enough to record intensity directly and yet would be rugged enough to survive the high intensities expected. As only a limited number of recorders were available, additional measurements were attempted with devices which were self-recording. Two types of such devices were used: panels of blackened metal foils similar to those used previously by USNRDL, and modifications of the black-ball gas calorimeter used with some success during Operation BUSTER by the Naval Research Laboratory (NRL).

The thermal measurements made in connection with the air temperature measurements of Project 8.2, were made on, or adjacent to, the 55-ft steel towers provided for the Project. These towers were located at stations ranging from ground zero to 9000 ft from ground zero. For Shots 3 and 4 measurements made at six U.S. Forest Service, Project 8.1, stations extended the range of measurements out to 20,000 ft from ground zero.

For each of the three shots in the T-7 Area seven disk calorimeters were given to WADC personnel for thermal measurements at Project 3.1 stations. Although these instruments were made and calibrated by Project 8.3 personnel, the installation and recording of data were accomplished by Project 3.1 personnel. Finally, three disk calorimeters were mounted in the B-50 bomber which served as drop plane for several of the detonations. The instruments were installed and operated by members of the 4925th Test Group (Atomic), but the records were turned over to Project 8.3 personnel for analysis.

The make-up and location of the stations at which thermal instrumentation was mounted by Project 8.3 are summarized in Tables 2.1 through 2.4. A plot-plan of a typical station is given in Fig. 2.1. Schematic station layouts for the T-7 and F Areas are shown in Figs. 2.2 and 2.3, respectively.

TABLE 2.1

Station Locations, Shot 1

Tower Station	Distance from GZ (ft)	Recorder[a] Station	Recorder Number	Calorimeters Grade	Calorimeters 3 ft	Calorimeters 10 ft	Calorimeters 50 ft	Foils 1 ft	Foils 10 ft	Foils 50 ft	Spheres Grade	Spheres 50 ft	Radio-meters[b] 10 ft
F-200	0	-	-	-	-	-	-	1	-	-	1	-	-
F-202	500	F-220	435	-	-	-	3	-	-	-	-	-	-
			047	-	-	2	-	3	1	2	1	1	1D
			005	3	-	-	-	-	-	-	-	-	-
F-204	1,000	-	-	-	-	-	-	1	-	-	1	-	-
F-206	1,500	-	-	-	-	-	-	1	-	-	1	-	-
F-208	2,000	F-221	436	-	-	-	3	-	-	-	-	-	-
			437	-	-	2	-	3	1	2	1	1	1D
			438	3	-	-	-	-	-	-	-	-	-
F-210	3,000	-	-	-	-	-	-	1	-	-	1	-	-

(a) Recorder stations located opposite corresponding tower stations. Cable lengths from instrument to recorder vary from 50-150 ft.

(b) D = disk radiometer.

TABLE 2.2

Station Locations, Shot 2

Tower Station	Distance from GZ (ft)	Recorder[a] Station	Recorder Number	Calorimeters Grade	Calorimeters 3 ft	Calorimeters 10 ft	Calorimeters 50 ft	Foils 1 ft	Foils 10 ft	Foils 50 ft	Spheres Grade	Spheres 50 ft	Radio meters[b] 10 ft
7-200	0	-	-	-	-	-	-	1	-	-	1	-	-
7-201	750	-	-	-	-	-	-	1	-	-	1	-	-
7-202	1,500	7-220	438	-	-	-	-	1	-	-	1	-	1W
			437	-	-	-	-	-	-	-	-	-	-
			436	-	-	4	-	-	-	-	-	-	-
7-204	3,000	7-221	435	3	-	1	-	1	-	-	1	-	2D
			005	-	-	-	2	-	-	-	-	-	-
7-206	4,500	-	-	-	-	-	-	1	-	-	1	-	-

(a) Recorder stations located opposite corresponding tower stations. Cable lengths from instrument to recorder vary from 50-150 ft.

(b) D = disk radiometer.
W = fine-wire radiometer.

TABLE 2.3

Station Locations, Shot 3

Tower Station	Distance from GZ (ft)	Recorder[(a)] Station	Recorder Number	Calorimeters Grade	Calorimeters 3 ft	Calorimeters 10 ft	Calorimeters 50 ft	Foils 1 ft	Foils 10 ft	Foils 50 ft	Spheres Grade	Spheres 50 ft	Radio-meters[(b)] 3 ft	Radio-meters[(b)] 10 ft
7-200	0	-	-	-	-	-	-	1	-	-	-	-	-	-
7-202	1,500	7-220	436	-	-	1	-	1	-	-	1	-	2D 1W	-
			438	-	-	-	-	-	-	-	-	-	1W	-
7-204	3,000	7-221	435	3	-	2	-	-	-	-	-	-	-	1D
			437	-	-	-	3	3	1	2	1	1	-	-
7-206	4,500	-	-	-	-	-	-	1	-	-	1	-	-	-
7-208	6,000	7-234	865	2	-	1	2	3	1	2	1	1	-	-
7-210	9,000	7-222	047	-	-	6	-	1	-	-	1	-	-	-
USFS	11,000	-	-	-	-	-	-	1	-	-	-	-	-	-
USFS	12,000	-	-	-	-	-	-	1	-	-	-	-	-	-
USFS	13,000	-	-	-	-	-	-	1	-	-	1	-	-	-
USFS	16,000	-	-	-	-	-	-	1	-	-	-	-	-	-
USFS	18,000	-	961	-	3	-	-	3	-	-	1	-	2D	-
USFS	20,000	-	-	-	-	-	-	1	-	-	-	-	-	-

(a) Recorder stations located opposite corresponding tower stations. Cable lengths from instrument to recorder vary from 50-150 ft.

(b) D = disk radiometer. W = fine-wire radiometer.

TABLE 2.4

Station Locations, Shot 4

Tower Station	Distance from GZ (ft)	Recorder[(a)] Station	Recorder Number	Calorimeters Grade	Calorimeters 3 ft	Calorimeters 10 ft	Calorimeters 50 ft	Foils 1 ft	Foils 10 ft	Foils 50 ft	Spheres Grade	Spheres 50 ft	Radio-meters[(b)] 3 ft	Radio-meters[(b)] 10 ft
7-200	0	-	-	-	-	-	-	2	-	-	-	-	-	-
7-202	1,500	7-220	436	-	-	1	-	2	-	-	-	-	2D 1W	-
			438	-	-	-	-	-	-	-	-	-	2W	-
7-204	3,000	7-221	435	3	-	2	-	1	-	-	2	2	-	1D
			437	-	-	-	3	-	-	-	-	-	-	-
7-206	4,500	-	-	-	-	-	-	1	-	-	1	-	-	-
7-208	6,000	7-234	865	2	-	1	2	1	-	-	1	2	-	-
7-210	9,000	7-222	047	-	-	6	-	1	-	-	1	-	-	-
USFS	11,000	-	-	-	-	-	-	1	-	-	1	-	-	-
USFS	12,000	-	-	-	-	-	-	1	-	-	1	-	-	-
USFS	13,000	-	-	-	-	-	-	1	-	-	1	-	-	-
USFS	14,500	-	-	-	-	-	-	1	-	-	-	-	-	-
USFS	16,000	-	-	-	-	-	-	1	-	-	1	-	-	-
USFS	18,000	-	961	-	3	-	-	2	-	-	1	-	2D	-

(a) Recorder stations located opposite corresponding tower stations. Cable lengths from instrument to recorder vary from 50-150 ft.

(b) D = disk radiometer. W = fine-wire radiometer.

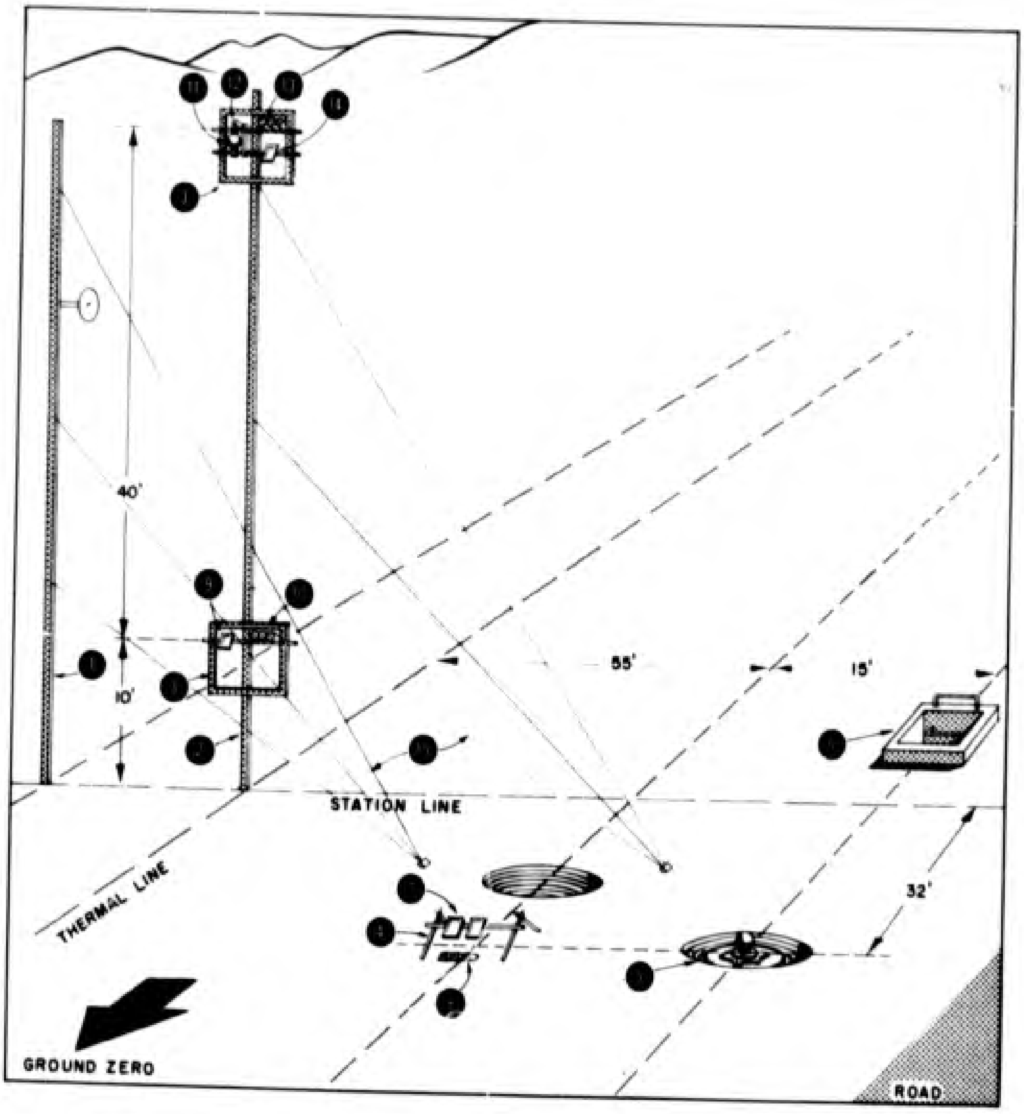

1. Blast Tower
2. Thermal Tower
3. Tower Instrument Support Frames
4. Surface Instrument Support Tubelox Frame
5. Sphere Calorimeter (At Grade)
6. Instrument Shelter
7. Passive Receivers (1-ft Elev)
8. Calorimeters or Radiometers (At Grade)
9. Passive Receiver (10-ft Elev)
10. Calorimeters or Radiometers (10-ft Elev)
11. Sphere Calorimeter (50-ft Elev)
12. Photronic Cell (50-ft Elev)
13. Calorimeters or Radiometers (50-ft Elev)
14. Passive Receiver (50-ft Elev)
15. Guy Wires (Left, Front Only Shown)

Fig. 2.1 Isometric Drawing of a Typical Station

UNCLASSIFIED

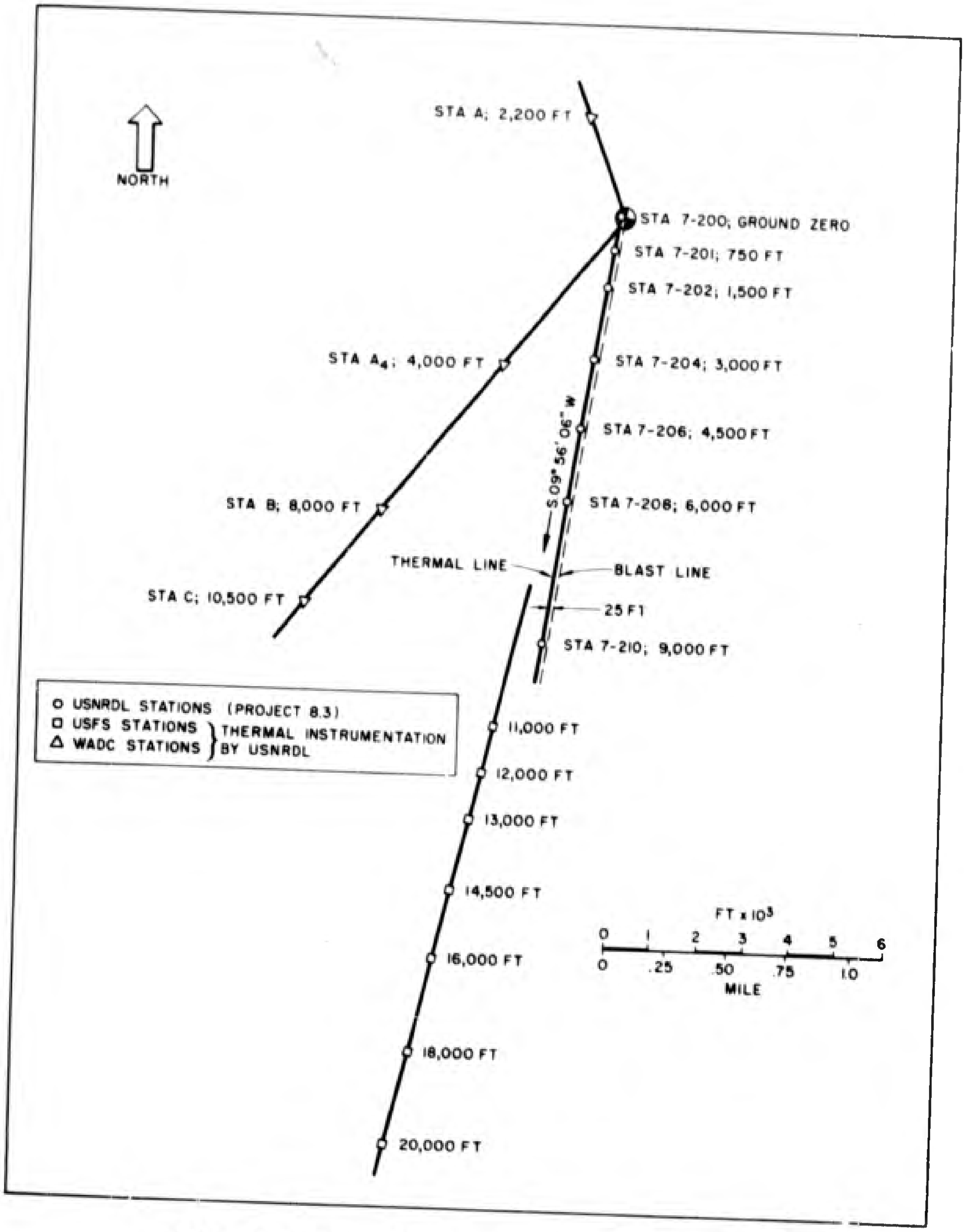

Fig. 2.2 Schematic Station Layout, T-7 Area

UNCLASSIFIED [redacted] ATOMIC ENERGY ACT 1946

UNCLASSIFIED Security Information

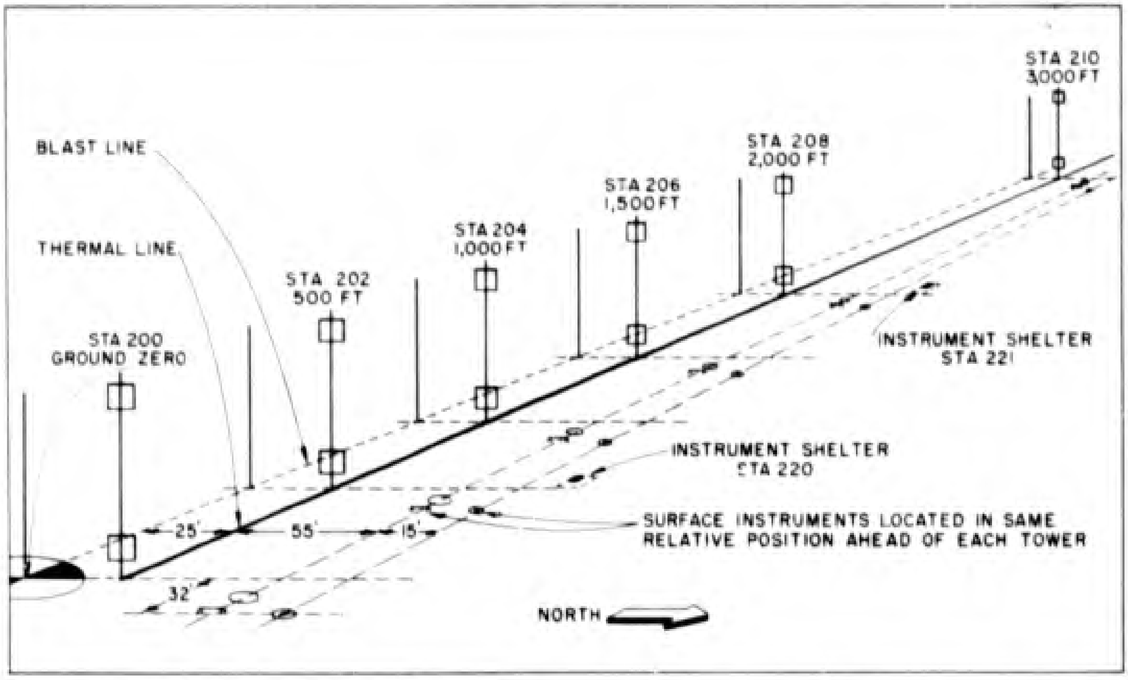

Fig. 2.3 Schematic Station Layout, F Area

2.2 DISK CALORIMETERS

2.2.1 Description

Although the USNRDL field calorimeter was modified slightly prior to Operation TUMBLER-SNAPPER, the basic design of the instrument did not change (Fig. 2.4). A disk-shaped energy receiver cut from copper and blackened on one face with electrolytically-deposited platinum and finish coated with camphor black, is exposed to thermal radiation through an appropriate filter. The receiving disks, 3/8 in. in diameter, vary in thickness from 0.020 in. to 0.125 in., the thicknesses being selected so that the temperature rise in each disk would never be appreciably greater than 150°C in order that the heat losses from the disk would not be excessive.

Except in the case of the thickest disk, a thermocouple consisting of 5-mil copper and constantan wire is soldered to the center of the unblackened face of the disk. The other end of the thermocouple wire is fastened to the reference junction, comprised of massive copper blocks housed in the calorimeter case. The electrical signal generated by the thermocouple is fed into one galvanometer of a 12-channel Heiland oscillographic recorder.

Each receiving disk is sufficiently thick to give a long time constant with respect to total energy measurements, that is, the receiver retains the energy absorbed during the detonation with a minimum of heat loss. However, since the thermal diffusivity of the disk is quite high, the rate of change of temperature at any point in the disk rapidly reaches a constant value for a constant input of energy, that is, the time constant for rate of energy received is short and differentiation of the recorded energy-vs-time curve will give an accurate intensity-vs-time curve.

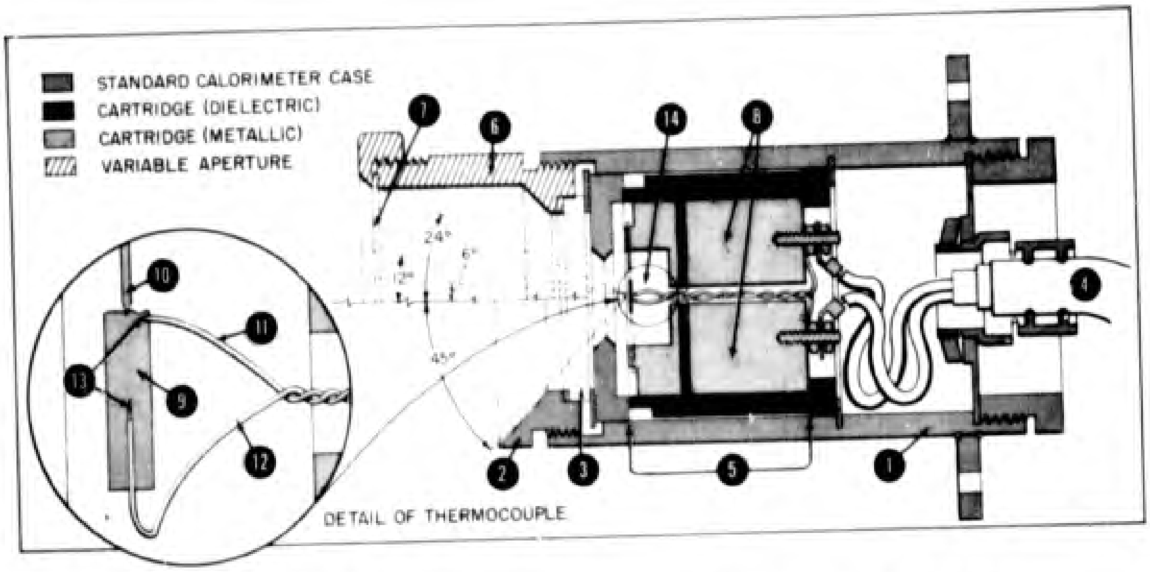

1. Std Calorimeter Case and Fittings (3-in. OD)
2. Std Aperture Ring (45° Half-angle Field)
3. Filter (Quartz, or Corning 2-58, 3-69, 7-56, or 0-52)
4. DHFTA-9 No. 10 Cable to Recorder
5. NRDL Mk 1 Field Calorimeter Cartridge
6. Variable Aperture Adapter Ring
7. Variable Aperture Plates (6°, 12°, or 24°)
8. Copper Reference Blocks
9. Thermocouple Button (0.375-in. D)
10. Phonograph Needle (Button Support)
11. Thermocouple Lead-in Wire (5-mil Copper)
12. Thermocouple Lead-in Wire (5-mil Constantan)
13. Drilled and Peened Connection of Lead-in Wires to 0.125-in. Thickness Button
14. Soldered Connection of Lead-in Wires to Thin Buttons

Fig. 2.4 Cross Section of Field Calorimeter

The time constant for intensity of each of the receiving disks was below the 20-msec time constant requirement as set by the Armed Forces Special Weapons Project (AFSWP). In the case of the 0.125-in. disk, however, the time constant was quite close to the 20-msec limit if the thermocouple was attached to the back surface of the disk. To shorten the response time of this instrument, the thermocouple was inserted close to the geometrical center of the disk through a small hole drilled through the periphery of the disk.*

The thicknesses of all the receivers used, together with an indication of the energies for which these thicknesses were selected, are shown in Table 2.5. In this table, column 3 gives the temperature in degrees centigrade above the ambient temperature, which the receiver will attain when exposed to the energy listed in column 2. Column 4 gives the voltage generated at the thermocouple and column 5 gives the voltage which the galvanometer records to produce the deflection in column 6. The difference in the two voltages listed is due to the necessity of introducing a series resistance into the thermocouple circuits in order to properly damp the galvanometer.

TABLE 2.5

Galvanometer Deflections for Various Energies and Disk Thicknesses

Thickness (in.)	Energy (cal/sq cm)	Temperature (^{o}C)	Thermocouple Signal (mv)	Recorded Signal (mv)	Deflection (cm)
0.125	40	150	6.8	3.2	4.3
0.0625	20	150	6.8	3.2	4.3
0.0312	10	150	6.8	3.2	4.3
0.025	5	95	4.2	2.0	2.7
0.020	3	70	3.2	1.5	2.0

For the measurement of total energy the receiving disks were mounted behind quartz filters which transmit in the region between approximately 2200 Å and 4.5 μ. A rough spectral breakdown was obtained by mounting receiving disks in back of Corning glass filter Nos. 0-52, 3-69, 2-58, and 7-56. These filters transmit, respectively, from 3600 Å, 5200 Å, 6400 Å, and 9500 Å through 2.5 μ. Transmission curves for all the filters used are shows in Figs. 2.5 and 2.6. Diaphragms of various sizes were mounted (Fig. 2.4) on the aperture of some of the calorimeters so that the effect of the field of view on the energy received could be determined.

2.2.2 Use as an Intensity Device

As mentioned above, the energy-vs-time traces recorded by the calorimeter circuits may be differentiated to give intensity-vs-time curves. This differentiation may be accomplished approximately by reading for a short time interval, Δt, the energy, Δq, recorded during that interval and plotting the average intensity for the time interval, $\frac{\Delta q}{\Delta t}$, as a close approximation to the true intensity, $\frac{dq}{dt}$. Depending upon the infor-

* This was done at the suggestion of H. C. Hottel.

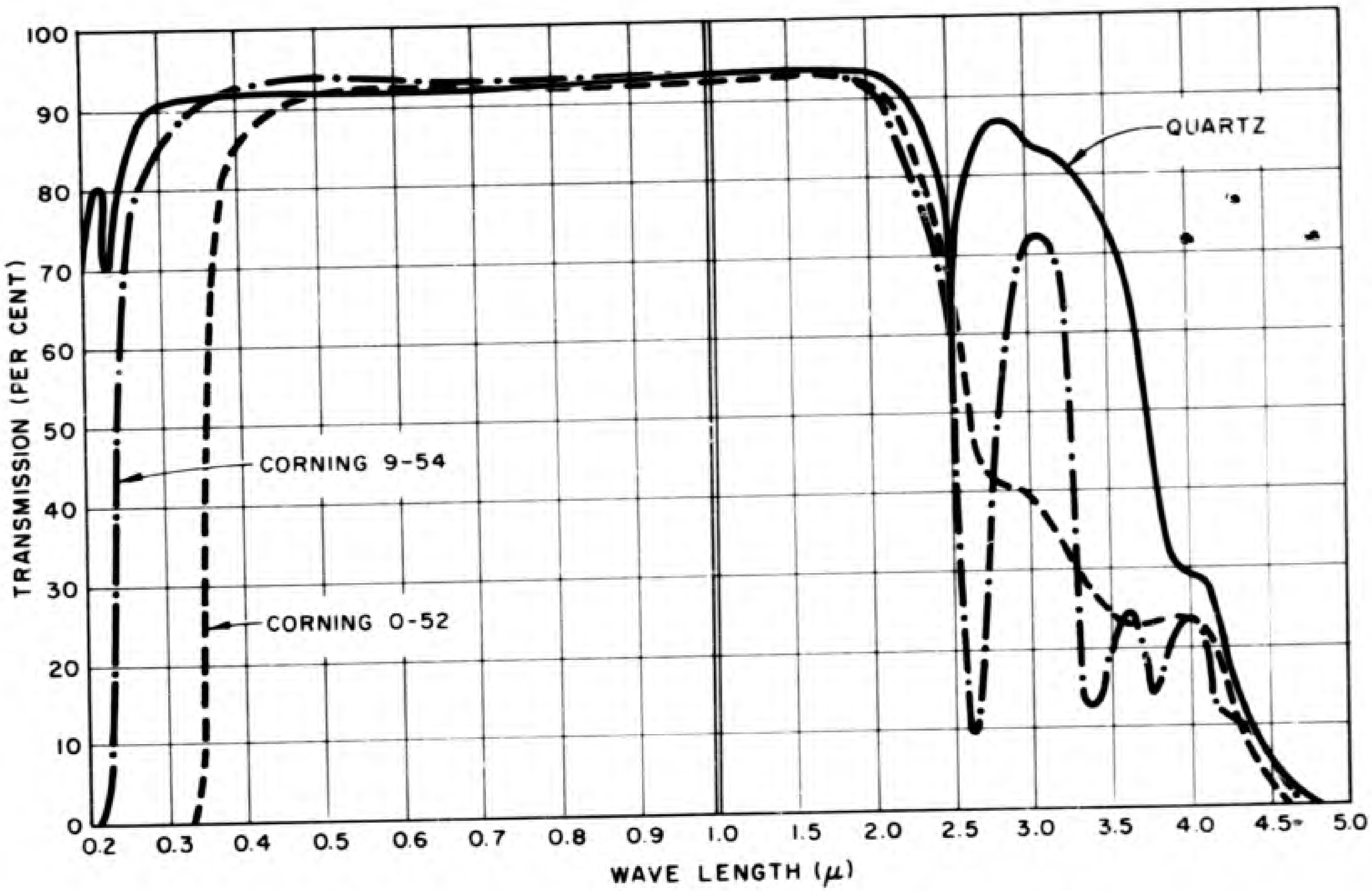

Fig. 2.5 Transmission Curves of Quartz and Corning Filters 9-54 and 0-52

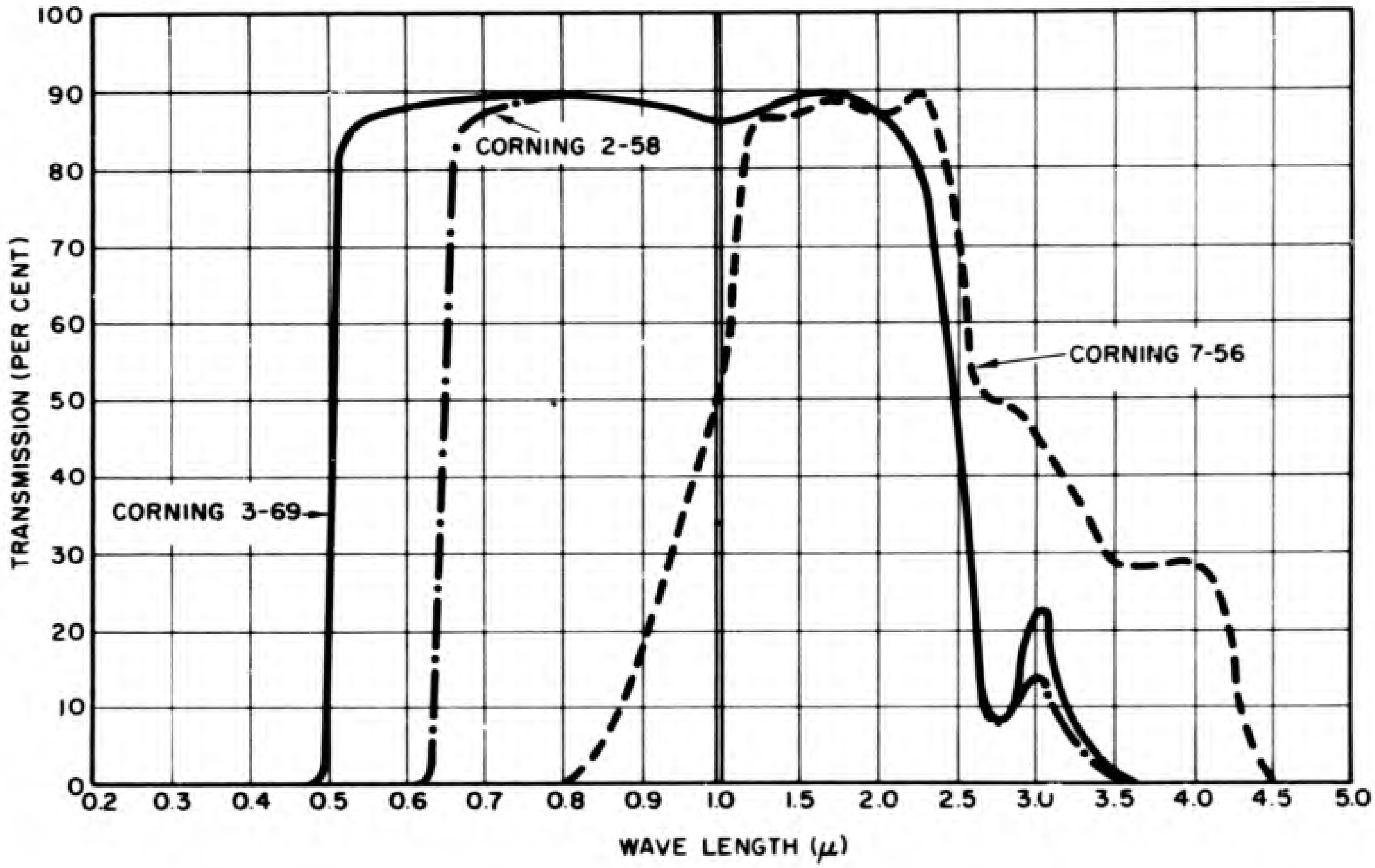

Fig. 2.6 Transmission Curves of Corning Filters 3-69, 2-58, and 7-56

mation desired, the differentiation technique may be carried out in one of two ways. The difference between the two techniques depends upon the fact that the errors in reading the calorimeter traces are of two types: (1) a calibration or scale error, which is a constant percentage regardless of the magnitude of the deflection, and (2) the reading error, which is constant in value and thus varies percentage-wise with the magnitude of the deflection.

The difference in the two techniques may be illustrated by taking as a typical case a trace with a total deflection of 3 cm, which, for weapons of a magnitude used in this operation, would have at peak intensity a peak deflection rate of about 6 cm/sec, falling off at 2 sec to about 2.5 per cent of that value. Using the four-fold magnification in a Universal Telereader, Type 17A, the error in reading a good Heiland galvanometer trace is not greater than ± 0.003 cm. The reading error for the total energy measurements then is 3 ± 0.003 cm, or 0.1 per cent, a negligible value.

However, as a time resolution of 20 msec is desired, the intensity curve must be based upon the deflection of the galvanometer during a 20-msec interval. At peak intensity, the error in this deflection would amount to 6 cm/sec x 0.02 sec = 0.12 cm, and this value would be known to ± 0.003 cm, an error of ± 2.5 per cent. However, at 2 sec the deflection during the 20-msec interval would be only 0.003 cm, and the uncertainty, then, would be equal in magnitude to the deflection itself.

If one restricts the need for a 20-msec time resolution to the interval around the peak intensity, where most damage is produced, it is possible by proper selection of Δt to maintain a fixed percentage error in the intensity value. Thus, if time intervals are chosen so as to maintain the energy interval found at peak intensity, 0.12 cm in the example above, the uncertainty in the energy for the time interval will remain constant and thus the uncertainty in the intensity will remain constant. This procedure gives the average intensity fairly accurately for the time interval over which the measurement is made.

In obtaining intensity-time curves, rectangles representing the time interval selected and the corresponding error in the intensity for each point may be plotted rather than the point itself. This procedure has the added advantage of having the long axis of the rectangle of uncertainty lie parallel to the curve in regions of slowly changing slope, thus simplifying the drawing of the curve.

2.3 DISK RADIOMETER

2.3.1 Historical

The use of the thick copper disk as a receiving element for measuring the intensity of the thermal radiation from a nuclear detonation was a secondary consideration in the original design of a disk calorimeter. The concept and the validity of differentiating the total energy curve recorded by the calorimeter to obtain a rate curve originated during Operation GREENHOUSE. However, the procedure is laborious and cannot very well be done in the field. An elaborate reading instrument is required in order to read the original traces with sufficient accuracy for the differentiation. The effect of electrical noise upon the record is disastrous when differentiation is attempted.

There has long been a need for a device which would record directly the intensity of the thermal pulse obtained in the field, and shortly after Operation BUSTER a limited amount of work was initiated in this direction both at USNRDL and at the Massachusetts Institute of Technology (MIT). The work was reviewed at the January, 1952, meeting of the AFSWP panel on thermal radiation and it was agreed that USNRDL would attempt to test a new type of radiometer during Operation TUMBLER-SNAPPER. At that time H. C. Hottel, of MIT, turned over to USNRDL a prototype of an instrument which was used during Operation TUMBLER-SNAPPER. Several similar instruments were built at USNRDL and also tested during these operations.

2.3.2 Description of the Instrument

The design proposed by H. C. Hottel was adopted because it was fairly easy to construct and, once made, proved to be very rugged for field use. A cross section of the radiometer is given in Fig. 2.7. The receiving element is a thin disk of constantan foil which covers a small hole drilled in a massive block of copper. The foil is held in place by an annular ring secured to the block by aligning screws. A very thin copper wire is soldered to the center of the back surface of the foil to provide the thermo-electric hot junction. The junction of the constantan foil and the massive copper block constitutes the cold junction. The energy absorbed by the foil rapidly dissipates into the block, so there is a relatively small temperature increase in the foil and a negligible rise in the temperature of the surface of the copper block. The central copper wire is fastened to a terminal in an insulated block at the back of the massive copper piece. A second terminal is made in the copper block and these two terminals are connected through appropriate resistances to the Heiland galvanometer. After the instrument is assembled, the front surface of the constantan foil is blackened with camphor smoke.

2.3.3 Calibration of the Disk Radiometer

According to H. C. Hottel, a theoretical calibration constant can be determined for these instruments by the use of the following equation for the steady state condition:

$$\frac{\Delta T}{I} = \frac{r^2}{4KY},$$

where I = Intensity of the absorbed radiant energy,
ΔT = Temperature difference between the edge and the center of the foil,
r = Radius of the circular foil as defined by the radius of the hole in the copper block,
Y = Thickness of the foil, and
K = Thermal conductivity of the foil.

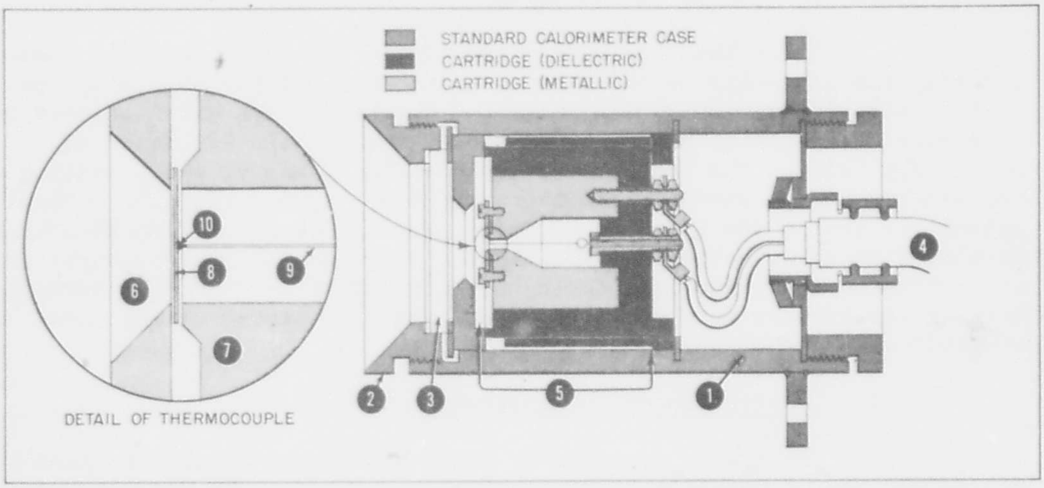

1. Std Calorimeter Case and Fittings (3-in. OD)
2. Std Aperture Ring (45° Half-angle Field)
3. Filter (Quartz or Corning 2-58)
4. DHFTA-9 No. 10 Cable to Recorder
5. MIT Foil Radiometer Cartridge
6. Secondary Aperture and Pressure Plate
7. Copper Reference Block
8. Constantan Foil
9. Copper Lead-in Wire
10. Lead-in Soldered to Foil

Fig. 2.7 Cross Section of Disk Radiometer

The calculated sensitivity for the instrument (MIT-3) given to USNRDL, is $\frac{\Delta T}{I}$ = 5.8°C/cal/sq cm/sec. The sensitivity as determined experimentally at MIT was 2.9°C/cal/sq cm/sec. The front surface of the MIT-3 radiometer was blackened before use at USNRDL. Recalibration at that time gave a sensitivity value of 8.0°C/cal/sq cm/sec. The latter value has been used in the reduction of all field data.

An estimate of the time constants for the instruments can be determined from the equation, $\tau = \frac{r^2 C_p \rho}{8K}$, where C_p and ρ are the specific heat and density, respectively, of the receiving element (the other quantities have been previously defined). Values of the time constant for the MIT-3 radiometer are as follows: theoretical, 0.0034 sec; experimental MIT, 0.012 sec; and experimental USNRDL, 0.013 sec. It may be seen that the experimental time constant is well below the requirement of 20 msec.

2.4 FINE-WIRE RADIOMETER

2.4.1 Description

The fine-wire radiometer used in Project 8.3 was inspired by the thermocouple devices used in the air temperature measurements of Project 8.2. For the air temperature measurements the heated air was drawn past a fine-wire silver-constantan thermocouple which was shielded from the thermal radiation. For the intensity measurements a similar fine-wire thermocouple is exposed to the fire ball and cooled by a high-velocity stream of air from a constant-temperature air supply.

The thermocouple was made of 2-mil constantan wire, half the length of which had been silver-plated, and was mounted adjacent to the end of a Pyrex tube in such a way that the silver-constantan junction was centered in the tube opening. The thermocouple reference junctions consisted of large brass blocks mounted inside a metal shield. Figure 2.8 shows a cross sectional view of the instrument. The output of the thermocouple is again recorded on a channel of the Heiland recorders used for the other Project 8.3 measurements. The entire recording circuit (except for a small portion of the thermocouple exposed to the thermal radiation) is electromagnetically shielded.

The cooling air was supplied by a 20-cu-ft compressed air tank buried in the ground behind the instruments. The air flow was controlled by means of a solenoid operated through an Agastat relay circuit similar to those used for the Project 8.2 temperature measurements. By maintaining a high air flow past the wire, the net heating of the wire upon absorption of the thermal radiation may be kept to reasonable values, and the time constant of the system is considerably reduced.

2.4.2 Theory

For any radiant flux incident a heat balance is established between the heating effect of the thermal radiation and the cooling of the air stream. The general expression for the heat balance is:

$$\alpha IDL = C_p \pi \frac{D^2}{4} L \rho \frac{dT}{dt} + h \pi DL(T - T_a), \qquad (2.1)$$

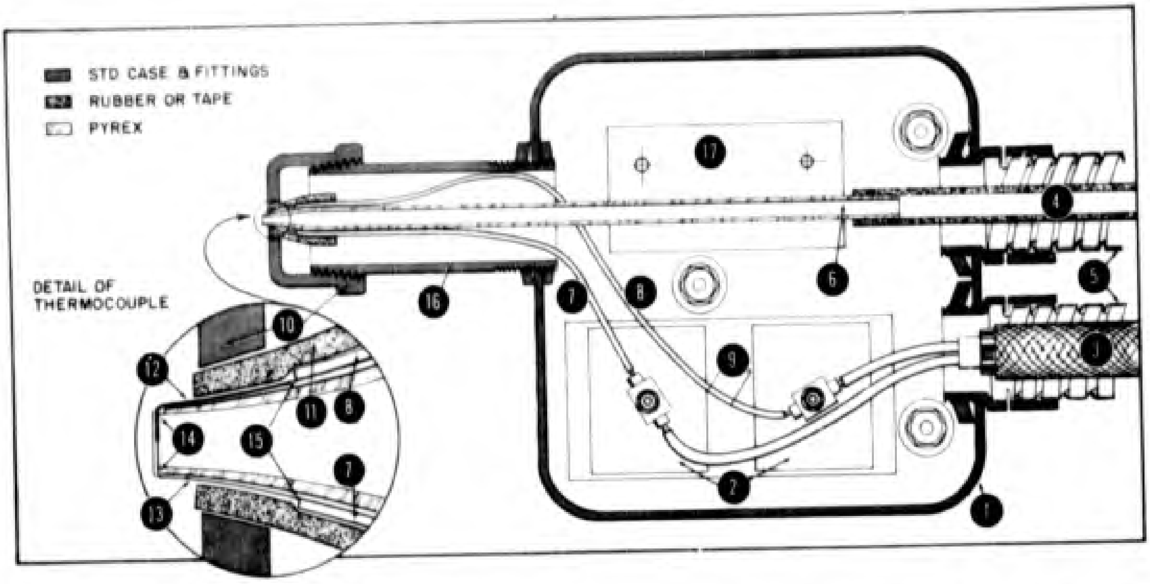

1. 4-11/16 in. Square Electrical Junction Box
2. Brass Reference Blocks
3. DHFTA-9 No. 10 Cable to Recorder
4. Air Supply (Rubber Hose, 1/4-in. ID)
5. 3/4-in. Flexible Metallic Conduit
6. Pyrex Nozzle Tube
7. Thermocouple Lead-in Wire (Constantan)
8. Thermocouple Lead-in Wire (Copper)
9. Thermocouple Identification Tag
10. Nozzle Guard (3/4-in. IPS Pipe Cap)
11. Dielectric Tape
12. Silver-plated Constantan Wire
13. 0.002-in. D Constantan Wire
14. Nozzle Notched to Receive Wire
15. Thermocouple Wires Soldered to Lead-in
16. 3/4-in. IPS Nipple
17. Nozzle Mounting Block

Fig. 2.8 Cross Section of Fine-wire Radiometer

where α = Absorptivity of the wire,
I = Irradiation (cal/sq cm/sec),
D = Diameter of wire (cm),
L = Length of wire (cm),
C_p = Specific heat of wire (cal/g/$^{\circ}$C),
ρ = Density of wire (g/cu cm),
T = Temperature of wire ($^{\circ}$C),
t = Time (sec),
h = Forced convection heat transfer coefficient for the wire in perpendicular air flow (cal/sq cm/$^{\circ}$C/sec), and
T_a = Air temperature ($^{\circ}$C).

From Equation 2.1 it may be seen that the temperature rise of the wire may be expressed by:

$$T - T_a = \frac{aI(1 - e^{-\frac{4h}{C_p \rho D}t})}{\pi h} \qquad (2.2)$$

Under equilibrium condition the sensitivity of the instrument is given by:

$$\frac{T - T_a}{I} = \frac{a}{\pi h} \qquad (2.3)$$

The time constant, τ, of the wire can be obtained from the exponent of Equation 2.2:

$$\tau = \frac{C_p \rho D}{4h} \text{ sec} \qquad (2.4)$$

An expression for the heat transfer coefficient, h, can be obtained from McAdams:[10]

$$\frac{hD}{k} = 0.32 + 0.43 \left(\frac{Dv\gamma}{\mu}\right)^{0.52}, \qquad (2.5)$$

where $\frac{hD}{k}$ = Nusselt's number (consistent units), and

$\frac{Dv\gamma}{\mu}$ = Reynold's number (consistent units).

For air at 20°C at a velocity of 450 ft/sec and for a 2.4-mil (0.006-cm) constantan wire, Equation 2.5 reduces to:

$$h = 0.14 \text{ cal/sq cm/}^{\circ}\text{C/sec} \qquad (2.6)$$

Substituting this value for h in Equation 2.4, and assuming $\frac{C_p \rho D}{4} = 0.0014$ for the constantan wire,

$$\tau = 0.010 \text{ sec} = 10 \text{ msec} \qquad (2.7)$$

For an air velocity of 450 ft/sec, and a wire absorptivity of 0.20, the sensitivity of the instrument becomes:

$$\frac{T - T_a}{I} = 0.46^{\circ}\text{C/cal/sq cm/sec} \qquad (2.8)$$

Since the thermocouple devices were developed for use in the air temperature measurements of Project 8.2 and adapted at the last minute for use as radiometers, no calibration other than the theoretical one was attempted. Because all the equipment was available for testing in the field, the instruments were installed as a check on the practicality of their operation. It was hoped that these radiometers would provide one additional curve of intensity vs time for comparison with those obtained with the other instruments.

2.5 PASSIVE-RECEIVER PANELS

During Operation TUMBLER-SNAPPER, measurements were made with panels of blackened metal foils similar to those used at Operations GREENHOUSE and BUSTER. The panels, made from the Operation GREENHOUSE panels by cutting them in half, were 8 x 10 in. in size, having 25 holes 15/16 in. in diameter drilled into the face covered by a 6-1/2-in. square Corning No. 0-52 or 9-54 filter. A complete description of these panels was given in the report on Operation GREENHOUSE.

The indicating materials used in these panels were cadmium, tin, lead, silver, and copper foils blackened with chemically or electrolytically deposited, finely divided metals. For each metal in each panel a range of thicknesses was exposed such that all expected values of energy from the detonation would be sufficient to melt some, but not all, of the foils. For each foil a curve relating the critical energy for melting, that is, the minimum amount of energy necessary to just melt through the foil, to time of exposure to the thermal radiation was determined in the laboratory (typical calibration curves are shown in Fig. 2.9). Thus, each series of foils serves as an instrument which, although it cannot measure exactly the radiation received, can closely bracket this value, if the time of exposure is known. Of course, it is necessary to obtain the time of exposure from one of the dynamic instruments.

The copper and silver foils were blackened essentially as they were for Operation GREENHOUSE[2], tin and cadmium as for Operation BUSTER[3], and lead with a copper-antimony black as described elsewhere[9]. The reflectance characteristics of the metals after blackening have been reported previously, but may be summed up as follows: the blackened foils absorb at least 96 per cent of the incident radiation of wave length 0.2 to 1 μ, at least 94 per cent from 1 to 1.5 μ and at least 85 per cent from 1.5 to 2.0 μ.

The metals used were grouped into two total energy ranges of three metals each and an upper range of two metals. For the range 0.5 to 30 cal/sq cm, cadmium, tin, and lead were used; for the range 30 to 70 cal/sq cm, silver, cadmium, and lead were used; for energies above 70 cal/sq cm, silver and copper were used with silver in two geometries to give an additional check.

The passive-receiver panels were exposed for two reasons. Since an energy measurement made with the foils depends upon an effect produced upon the foils, and since this effect will not be produced at intensities below a certain critical intensity, the foils measure effective, rather than the true, total energy. Where measurements were made with the foil panels at stations at which measurements were also made with other instruments, the measurements served as a check of the degree to which this effective energy approximates the true energy.

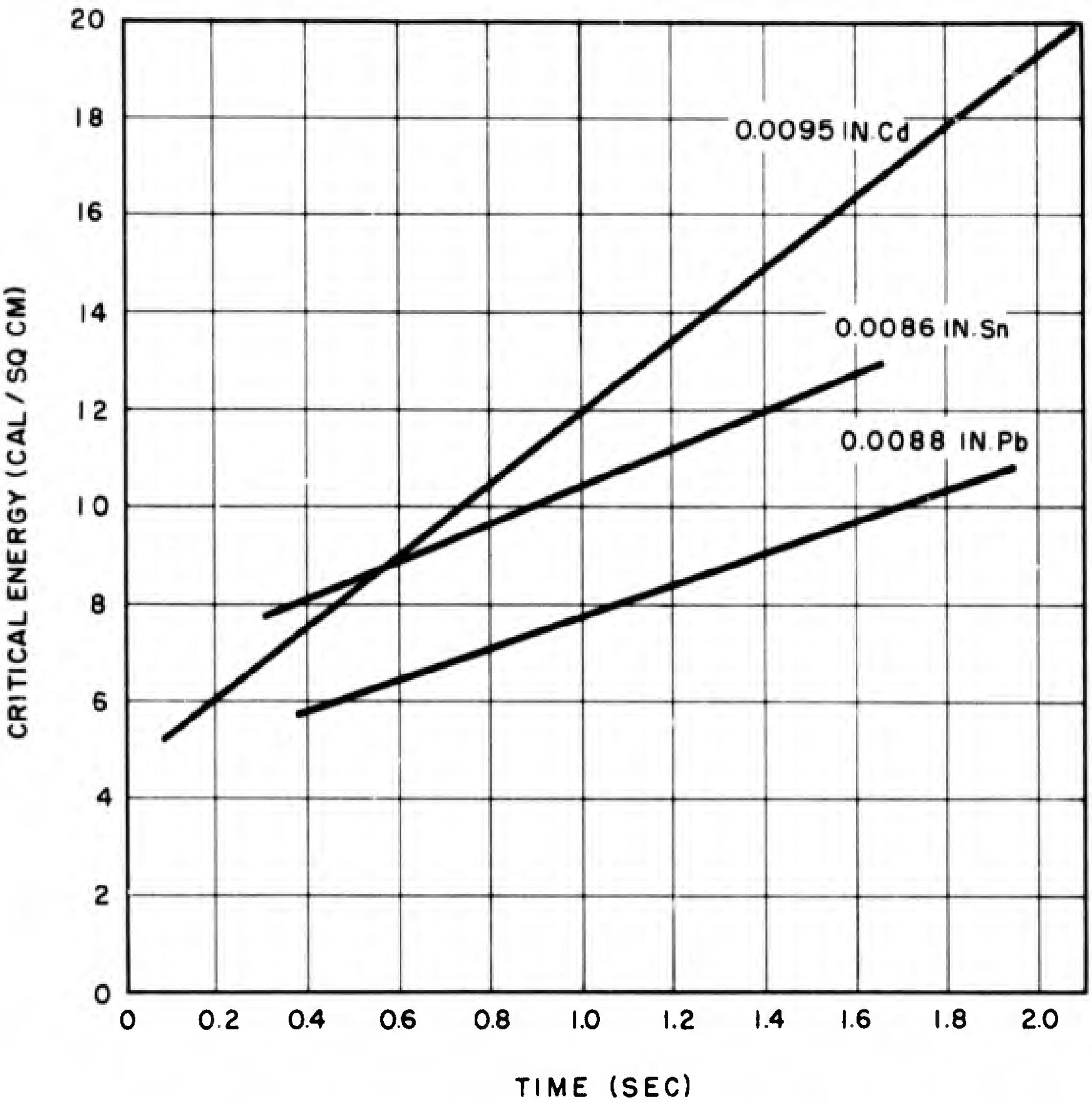

Fig. 2.9 Typical Calibration Curves for Passive Receivers

Since the shape of the thermal pulse varies with the yield of the weapon, and since the energy in a long, low-intensity pulse would not be effective in producing damage to the foils, it was expected that the ratio of effective energy to true energy would decrease with increasing yield. Having established a ratio of effective to true energy for a particular weapon, the foil panels could then be used to provide an indication of a value of true thermal energy at stations at which no recording channels were available for obtaining the true value directly.

The total number of panels exposed during the four shots was 60: 16 on the first shot, 5 on the second, 24 on the third, and 15 on the last. For each panel position a value of expected energy was calculated and an energy range for each panel was found by multiplying this expected value by 0.3 and 1.3 for the 0.5- to 30-cal/sq cm range, 0.25 and 1.5 for the 30- to 70-cal/sq cm range, and 0.21 and 1.7 for the range extending upwards from 70 cal/sq cm. For each of these ranges a geometrical progression of eight steps of energy values was calculated between the limits of the range. Based upon the laboratory calibrations, corresponding thicknesses of the three metals were determined after making assumptions on field pulse time. Some simplification was accomplished by grouping almost-equal thicknesses and similar panels.

It was found that all of the ranges fell nicely into 11 groups, thus reducing the complexity of fabrication by a large factor. The 60 panels used included 27 thicknesses of cadmium ranging from 0.8 to 62 mil, 23 thicknesses of tin from 0.6 to 43 mil, 26 thicknesses of lead from 0.8 to 55 mil, 19 thicknesses of silver from 1 to 125 mil, and 22 thicknesses of copper from 1.1 to 80 mil. With a few exceptions the geometry of the receivers was the same as that used in the previous operations: 13/16-in.-D disks with apertures which permitted them to receive radiation on an area of 3/8-in. D in the center. The foils were also exposed in two other types of geometry. Strips 13/16 in. long and 1/8 in. wide were used in the high energy range as a third indicator. Disks 13/32 in. in diameter, attached to the insulating washers by three tabs, 1/16 in. wide and 3/16 in. long, were incorporated into the lowest-energy panels, since they are more sensitive than the standard size disk.

2.6 SPHERE CALORIMETERS

The sphere calorimeter has been designed by NRL personnel and used by them during Operation BUSTER - JANGLE. A photograph of the instrument is shown in Fig. 2.10. Its principle of operation is based on the general gas law. The gas is air, enclosed (at constant volume) in a copper sphere. The air is heated when thermal radiation falls on the sphere. The resulting increase in pressure of the air moves a beryllium-copper diaphragm in the bottom of the sphere. The deflection of the diaphragm is measured by a dial indicator. The indicator is mounted below the diaphragm in such a manner that the contact point of the indicator rides on a button in the center of the diaphragm. The indicator is so constructed that it registers movements in a positive direction only. To prevent spurious readings due to diurnal fluctuations of temperature and pressure, a slow leak is provided in both the sphere and the bottom cover.

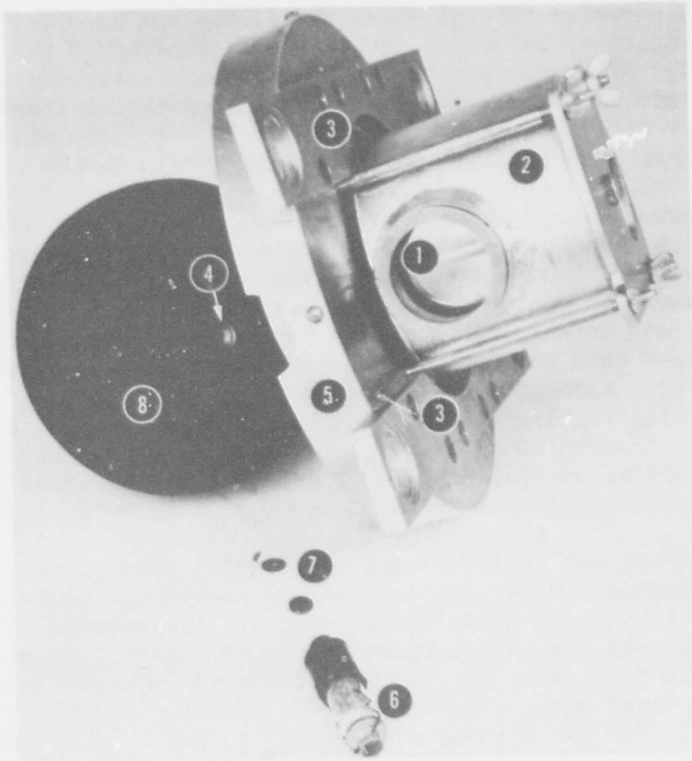

1. Dial Indicator
2. Diaphragm and Indicator Case
3. Base Bracket
4. Breather Connection Fitting
5. Guard Ring
6. Desiccator Plug
7. Breather Aperture Washer
8. Sphere

Fig. 2.10 Sphere Calorimeter

With considerable care and effort reasonable data were obtained during Operation BUSTER, but the Operation JANGLE results were not as satisfactory. The instruments were calibrated by NRL personnel and transferred to USNRDL personnel at the Nevada Proving Grounds during Operation TUMBLER. Since the instruments were still in the development stage, and since Project 8.3 personnel did not have time to familiarize themselves with the operation of the device, not too much hope was held for successful performance during Operation TUMBLER-SNAPPER. However, it was expected that experience with the calorimeters during this field operation would promote successful use of these devices in future operations.

2.7 CIRCUITS

Two types of electrical circuits were involved in this operation: the power and signal circuits or which all instruments were operated, and the recording circuits through which the electrical impulses produced by the thermal radiation detection devices were recorded by the Heiland galvanometers. All power required to operate the instruments was provided by 24-v aircraft batteries located in the instrument shelters. All recorders were activated by the minus 5-sec EG&G signals which actuated secondary relays used to close the power circuits. In the power circuits, Agastat time-delay relays were used to close the circuits, hold them closed for predetermined periods of time and then to open them. For recording of thermocouple outputs, a completely shielded circuit, properly grounded, was made up of two-conductor armored cable (the armor served as a shield) between the calorimeters and a closed junction box in the instrument shelter, and between the junction box and the Heiland recorders. The junction box was used to mount appropriate resistors, to obtain proper sensitivity and damping for the galvanometers, and as a convenient place for applying electrical calibration signals. As a check on the protection offered by the armored cable, several other types of cables were used at the 10-ft elevation at Station 7-202, Shot No. 2. The types of cable used were Romex, Romex in flexible metallic conduit, and twisted bell wire.

Since instrument shelters were provided at each station at which dynamic instrumentation for Project 8.3 was placed, no extremely long lengths of cable were used for the Project 8.3 instruments. The same recorders were used for this project as for Project 8.2 measurements. For the instruments mounted on the tower the armored cable was run down the inside of the tower post, thence into 2-ft trenches and into the instrument shelters. For the instruments mounted on the Tubelox racks, the cable was again run in trenches to the instrument shelters. A block diagram of a typical electrical circuit is shown in Fig. 2.11.

2.8 MOUNTING

For maximum ease and flexibility all instrument mounts were designed to fasten to 2-in.-OD Tubelox pipe. All instrumentation on the towers was supported by horizontal Tubelox lengths attached by U-bolts to the 6- x 6-ft mounting frames provided at the 10- and 50-ft elevations on the towers. Surface-mounted instruments were supported and anchored by a pair of 6- x 6-ft right-angle "A" frames set in the ground 3 ft apart with their bases parallel to the blast line and their apices 2 ft above grade. The instruments were mounted on stringers across the sloping front face of this framework. Standard 8-in.-D Tubelox base plates were attached by bayonet fittings to the four legs of the framework. The base of each frame was buried in the ground at distances 55 ft to the left and 32 ft forward (toward ground zero) of the corresponding thermal tower.

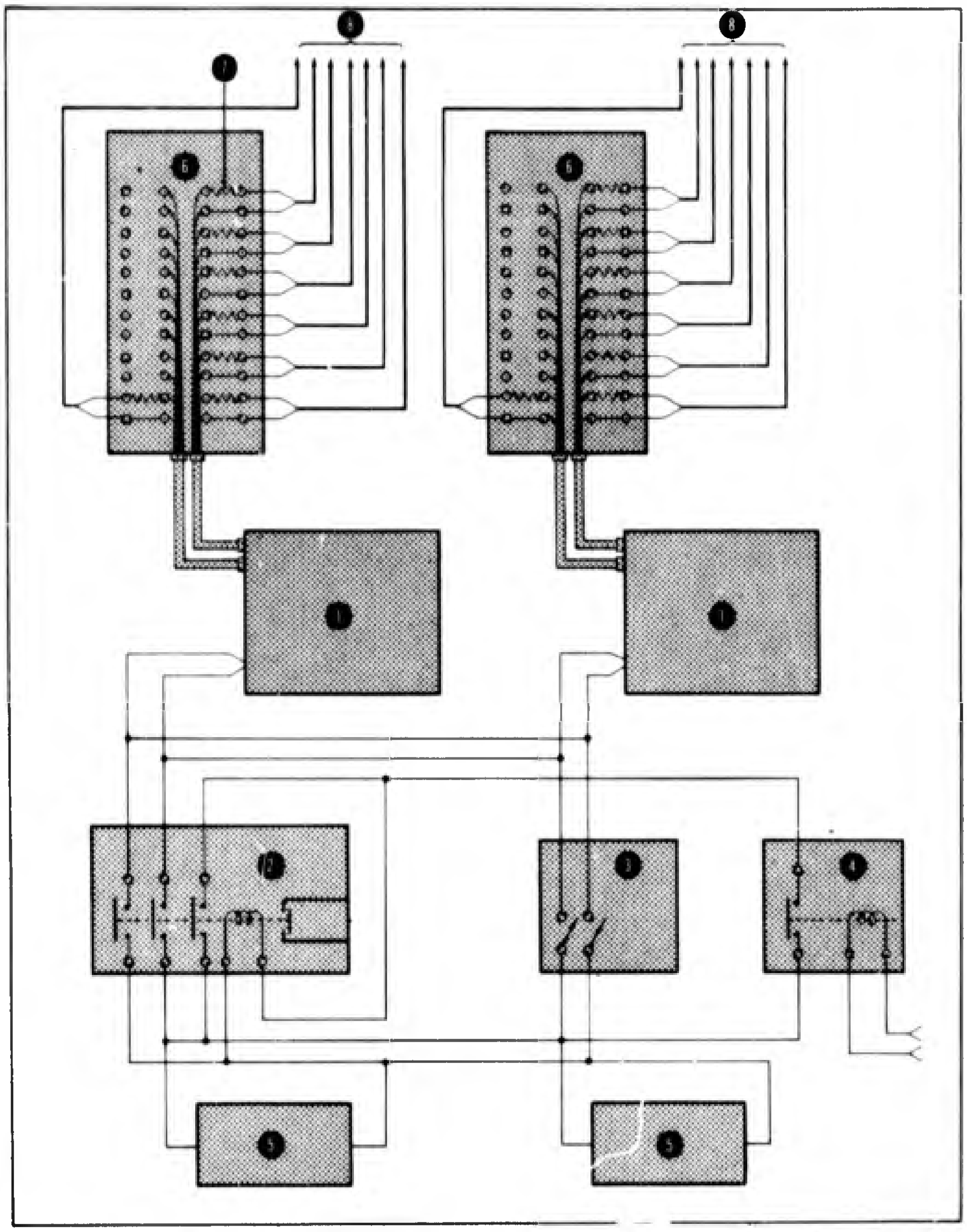

1. 12-channel 24-v Heiland Oscillograph Recorder
2. "Agastat" Time Delay Relay
3. Recorder Test Switch
4. "EG&G" Signal Relay
5. 24-v, 51-amp-hr Batteries
6. Recording Circuit Junction Boxes
7. Impedance Matching Resistors
8. DHFTA-9 No. 10 Cables to Calorimeters

Fig. 2.11 Circuit Diagram of Typical Instrument Station

A view of a typical grade-level installation is given in Fig. 2.12. The mounting of the instruments at the 10- and 50-ft elevations on the tower is shown in Figs. 2.13 and 2.14, respectively. An over-all view of the complete installation is given in Fig. 2.15. In this figure the ground installation can be seen in the lower right hand corner.

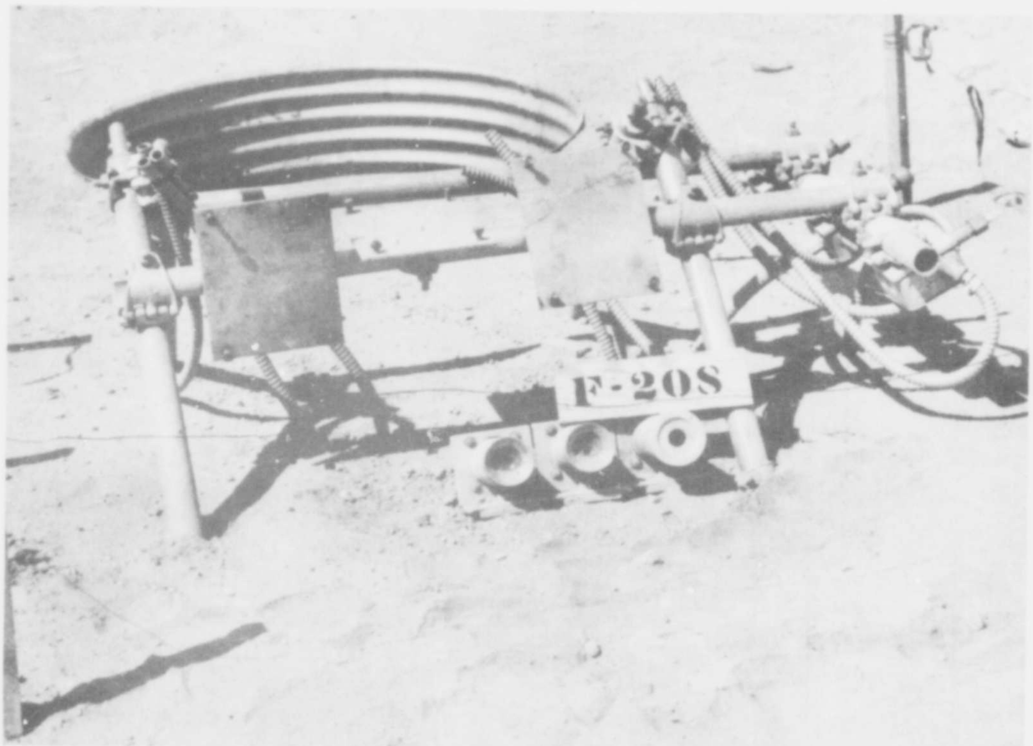

Fig. 2.12 Typical Ground Level Installation

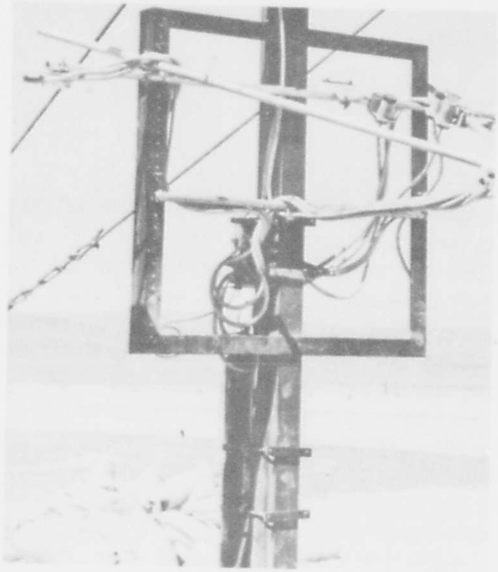

Fig. 2.13 Typical 10-ft Installation

Fig. 2.14 Typical 50-ft Installation

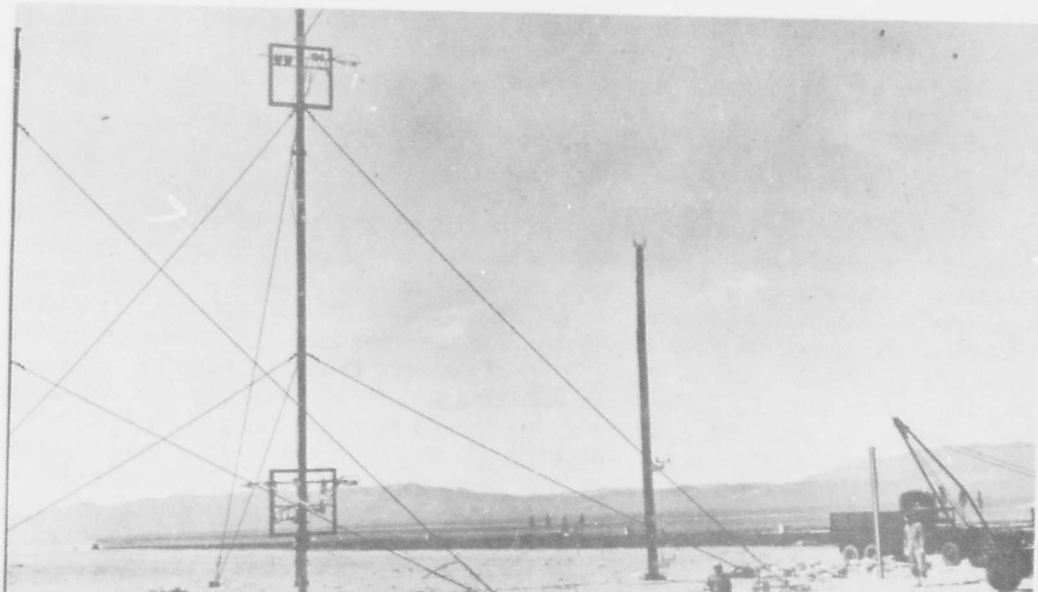

Fig. 2.15 Typical Station

CHAPTER 3

CALIBRATION

3.1 GENERAL

The procedures used to calibrate the field instruments were of two essentially independent types: thermal and electrical. The thermal calibrations concerned the thermal properties of the measuring instrument itself, and were usually made by a comparison of the response of the instrument being calibrated with the known response of another instrument or laboratory standard. This comparison could involve visual observation of damage, as in the case of the passive receivers, or measurement of thermoelectric output, as in the case of the disk calorimeter or radiometer. Since there was little likelihood of a change in the thermal properties of the instruments after assembly, the thermal calibrations were generally performed in the laboratory, both before and after the field phases of the operation, with some check calibrations in the field.

In the case of the disk calorimeters and the radiometers, the thermal pulse generates an electrical signal. This signal is carried by a circuit and recorded by a galvanometer which is not part of the detection device. An electrical calibration is necessary in addition to the thermal calibrations. The electrical calibration took into account the characteristics of the electrical circuit used to record the thermoelectric signal generated by the particular detection device. Consequently, this type of calibration was performed in the field using the circuits that were used during the test itself.

3.2 THERMAL CALIBRATIONS

The laboratory source and apparatus used for the thermal calibration of the instruments have been previously described[2,3]. Briefly, the exposure equipment consists of a Navy 36-in. searchlight as a source of nearly parallel radiation, and a second searchlight mirror to collect this parallel radiation and bring it to a focus to form an image of the carbon. Exposure times are controlled either by a high-speed air shutter[9], or by using a sweeping technique, i.e., by rotating the source so that the focused image sweeps past the exposure aperture. Primary measurements of the energy delivered by the source were made with an absolute water-flow calorimeter[12]. The source was then used to calibrate certain secondary calorimeters[11], similar in design to those used in the field. A further check is obtained by comparing the experimental calibration of the secondary calorimeters with theoretical calculations based upon geometrical considerations and the properties of the calorimeter receiver.

 UNCLASSIFIED

All of the instruments were given check calibrations in the field using a portable calibrator consisting of a 1,500-w Wolfram projection lamp and a 29-cm elliptical mirror with foci at 16 and 25 cm from its vertex[5]. This portable calibrator was also used for the primary calibration of some of the USNRDL disk radiometers.

3.3 ELECTRICAL CALIBRATIONS

Since it is impossible to set up in advance exact duplicates of the unknown field circuits, it becomes necessary to make electrical calibrations in the field. Because of the vast number of circuits to be calibrated in a limited time and with limited personnel, the Instruments Branch, Nucleonics Division, USNRDL, was asked to construct a calibration set that would maintain a high degree of accuracy under the strain of rough handling and field conditions.

The test set provided was capable of both the measurement of resistance, with a bridge circuit, and the generation of voltage signals from a low-impedance voltage generator. The set consisted of a Leeds and Northrup 24-ohm galvanometer, a Standard cell, a Burgess 1-1/2-v dry cell, and necessary switches and resistors. One circuit provides voltage signals of 1, 2, 3, 4, 5, 10, 20, and 30 mv with an accuracy of 0.005 mv for an external resistance range of 20 to 110 ohms. A second circuit consists of a resistance bridge capable of an accuracy of 0.1 ohm over a range from 0 to 100 ohms. The voltage generation circuit is used for calibration purposes and the resistance bridge for the adjustment of circuit resistances to obtain proper damping for the galvanometer used for recording the signal. A circuit diagram is shown in Fig. 3.1.

For circuit calibration, the field circuit was opened in the junction box, and the test leads attached so that the test set was connected in series in the circuit. The Heiland recorder was started and a calibration performed. This same procedure was followed for the other circuits of the recorder until all 12 circuits had been calibrated, the total process taking a little more than 10 min. Use of the test set made it possible to make calibrations in a short interval of time, an advantage that was particularly suited for the highly radioactive areas encountered in check calibrations made on the recovery trips following a detonation.

After the recording paper was developed, the calibrations were easily identified and measured. A typical set of calibrations takes about 10 ft of recorder paper and can thus be run on the same roll of paper that is used during the actual test. The individual circuit calibration gives the deflection of the galvanometer produced by the voltage applied to the actual field circuit. For each circuit, the set of calibrations gives the degree of linearity of scale over the range of voltages to be encountered during the detonation. A typical calibration trace is shown in Fig. 3.2.

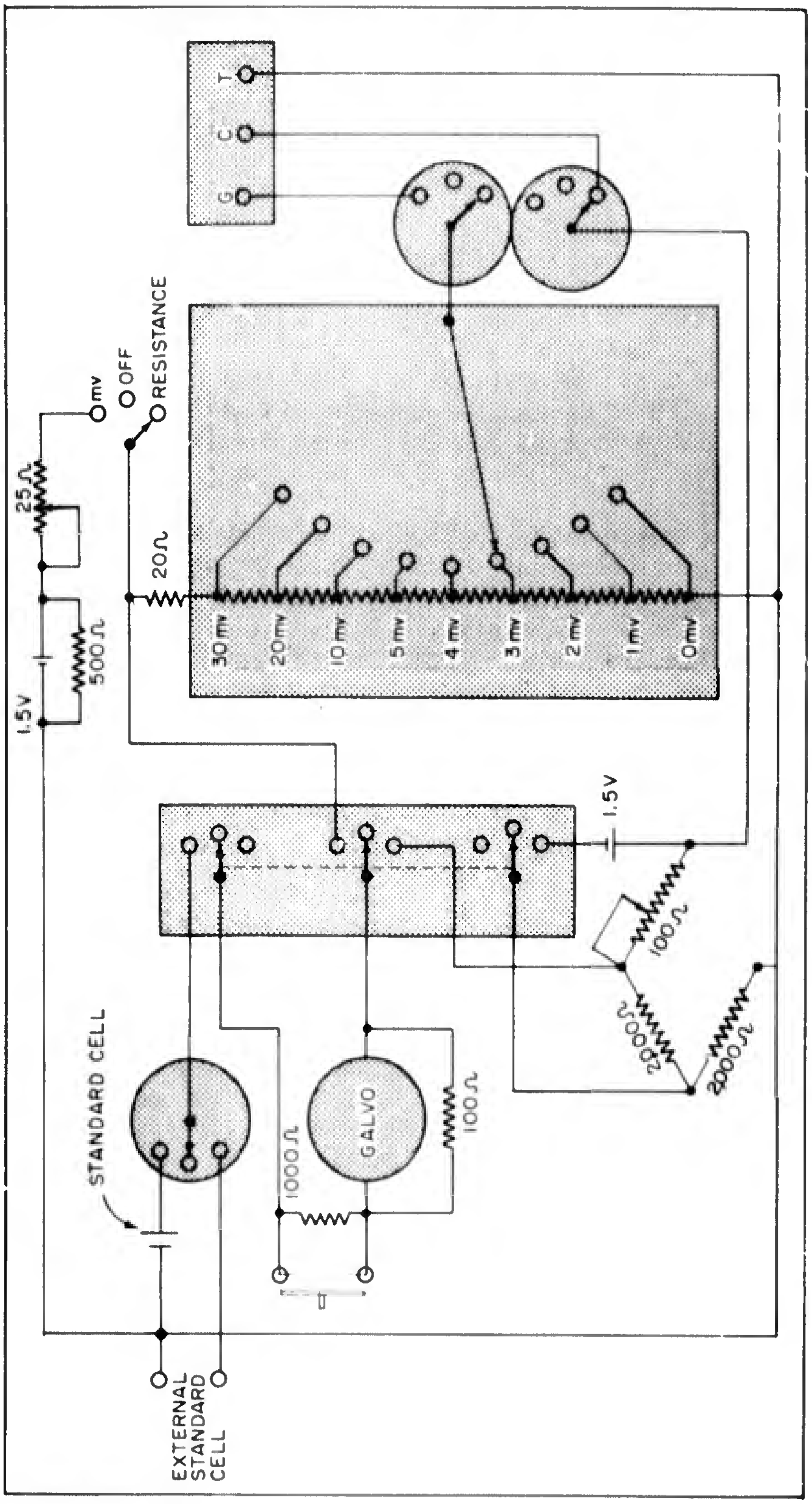

Fig. 3.1 Wiring Diagram of Electrical Test Set

3.4 FIELD CALORIMETERS

The 36-in. searchlight source has a high degree of convergence (cone of approximately 60° half-angle). The geometry of the calibrating equipment necessitated exposure of the receiving disk of the field calorimeter with filter removed. A further complication introduced by the high convergence was the fact that exposure of the field calorimeters, especially those with thick receivers, directly to this beam would result in a fairly large amount of energy striking the edges of the receivers. In order to eliminate the necessity for correcting for edge effects, a new aperture plate was designed for the Mark VI laboratory secondary calorimeter which would also accommodate the field calorimeters. The aperture diameter and the aperture-receiver spacing were adjusted so that all the energy passing through the aperture hit the front surface of the receiver in both the laboratory and field instruments. The calibration factor of the field calorimeter is:

$$k \text{ (cal/sq cm/mv)} = \frac{A_1}{A_2} \cdot \frac{V_1}{V_2} \cdot k_1,$$

where A_1 = Area of Mark VI aperture when calibrated against absolute water-flow calorimeter (sq cm),
A_2 = Area of field calorimeter receiver (sq cm),
V_1 = Signal from Mark VI when exposed to beam (mv),
V_2 = Signal from field calorimeter when exposed to beam (mv), and
k_1 = Calibration constant of Mark VI (cal/sq cm/mv).

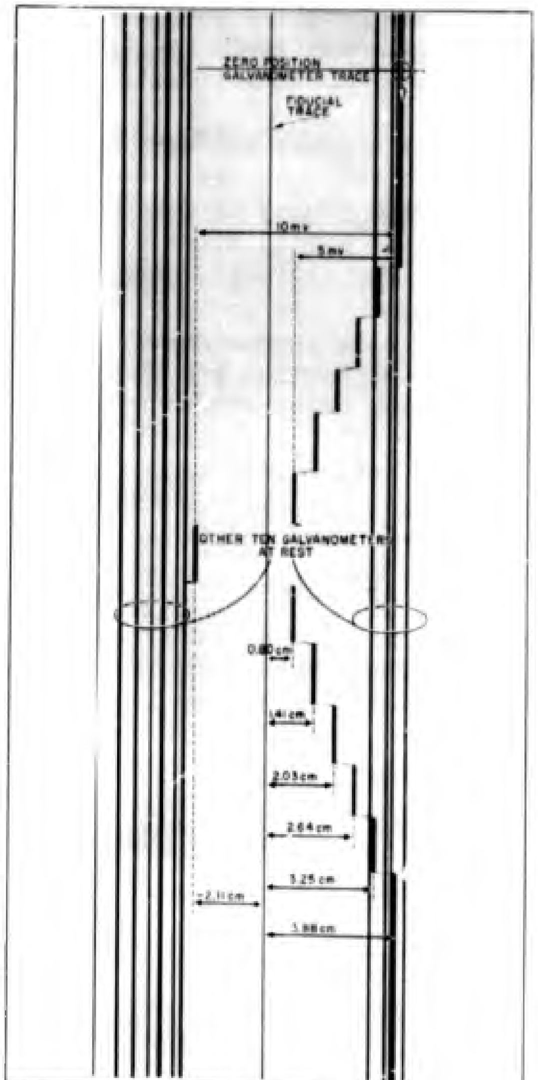

CALORIMETER CALIBRATION SHEET

RECORDER NO ______ STATION NO ______ SHOT NO ______

	FIDUCIAL	MV	2 MV	3 MV	4 MV	5 MV	10 MV	MEAN	MV/CM
READING	3.88	3.25	2.64	2.03	1.41	0.80	-2.11		
DELTA		0.63	1.24	1.85	2.47	3.08	5.99		
CM/MV		0.63	0.61	0.62	0.62	0.62	0.60	0.61	1.64

Fig. 3.2 Sample Calibration Record Obtained with Test Set

It is evident from the equation that this type of calibration necessitates an accurate measurement of the receiver area. However, it is felt that this measurement can be made much more accurately than any type of correction for edge effects.

The signals produced by both the laboratory and field calorimeters were recorded, through a voltage divider, on a Brown Electronik Potentiometer with ranges of 0 - 0.5 and 0 - 2.5 mv. In order to keep the decay corrections small, exposure times of 1 sec or less were used on all but the thickest (125-mil) disks, for which an exposure time of 2 sec was used. As the pen speed of the recorder was such that the pen would travel full scale in approximately 3.3 sec, the voltage divider was adjusted so that the deflection was about 1/3 full scale. Using this technique, equilibrium temperatures were established and recorded in a little over 1 sec for all cases except the thickest disks. The decay corrections in the calibration were therefore never more than a few per cent. Each calorimeter was calibrated at two energy levels in order to determine the influence of the change of thermoelectric power with temperature.

In addition to the experimental calibration, a theoretical calibration was made by weighing each disk and measuring the thermoelectric output of the thermocouple wire used. From this data, and taking the heat capacity of copper as 0.093 cal/g/°C and an absorptivity of 1 for the blackened face, the theoretical calibration factor was obtained from the formula:

$$k \text{ (cal/sq cm/mv)} = \frac{MC}{AE},$$

where M = Mass of receiver (g),
A = Area of receiver (sq cm),
C = Heat capacity of copper (cal/g/°C), and
E = Average thermoelectric power of the copper-constantan thermocouple over applicable temperature range (mv/°C).

Table 3.1 gives the results of the experimental and theoretical determination of the calibration factor. Columns 2 and 3 give the experimentally-determined calibration factor for the two energy levels. Columns 4 and 5 give the experimental calibration factor per gram, and columns 6 and 7 give the theoretically-calculated calibration factor per gram using an average thermoelectric power over the temperature rise produced by the two energy levels. Columns 8 and 9 are the ratios of the experimental to the theoretical calibration factors. It can be seen that in no case is there as large a difference as 10 per cent between the experimental and theoretical factors and on the average the difference is only a few per cent. Column 10 is the average experimental calibration factor used.

TABLE 3.1

Thermal Calibration Factors for Disk Calorimeters

Cal. No.	Exp. Calib. Factor (cal/sq cm/mv)		Exp. Calib. Factor per Gram of Receiver (cal/sq cm/mv/g)		Theo. Calib. Factor per Gram of Receiver (cal/sq cm/mv/g)		Ratio of Exp. to Theo. Calib. Factor		Av. Exp. Calib. Factor (cal/sq cm/mv)
	High Energy[a]	Low Energy[b]	High Energy	Low Energy	High Energy	Low Energy	High Energy	Low Energy	
Red 2	5.28	5.97	2.64	2.98	2.86	3.00	0.92	0.99	5.62
3	5.67	6.01	2.67	2.84	2.86	3.00	0.93	0.96	5.84
4	5.67	6.22	2.82	3.10	2.86	3.00	0.99	1.03	5.95
5	5.92	6.24	2.75	2.90	2.86	3.00	0.96	0.97	6.08
8	5.64	5.81	2.74	2.82	2.86	3.00	0.96	0.94	5.72
9	5.79	6.25	2.73	2.95	2.86	3.00	0.96	0.98	6.02
10	5.43	6.18	2.62	2.98	2.86	3.00	0.92	0.99	5.80
12	5.64	6.18	2.71	2.97	2.86	3.00	0.95	0.99	5.91
13	5.58	5.91	2.66	2.81	2.86	3.00	0.93	0.94	5.74
14	5.33	5.60	2.68	2.82	2.86	3.00	0.94	0.94	5.47
15	5.38	5.51	2.65	2.72	2.86	3.00	0.93	0.91	5.45
16	5.22	5.32	2.73	2.79	2.86	3.00	0.96	0.93	5.27
						Av---	0.95	0.96	--
Black 1	3.15	3.32	3.06	3.22	3.00	3.11	1.02	1.04	3.24
2	3.21	3.40	3.11	3.30	3.00	3.11	1.04	1.06	3.30
4	3.03	3.17	2.94	3.07	3.00	3.11	0.98	0.99	3.10
5	3.01	3.11	2.90	2.99	3.00	3.11	0.97	0.96	3.06
7	3.19	3.20	3.07	3.08	3.00	3.11	1.02	0.99	3.20
8	3.15	3.20	3.06	3.10	3.00	3.11	1.02	1.00	3.18
9	3.14	3.10	3.08	3.04	3.00	3.11	1.03	0.98	3.12
						Av---	1.01	1.00	--
White 1	1.43	1.44	2.82	2.84	2.93	3.11	0.96	0.91	1.44
2	1.46	1.53	2.87	3.01	2.93	3.11	0.98	0.97	1.50
3	1.45	1.55	2.82	3.02	2.93	3.11	0.96	0.97	1.50
4	1.45	1.62	2.85	3.18	2.93	3.11	0.97	1.02	1.54
5	1.42	1.49	2.77	2.91	2.93	3.11	0.95	0.94	1.46
						Av---	0.96	0.96	--
Grey 1	1.16	1.15	3.00	2.98	2.82	3.06	1.06	0.97	1.16
2	1.18	1.18	2.96	2.96	2.82	3.06	1.05	0.97	1.18
3	1.09	1.13	2.82	2.93	2.82	3.06	1.00	0.96	1.11
4	1.13	1.20	2.90	3.08	2.82	3.06	1.03	1.01	1.16
5	1.07	1.10	2.77	2.85	2.82	3.06	0.98	0.95	1.08
6	1.18	1.24	2.99	3.14	2.82	3.06	1.06	1.03	1.21
7	1.12	1.14	2.90	2.95	2.82	3.06	1.03	0.96	1.13

TABLE 3.1 (Continued)

Thermal Calibration Factors for Disk Calorimeters

Cal. No.	Exp. Calib. Factor (cal/sq cm/mv)		Exp. Calib. Factor per Gram of Receiver (cal/sq cm/mv/g)		Theo. Calib. Factor per Gram of Receiver (cal/sq cm/mv/g)		Ratio of Exp. to Theo. Calib. Factor		Av. Exp. Calib. Factor (cal/sq cm/mv)
	High Energy[a]	Low Energy[b]	High Energy	Low Energy	High Energy	Low Energy	High Energy	Low Energy	
8	1.14	1.17	3.00	3.08	2.82	3.06	1.06	1.01	1.16
9	1.11	1.22	2.79	3.06	2.82	3.06	0.99	1.00	1.16
10	1.16	1.23	2.93	3.11	2.82	3.06	1.04	1.02	1.20
11	1.19	1.15	3.06	2.96	2.82	3.06	1.09	0.97	1.17
12	1.11	1.18	2.85	3.03	2.82	3.06	1.01	0.99	1.14
13	1.10	1.16	2.85	3.00	2.82	3.06	1.01	0.98	1.13
14	1.14	1.18	2.95	3.06	2.82	3.06	1.05	1.00	1.16
						Av---	1.03	0.98	--
Brass 1	0.94	0.98	2.99	3.12	3.04	3.20	0.98	0.98	0.96
3	0.97	1.10	3.05	3.46	3.04	3.20	1.00	1.08	1.04
6	0.95	1.02	3.06	3.28	3.04	3.20	1.01	1.02	0.98
8	0.93	0.93	2.99	2.99	3.04	3.20	0.98	0.93	0.93
						Av---	0.99	1.00	--

(a) The high energies delivered were 23, 12, 7, 7, and 7 cal/sq cm for the Red, Black, White, Grey, and Brass calorimeters, respectively.

(b) The low energies delivered were 11, 7, 3, 3, and 3 cal/sq cm for the Red, Black, White, Grey, and Brass calorimeters, respectively.

As can be seen from Table 3.1 the calibration factor is not constant, owing to the slight change in thermoelectric power with temperature. Practically, however, the use of an average value leads to no appreciable error over the limited temperature range normally covered by the calorimeters. In those few cases where abnormally small or large signals were obtained, a small correction was applied on the basis of the experimentally-determined thermoelectric power.

3.5 RADIOMETERS

Only the MIT-3 radiometer was calibrated with the laboratory thermal source, as the other radiometers were not completed until after departure for the field. The other radiometers were calibrated between Shots 2 and 3 using the portable calibrator. The voltage on the calibrator was maintained at a constant value and the calibration factors were determined by taking the ratio of the deflections of the various radiometers to the deflection obtained by the MIT-3. The results of the disk radiometer calibrations are shown in Table 3.2.

TABLE 3.2

Calibration Factors for Disk Radiometers (Field)

Instrument	Calibration Factor (cal/sq cm/sec/mv)
MIT-3	2.9[a]
USNRDL K-1	5.9
USNRDL K-2	2.8
USNRDL K-3	4.8
USNRDL K-5	2.9
USNRDL K-8	3.3

(a) Obtained using laboratory source.

3.6 PASSIVE RECEIVERS

To use the series of blackened metal foils as a measuring device it is necessary to be able to assign a value to the energy pulse which is bracketed by two foils in a series. This value may be determined in one of two ways, neither of which is as simple as may appear at first glance. The first method, a theoretical approach, is to calculate, using known constants of the metal and heat transfer equations, the energy necessary to produce a given effect upon any foil. To date, the appropriate equations and constants are not sufficiently well known to allow much faith in calculations of this type. The other method, an empirical approach, involves the measurement of effects on foils using a known source of thermal radiation. This procedure is strictly accurate only if all important parameters in both the calibrating exposure and the measurement exposure are carefully controlled.

A discussion of current estimates of the importance of the various parameters may be found in the report on Operation GREENHOUSE. Perhaps the most important variable which has not been eliminated, and which has been found to affect seriously the quantity of thermal energy necessary to produce a certain effect on a metal foil, is the time in which this energy is received. For each effect on a given metal foil there exists not only one critical energy, but a curve of critical energy vs time. Before a series of foils could be used to determine a unique energy value, for an unknown radiant energy pulse, it would be necessary to obtain the time and shape of this pulse.

The passive receivers were calibrated in the laboratory by exposure to the 36-in. searchlight source. Calibration curves showing critical energy vs time of exposure, as defined in the Operation GREENHOUSE report, were obtained for all thicknesses of the five metals used. The critical effects were selected on the basis of reproducibility and ease of determination.

The criteria for threshold, as previously determined during calibration, were first surface-melt for cadmium, and first melt-through for the other metals. For the three-legged disks, surface-melt was substituted for melt-through as the criterion for tin. Distortion of the edge of the strip had been chosen as the silver-strip threshold. Application of these criteria to damage produced by the incident radiation, in the laboratory and in the field, enable an estimation to be made of the energy received by the series of foils during the detonation.

CHAPTER 4

RESULTS

4.1 GENERAL

After each detonation the shot area was re-entered at the earliest moment following clearance by the Radiological Safety group. The recorder paper and foil panels were recovered, and the readings on the sphere calorimeters were recorded.

Some loss of data occurred because of the unsatisfactory operation of two of the Heiland recorders. For Shot 1, one of the recorders used at Station 202 failed to operate, and a second operated intermittently. In the case of Shot 2, one of the recorders used for Station 204 failed to operate satisfactorily. Since this was the same recorder that operated intermittently during Shot 1, it was replaced prior to Shot 3 by a new one, procured from the Heiland Research Corporation. All of the recorders operated satisfactorily on Shots 3 and 4. Very little usable data were obtained at Station 7-202, Shot 4, as the shock wave completely destroyed the station. No electrical pickup of magnitude sufficiently high to negate total energy determinations was observed except at Station 7-202, Shot 2, where several types of cable were used as a check on the shielding protection afforded by the various types of cables. The pickup recorded at Station 7-204, Shot 4, however, was sufficiently high to render questionable the intensity-time curves from some of the calorimeters at this station.

4.2 CALORIMETERS

The data from the original Heiland tracings were obtained using the Universal Telereader. These data were used to plot intensity-vs-time curves and to obtain total energy values for each calorimeter. The total energy received by each calorimeter disk is given in Tables 4.1 through 4.4. In these tables, column 1 gives the station number, column 2 the slant range from point of detonation, column 3 the field of view of the calorimeter, column 4 the orientation, column 5 the angle from horizontal, column 6 the elevation, column 7 the calorimeter number, column 8 the type of filter used, column 9 the total energy received under the filter, and column 10 the total energy incident on the calorimeter in the wave length region defined by the filter used. The values reported in column 10 are obtained by making corrections to the values in column 9 for the transmission of the filters in the flat portions of their transmission curves. This correction amounted to about 8 per cent for quartz, 8 per cent for 9-54, 8 per cent for 0-52, 10 per cent for 3-69, 12 per cent for 2-58, and 12 per cent for 7-56.

TABLE 4.1

Calorimeter Results, Shot 1

Station	Slant Range (ft)	Half-angle of Field of View (deg)	Orientation[a]	Angle from Horizontal (deg)	Elevation (ft)	Cal. No.	Filter	Total Energy under Filter (cal/sq cm)	Total Energy Incident[b] (cal/sq cm)
F-202	970	45	AZ	+ 58	10	Red 3	Quartz	Recorder Failure	
	980	45	AZ	+ 58	0	Red 6	Quartz	Recorder Failure	
	980	45	AZ	+ 58	0	Red 5	Quartz	Recorder Failure	
	940	30	AZ	+ 58	50	Red 9	Quartz	42.6	46.3
	970	30	AZ	+ 58	10	Red 2	Quartz	Recorder Failure	
	980	30	AZ	+ 58	0	Red 4	Quartz	Recorder Failure	
	940	45	GR	- 58	50	Black 1	Quartz	7.0	7.6
	940	15	GR	- 58	50	Black 2	Quartz	0.59	0.64
F-208	2,210	45	AZ	+ 21	10	Grey 3	Quartz	8.0	8.7
	2,220	45	AZ	+ 21	0	Grey 6	Quartz	7.5	8.7
	2,220	45	AZ	+ 21	0	Grey 5	Quartz	6.9	7.5
	2,200	15	AZ	+ 21	50	Grey 1	Quartz	7.0	7.6
	2,210	15	AZ	+ 21	10	Grey 2	Quartz	6.7	7.2
	2,220	15	AZ	+ 21	0	Grey 4	Quartz	-0-	-0-
	2,200	45	GR	-21	50	Brass 1	Quartz	5.1[c]	5.5[c]
	2,200	15	GR	-21	50	Brass 8	Quartz	0.14	0.15

(a) AZ = Calorimeter aligned toward air zero. GR = Calorimeter aligned to measure radiation reflected from the ground in front of station.

(b) Not corrected for atmospheric attenuation.

(c) Field of view included part of the fire ball energy as well as the energy reflected from the ground.

TABLE 4.2

Calorimeter Results, Shot 2

Station	Slant Range (ft)	Half-angle of Field of View (deg)	Orientation[a]	Angle from Horizontal (deg)	Elevation (ft)	Cal. No.	Filter	Total Energy under Filter (cal/sq cm)	Total Energy Incident[b] (cal/sq cm)
7-202	1,760	45	AZ	+ 36	10	White 4	Quartz	11.9	12.9
	1,760	45	AZ	+ 36	10	White 1	Quartz	11.2	12.2
	1,760	45	AZ	+ 36	10	White 5	Quartz	10.5	11.4
	1,760	45	AZ	+ 36	10	White 3	Quartz	Galvanometer burn-out	
7-204	3,070	45	AZ	+ 20	10	Grey 5	Quartz	3.7	4.0
	3,080	45	AZ	+ 20	0	Brass 3	Quartz	4.1	4.5
	3,080	45	AZ	+ 20	0	Grey 2	Quartz	3.9	4.3
	3,080	45	AZ	+ 20	0	Grey 1	Quartz	4.0	4.4
	3,050	15	AZ	+ 20	50	Brass 8	Quartz	3.2	3.5
	3,050	45	GR	-57	50	Brass 1	Quartz	0.27	0.29

(a) AZ = Calorimeter aligned toward air zero. GR = Calorimeter aligned to measure radiation reflected from the ground in front of station.

(b) Not corrected for atmospheric attenuation.

TABLE 4.3

Calorimeter Results, Shot 3

Station	Slant Range (ft)	Half-angle of Field of View (deg)	Orientation[a]	Angle from Horizontal (deg)	Elevation (ft)	Cal. No.	Filter	Total Energy under Filter (cal/sq cm)	Total Energy Incident[b] (cal/sq cm)
7-202	3,440	45	AZ	+66	10	Red 11	Quartz	31.7	34.5
7-204	4,500	45	AZ	+48	10	Red 12	Quartz	36.9	40.1
	4,510	45	AZ	+48	0	Red 14	Quartz	31.7	34.5
	4,510	45	AZ	+48	0	Red 15	Quartz	30.8	33.5
	4,470	15	AZ	+48	50	Red 9	Quartz	34.6	37.7
	4,500	15	AZ	+48	10	Red 4	Quartz	31.7	34.5
	4,510	15	AZ	+48	0	Red 13	Quartz	13.0	14.1
	4,470	45	GR	-50	50	Black 3	Quartz	0.57	0.62
	4,470	15	GR	-50	50	Black 4	Quartz	0.37	0.40
7-208	6,810	45	AZ	+29	50	Black 6	Quartz	17.8	19.4
	6,830	45	AZ	+29	0	Black 2	Quartz	16.6	18.1
	6,830	7.5	AZ	+29	10	Black 7	Quartz	9.9	10.8
	6,830	7.5	AZ	+29	0	Black 1	Quartz	7.6	8.3
	6,810	45	GR	-50	50	Black 5	Quartz	1.7	1.9
7-210	9,530	45	AZ	+20	10	White 1	Quartz	8.3	8.9
	9,530	45	AZ	+20	10	White 3	Quartz	0.78	0.84
						White 4[c]	0-52		
	9,530	45	AZ	+20	10	Grey 7	3-69	5.7	6.3
	9,530	45	AZ	+20	10	Grey 8	2-58	4.3	4.9
	9,530	45	AZ	+20	10	Brass 3	Spec.	2.8	3.9
	9,530	45	AZ	+20	10	Brass 8	7-56	2.0	2.3
USFS	18,300	30	AZ	+10	3	Grey 12	Quartz	2.0	2.2
	18,300	30	AZ	+10	3	Brass 1	Quartz	2.0	2.2
	18,300	30	AZ	+10	3	Grey 6+13	Quartz	---	---

(a) AZ = Calorimeter aligned toward air zero. GR = Calorimeter aligned to measure radiation reflected from the ground in front of station.

(b) Not corrected for atmospheric attenuation.

(c) Calorimeters connected in series but with opposite polarity.

TABLE 4.4

Calorimeter Results, Shot 4

Station	Slant Range (ft)	Half-angle of Field of View (deg)	Orienta-tion[a]	Angle from Horizontal (deg)	Elevation (ft)	Cal. No.	Filter	Total Energy under Filter (cal/sq cm)	Total Energy Incident[b] (cal/sq cm)
7-202	1,700	45	AZ	+38	10	Red 11	Quartz	63.4[c]	69.0[c]
7-204	3,010	45	AZ	+21	10	Red 12	None	50.3	50.3
	3,020	45	AZ	+21	0	Red 14	Quartz	39.6	43.2
	3,020	45	AZ	+21	0	Red 15	Quartz	40.1	43.6
	2,990	30	AZ	+21	50	Red 9	Quartz	53.2	57.8
	3,010	15	AZ	+21	10	Red 4	Quartz	51.6	56.2
	3,020	15	AZ	+21	0	Red 13	Quartz	24.3	26.5
	2,990	45	GR	-50	50	Black 3	Quartz	Bad record	
	2,990	15	GR	-50	50	Black 4	Quartz	0.15	0.16
7-208	5,890	45	AZ	+11	50	Black 6	Quartz	15.5	16.9
	5,920	45	AZ	+11	0	Black 2	Quartz	14.0	15.2
	5,910	30	AZ	+11	10	Black 7	Quartz	15.0	16.3
	5,920	7.5	AZ	+11	0	Black 1	Quartz	5.6	6.1
	5,890	45	GR	-50	50	Black 5	Quartz	0.8	0.9
7-210	8,900	45	AZ	+ 7	10	White 1	Quartz	6.3	6.8
	8,900	45	AZ	+ 7	10	White 3	Quartz	0.61	0.67
						White 4[d]	0-52		
	8,900	45	AZ	+ 7	10	Grey 7	3-69	4.3	4.8
	8,900	45	AZ	+ 7	10	Grey 8	2-58	3.3	3.8
	8,900	45	AZ	+ 7	10	Brass 3	Spec.	2.1	2.9
	8,900	45	AZ	+ 7	10	Brass 8	7-56	1.5	1.7
USFS	18,000	30	AZ	+ 3.5	3	Grey 12	Quartz	1.4	1.5
	18,000	30	AZ	+ 3.5	3	Brass 1	Quartz	1.4	1.5
	18,000	30	AZ	+ 3.5	3	Grey 6+13	Quartz	---	---

(a) AZ = Calorimeter aligned toward air zero. GR = Calorimeter aligned to measure radiation reflected from the ground in front of station.

(b) Not corrected for atmospheric attenuation.

(c) Total energy received up to arrival of shock wave, at 0.58 sec.

(d) Calorimeters connected in series but with opposite polarity.

These tables list only the results of measurements made by USNRDL personnel along the blast line. Results of the measurements made in cooperation with Project 3.1 personnel, in connection with the thermal damage to parked aircraft, are given in Appendix A. Results of the measurements made in cooperation with the 4925th Air Bombardment Group, in connection with the thermal energy incident upon the drop aircraft, are given in Appendix B.

4.3 RADIOMETERS

The original Heiland records were read with the Universal Telereader.

An intensity-vs-time curve was plotted for each radiometer, and in the case of the foil radiometers, was integrated to obtain the total energy. No integration was carried out for the fine-wire radiometer curves because these instruments were not calibrated.

The total energy values were obtained by integration of the intensity-vs-time curves from 0 to 2 sec. The 2-sec interval was chosen because at the end of 2 sec, for the weapons of the size concerned, the intensity has decreased to a small fraction of the peak intensity, and carrying the integration to longer times increases the uncertainties in the reduction of data, but adds little information of importance.

The radiometer results are listed in Table 4.5. Column 7 of the table gives the maximum intensities, and column 8 the total energies received in the time interval from 0 to 2 sec. For comparison purposes, similar data are given in columns 9 and 10 for the calorimeters at the same locations. In general, the agreement between the calorimeter and radiometer results is quite good, and in only one case did the values differ by more than the experimental error of the radiometers, which is about 15 per cent.

TABLE 4.5

Disk Radiometer Results[a]

Shot	Station	Height (ft)	Filter	Half-angle of Field of View (deg)	Instrument Type	Maximum Intensity, Radiometers (cal/sq cm/sec)	Total Energy to 2.0 sec, Radiometers (cal/sq cm)	Maximum Intensity, Calorimeters (cal/sq cm/sec)	Total Energy to 2.0 sec, Calorimeters (cal/sq cm)
1	F-208	10	Quartz	45	K	20	8.0	22	8.0
2	7-204	10	Quartz	45	K	11	4.4	10	3.9
	7-204	10	Quartz	45	MIT	10	3.5	10	3.9
3	7-202	3	2-58	45	K	43	25	--	---(b)
	7-202	3	2-58	45	K	Burn out		--	---
	7-204	10	Quartz	45	K	Off scale		79	31
	USFS	3	Quartz	24	K	5.4	2.0	4.3	1.7
	USFS	3	Quartz	24	MIT	4.7	1.6	4.3	1.7
4	7-204	10	Quartz	45	K	Burn out		120	48
	USFS	3	Quartz	24	K	3.9	1.4	3.8	1.2
	USFS	3	Quartz	24	MIT	3.6	1.2	3.8	1.2

(a) Not corrected for filter or atmospheric attenuation.

(b) No energy values given for calorimeter because presence of serious dust obscurations at this station would make any comparison of little value.

4.4 PASSIVE RECEIVERS

The panels of metal foils recovered after the shots were returned to the Laboratory, and a careful assessment made of the damage produced to each foil. In all cases, the panels were read independently by three observers. Each observer recorded the thicknesses of metal which bracketed the chosen effect, and, from the degree of melt of the thinner of the two, estimated and recorded that thickness which would have shown the threshold criterion. The mean value for each indicator was then determined from the three thickness estimates.

The field pulse time was obtained from the calorimetry data by approximating the rise and fall portions of the field pulse with straight lines, without changing the total energy or the peak intensity, and reading the time between the two abscissa intercepts. The energies were then obtained directly from the foil calibration curves. Tables 4.6, 4.7, 4.8, and 4.9 give results of the passive-receiver panels. In these tables column 8 is the energy received under the filter and 9 is the total energy received at the station. This value is obtained by correcting column 7 for the peak transmission of the two filters used (Corning No. 0-52 and 9-54). In addition a correction of approximately 10 per cent was added to the energy values obtained by the foils under the 0-52 filters for the energy lost below 0.36 μ, which is the lower wave length cut-off of the filter.

TABLE 4.6

Passive-receiver Results, Shot 1

Station	Slant Distance (ft)	Height above Grade (ft)	Angle from Horizontal (deg)	Metal	Indicated Total Energies (cal/sq cm)			Energy at Station (cal/sq cm)
					Bracketing	Estimated	Mean Estimated	
Alignment: Facing Air Zero[a]								
200	802	2	90	Ag	38.2-4[illegible].4	41.9	43.3	47.1
				Cu	34.5-[illegible]4.4	41.9		
				Ag[b]	33.0-62.4	46.1		
202	940	50	56	Ag	33.2-45.4	38.2	41.3	44.9
				Cd	24.0-31.1	28.4		
				Pb	51.6-----	57.2		
202	970	10	58	Ag	33.2-45.4	38.2	39.5	42.9
				Cd	24.0-31.1	28.8		
				Pb	51.6-----	51.6		
202	980	2	58	Ag	13.8-80.1	56.2	43.3	47.1[c]
				Cd	18.7-31.1	27.2		
				Pb	31.9-51.6	46.5		
204	1,340	2	39	Cd	14.6-18.3	14.9	21.0	22.8
				Sn	24.1-30.2	28.3		
				Pb	18.9-24.2	19.7		
206	1,760	7	28	Cd	10.2-12.3	10.4	11.9	12.9
				Sn	13.3-----	13.2		
				Pb	11.2-14.6	12.1		
208	2,200	50	21	Cd	7.3- 9.0	7.4	7.5	8.1
				Sn	6.9- 9.3	8.7		
				Pb	6.3- 8.5	6.3		
208	2,210	10	22	Cd	5.9- 7.3	5.9	7.0	7.6
				Sn	6.9- 9.3	8.3		
				Pb	6.3- 8.5	6.7		
208	2,220	2	22	Cd	5.9- 7.3	5.9	7.0	7.6
				Sn	6.9- 9.3	8.7		
				Pb	6.3- 8.5	6.3		

TABLE 4.6 (Continued)

Passive-receiver Results, Shot 1

Station	Slant Distance (ft)	Height above Grade (ft)	Angle from Horizontal (deg)	Metal	Indicated Total Energies (cal/sq cm) Bracketing	Estimated	Mean Estimated	Energy at Station (cal/sq cm)
210	3,170	2	15	Cd	2.7- 3.4	3.1	3.5	3.8
				Sn	3.2- 3.8	3.2		
				Pb	3.9- 5.2	4.1		
Alignment: Ground Reflection(d)								
202	940	50	-56	Cd	---	---	8.8	9.6
				Sn	9.3-13.3	10.6		
				Pb	6.0- 8.2	7.1		
208	2,200	50	-21	Cd	5.0-----	5.3	5.6	6.1
				Sn	6.0-----	6.0		
				Pb	5.2- 5.8	5.6		
Alignment: Panel Vertical(e)								
202	980	2	0	Cd	14.6-18.3	14.9	21.1	22.9
				Sn	24.1-30.2	24.2		
				Pb	24.2-27.4	24.2		
208	2,220	2	0	Cd	4.9- 5.9	5.8	7.1	7.7
				Sn	6.9- 9.3	8.7		
				Pb	6.4- 8.5	6.8		
Alignment: Panel Horizontal(f)								
202	930	2	90	Ag	25.9-33.2	29.6	28.9	31.1
				Cd	24.0-31.1	24.3		
				Pb	32.8-52.2	32.8		
208	2,220	2	90	Cd	0.9- 1.3	1.1	0.9	1.1
				Sn	---- 0.9	0.8		
				Pb	---- 1.1	0.7		

(a) Aligned facing the expected (not the actual) point of detonation.

(b) Strip geometry.

(c) Panel damaged by blast; thicknesses around threshold for silver and cadmium were missing.

(d) Aligned to measure radiation reflected from earth in front of station at specular angle.

(e) Aligned to measure radiation as received by a vertical surface.

(f) Aligned to measure radiation as received by a horizontal surface.

TABLE 4.7

Passive-receiver Results, Shot 2

Station	Slant Distance (ft)	Height above Grade (ft)	Angle from Horizontal (deg)	Metal	Indicated Total Energies (cal/sq cm) Bracketing	Estimated	Mean Estimated	Energy at Station (cal/sq cm)
Alignment: Facing Air Zero[a]								
200	1,120	2	90	Cd	23.9-32.5	24.4	30.2	36.1
				Sn	30.2-44.0	31.0		
				Pb	31.9-----	35.2		
201	1,280	2	58	Cd	18.3-18.7	18.7	20.8	24.9
				Sn	24.1-----	24.1		
				Pb	18.8-24.2	19.6		
202	1,770	2	36	Cd	9.0-10.3	9.0	11.3	13.5
				Sn	11.2-----	13.8		
				Pb	11.2-12.0	11.2		
204	3,080	2	20	Cd	2.0-----	3.0	3.5	4.2
				Sn	2.6-----	3.8		
				Pb	2.7-----	3.8		
206	4,510	2	14	Cd	1.2- 1.5	1.3	1.4	1.7
				Sn	1.3- 2.0	1.7		
				Pb	1.1- 1.8	1.1		
				Cd[b]	1.0- 1.3	1.1	1.3	
				Sn[b]	0.9- 1.3	1.1		
				Pb[b]	1.1- 1.7	1.6		

(a) Aligned facing the expected (not the actual) point of detonation.

(b) Three-legged disk geometry.

U[redacted]SIFIED

TABLE 4.8

Passive-receiver Results, Shot 3

Station	Slant Distance (ft)	Height above Grade (ft)	Angle from Horizontal (deg)	Metal	Indicated Total Energies (cal/sq cm) Bracketing	Estimated	Mean Estimated	Energy at Station (cal/sq cm)
Alignment: Facing Air Zero[a]								
202	3,450	2	90	Ag	48.9-65.0	54.3	49.7	59.4
				Cu	47.0-49.3	48.1		
				Ag[b]	44.8-86.2	46.6		
202	3,450	2	66	Ag	34.4-48.9	44.8	45.8	54.8
				Cu	38.4-47.0	42.9		
				Ag[b]	34.2-63.8	49.6		
204	4,470	50	47	Ag	26.9-28.2	27.7	26.0	28.3
				Cd	19.8-25.0	24.3		
				Pb	25.2-28.2	26.0		
204	4,500	10	47	Ag	26.9-28.2	27.9	25.6	27.8
				Cd	19.8-25.0	21.6		
				Pb	25.2-28.2	27.4		
204	4,510	2	48	Ag	26.9-28.2	27.7	24.2	26.3
				Cd	19.8-25.0	22.1		
				Pb	19.8-25.2	22.7		
206	5,590	2	36	Cd	12.9-15.3	14.7	15.5	18.5
				Sn	14.6-19.7	15.9		
				Pb	15.1-17.9	15.9		
208	6,810	50	29	Cd	----- 9.5	9.0	10.6	11.5
				Sn	9.5-13.4	11.6		
				Pb	11.1-15.1	11.1		
208	6,830	10	29	Cd	9.5-10.8	9.5	11.5	12.5
				Sn	13.4-13.7	13.4		
				Pb	11.1-15.1	11.5		
208	6,830	2	29	Cd	----- 9.5	9.0	10.6	11.5
				Sn	9.5-13.4	11.5		
				Pb	11.1-15.1	11.2		
210	9,540	2	20	Cd	5.3- 7.4	6.4	6.7	7.3
				Sn	5.6- 8.1	7.2		
				Pb	6.3- 6.7	6.5		
11,000	11,500	3	17	Cd	3.4- 4.5	3.4	4.1	4.9
				Sn	4.1- 5.6	4.1		
				Pb	4.0- 6.0	4.9		
12,000	12,400	3	15	Cd	2.9- 3.4	3.2	3.4	4.1
				Sn	3.0- 4.1	3.0		
				Pb	4.0- 5.2	4.0		
13,000	13,400	3	14	Cd	2.9- 3.4	3.0	3.2	3.6
				Sn	2.5- 3.0	2.6		
				Pb	3.7- 4.0	3.9		
16,000	16,300	3	12	Cd	1.6- 2.2	2.0	2.3	2.8
				Sn	1.5- 2.5	2.1		
				Pb	2.7- 3.7	2.7		

UN[redacted]IFIED
Security Information

[redacted]
ATOMIC ENERGY ACT 1946

TABLE 4.8 (Continued)

Passive-receiver Results, Shot 3

Station	Slant Distance (ft)	Height above Grade (ft)	Angle from Horizontal (deg)	Metal	Indicated Total Energies (cal/sq cm) Bracketing	Estimated	Mean Estimated	Energy at Station (cal/sq cm)
18,000	18,300	3	10	Cd	1.1- 1.6	1.3	1.6	1.9
				Sn	1.5- 2.5	1.5		
				Pb	2.0- 2.7	2.0		
18,000	18,300	3	10	Cd	1.1- 1.6	1.2	1.8	2.2
				Sn	1.5- 2.5	2.2		
				Pb	2.0- 2.1	2.0		
20,000	20,200	3	9	Cd	0.9- 1.1	1.1	0.9	1.4
				Sn	---- 1.1	0.8		
				Pb	---- 1.3	0.8		
				Cd(c)	1.6- ---	1.7	1.4	
				Sn(c)	1.0- 1.4	1.3		
				Pb(c)	1.1- 1.4	1.2		
(Special panel) 18,000	18,300	3	10	Cd(c)	1.9- 2.3	2.2	1.7	1.8
				Sn(c)	1.0- 1.4	1.1		
				Pb(c)	1.7- 2.0	1.8		
Alignment: Ground Reflection(d)								
204	4,470	50	-47	Cd	----- 5.9	---	---	6
				Sn	----- 5.4	---		
				Pb	----- 6.5	---		
208	6,810	50	-45	Cd	----- 3.4	3.1	2.4	2.6
				Sn	----- 2.5	1.5		
				Pb	----- 3.7	2.5		
Alignment: Panel Vertical(e)								
204	6,830	2	0	Ag	15.3-26.0	19.4	16.1	17.5
				Cd	12.9-15.3	14.9		
				Pb	12.1-15.1	13.9		
208	6,830	2	0	Cd	----- 9.5	9.0	9.1	9.9
				Sn	9.5-13.4	9.5		
				Pb	7.8-11.1	8.8		
Alignment: Panel Horizontal(f)								
204	4,510	2	90	Ag	26.0-26.9	26.4(g)	10.9	11.8
				Cd	-----12.9	11.5		
				Pb	-----12.1	10.3		
208	6,830	2	90	Cd	5.3- 6.6	5.4	4.5	4.9
				Sn	2.5- 3.0	2.9		
				Pb	4.0- 6.0	5.2		

(a) Aligned facing the expected (not the actual) point of detonation.
(b) Strip geometry.
(c) Three-legged disk geometry.
(d) Aligned to measure radiation reflected from earth in front of station at specular angle.
(e) Aligned to measure radiation as received by a vertical surface.
(f) Aligned to measure radiation as received by a horizontal surface.
(g) Reinforced by radiation reflected from aluminum faceplate and was not included in calculating total energy.

TABLE 4.9

Passive-receiver Results, Shot 4

Station	Slant Distance (ft)	Height above Grade (ft)	Angle from Horizontal (deg)	Metal	Indicated Total Energies (cal/sq cm) Bracketing	Estimated	Mean Estimated	Energy at Station (cal/sq cm)
Alignment: Facing Air Zero[a]								
200	1,060	2	90		Not recoverable			
200	1,060	2	90		Not recoverable			
202	1,700	2	38		Not recoverable			
202	1,700	2	38		Not recoverable			
204	3,020	2	21	Ag	33.2-45.4	42.2	41.1	49.2
				Cu	34.5-44.4	39.2		
				Ag[b]	33.0-62.4	41.8		
206	4,460	2	14	Ag	13.8-23.4	18.0	16.0	19.1
				Cd	14.4-18.3	14.9		
				Pb	14.6-18.9	15.0		
208	5,920	2	11	Cd	----- 9.0	8.5	9.2	11.0
				Sn	9.5-13.3	9.5		
				Pb	8.5-10.6	9.5		
210	8,900	2	7	Cd	3.4- 4.3	3.5	4.1	4.9
				Sn	3.7- 5.4	3.9		
				Pb	3.9- 5.8	5.0		
11,000	11,050	3	6	Cd	2.7- 3.4	3.0	2.6	3.1
				Sn	1.3- 2.0	1.7		
				Pb	2.7- 3.4	3.0		
12,000	12,040	3	6	Cd	1.5- 2.0	2.0	2.2	2.6
				Sn	2.0- 2.6	2.0		
				Pb	1.8- 2.7	2.6		
13,000	13,020	3	5	Cd	1.5- 2.0	1.8	1.8	2.2
				Sn	1.3- 2.0	1.7		
				Pb	1.8- 2.7	1.8		
14,500	14,500	3	4	Cd	1.3- 1.5	1.3	1.6	1.9
				Sn	1.3- 2.0	1.7		
				Pb	1.8- 2.7	1.8		
16,000	16,000	3	4	Cd	0.9- 1.3	1.1	1.1	1.3
				Sn	1.0- 1.3	1.2		
				Pb	---- 1.1	0.9		
18,000	18,000	3	4	Cd	0.9- 1.3	0.9	0.8	1.2
				Sn	---- 1.0	0.7		
				Pb	---- 1.1	0.8		
				Cd[c]	1.1- 1.3	1.2	1.1	
				Sn[c]	0.9- 2.0	1.0		
				Pb[c]	---- 1.0			
18,000	18,000	3	4	Cd	0.9- 1.3	0.9	0.8	1.1
				Sn	---- 1.0	0.7		
				Pb	---- 1.1	0.8		
				Cd[c]	1.1- 1.3	1.2	1.0	
				Sn[c]	0.9- 2.0	1.0		
				Pb[c]	---- 1.0	0.9		

(a) Aligned facing the expected (not the actual) point of detonation.
(b) Strip geometry.
(c) Three-legged disk geometry.

4.5 SPHERE CALORIMETERS

Unfortunately, no usable data were obtained from the sphere calorimeters. The results obtained were widely scattered and differed from the other measurements by as much as an order of magnitude. The biggest difficulty with these instruments seemed to be in the adjustment of the brake attached to the dial indicator. If this brake is made too loose, severe deflections are produced by the shock wave and if too tight, the indicator moves in spurts and low results are obtained.

CHAPTER 5

DISCUSSION OF RESULTS

5.1 CALORIMETERS

Generally speaking, the data obtained during these operations were about as expected. The total energy data obtained from the calorimeters during the four shots are shown in station-to-station comparisons in Figs. 5.1 through 5.4. The energy values represented as points in these figures were taken from column 10, Tables 4.1 through 4.4, and corrected for atmospheric attenuation, taking a transmission of 96 per cent per mile for Shots 1 and 2, and 95 per cent per mile for Shots 3 and 4. Only the data from those calorimeters which had the full field of view, unobscured by dust, were used for these plots. The lines have been drawn on the basis of the calorimeter data, but with the theoretical (inverse-square) slope.

The atmospheric transmission coefficients used were obtained by the Naval Research Laboratory (NRL)1/. They were specified for collimated or narrow beam conditions, and are therefore not strictly applicable to the wide-field-of-view calorimeters. According to E. O. Hulbert8/ "the effect of field of view of the receiver upon the energy received through the atmosphere from a point source at a distance is expressed by

$$R_A = R_c + g\ (1 - R_c)\ f\ (A) \qquad (5.1)$$

when R_c is the energy received by a receiver of very small (zero) field of view. R_c is calculated from the atmospheric attenuation coefficient for collimated light ..... . R_A is the energy received by the same receiver with circular field of view A radians in diameter, with axis pointing at the source. g depends on the reflectivity of the surface and f (A) on the polar diagram of scattering. From experiments with a source and a receiver on the surface of average reflectivity, for wave lengths 3600 to 6200Å, for v (visibility) about 5 to 50 km, and for A 5 to 25°, gf(A) was found to be 0.5 $(1 - e^{-A})$. Then Equation 5.1 becomes

$$R_A = R_c + 0.5\ (1 - R_c)\ (1 - e^{-A})." \qquad (5.2)$$

Equation 5.2 shows that use of the collimated transmission values for correcting data obtained with the wide field of view of these instruments will result in an over-correction. Calculations on the amount of over-correction, for the data obtained, using Equation 5.2 show that in the worst case (greatest slant range) the over-correction amounts to about

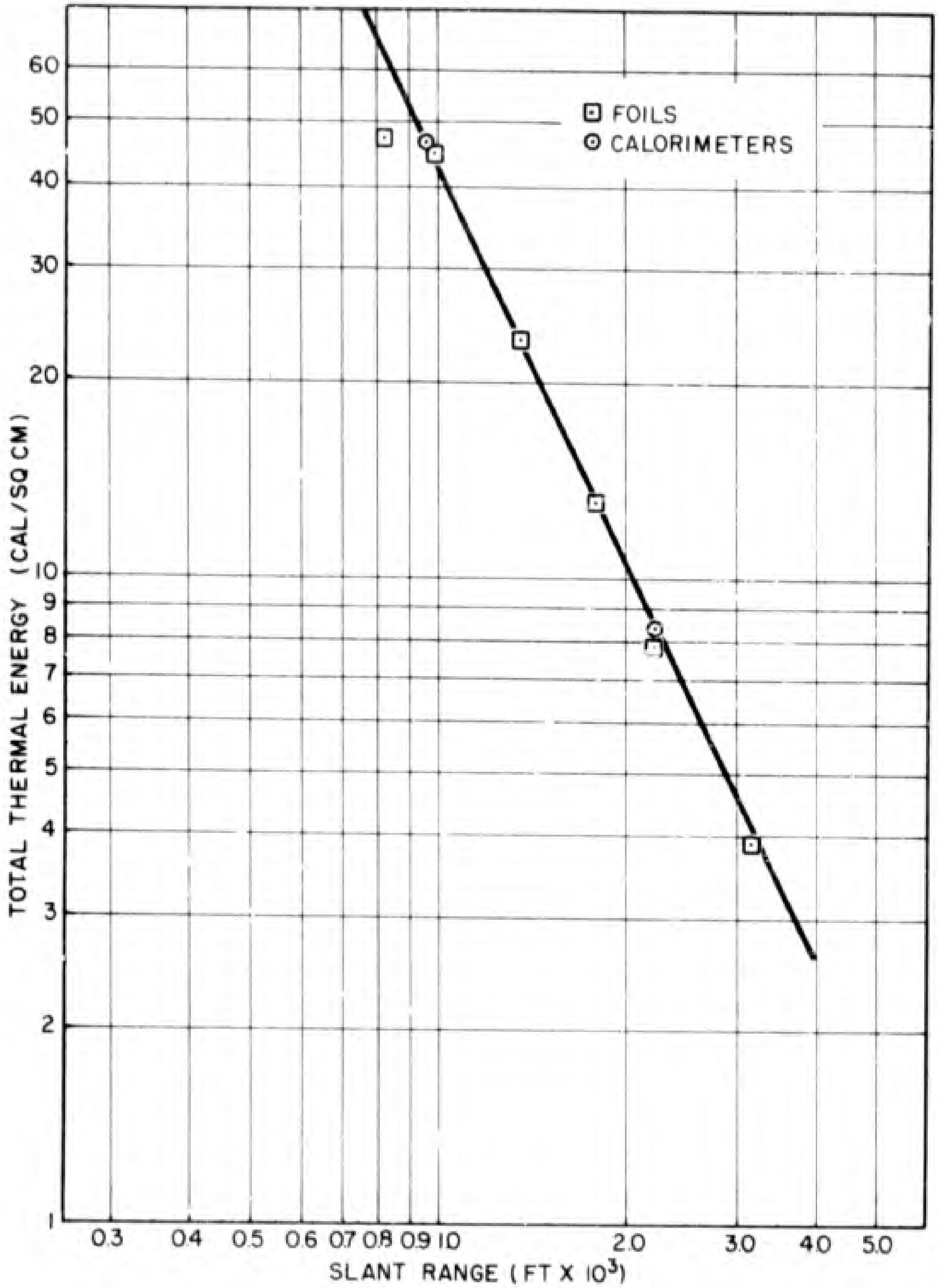

Fig. 5.1 Energy (Corrected for Atmospheric Attenuation) vs Slant Range, Shot 1. Calorimeters and Foils

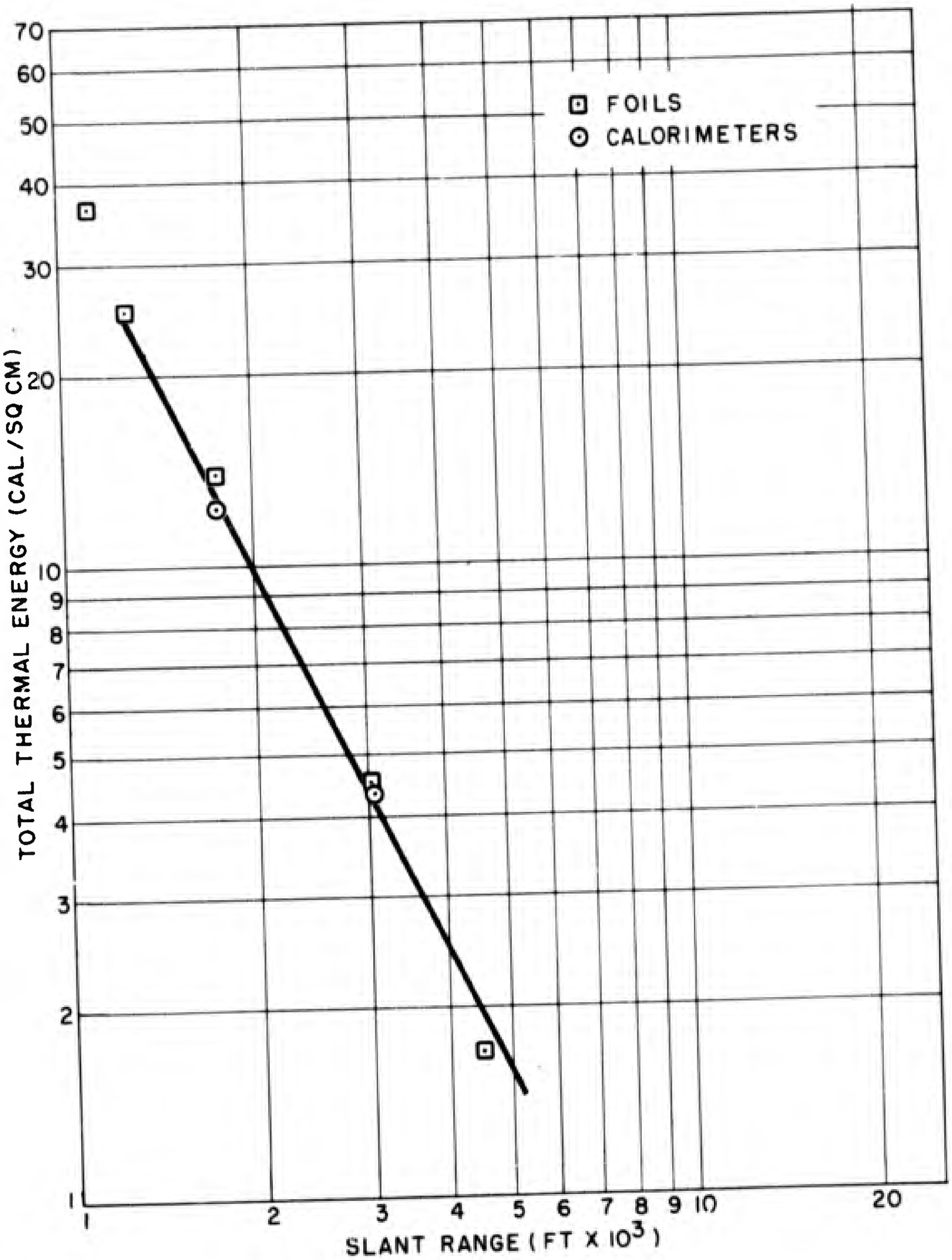

Fig. 5.2 Energy (Corrected for Atmospheric Attenuation) vs Slant Range, Shot 2. Calorimeters and Foils

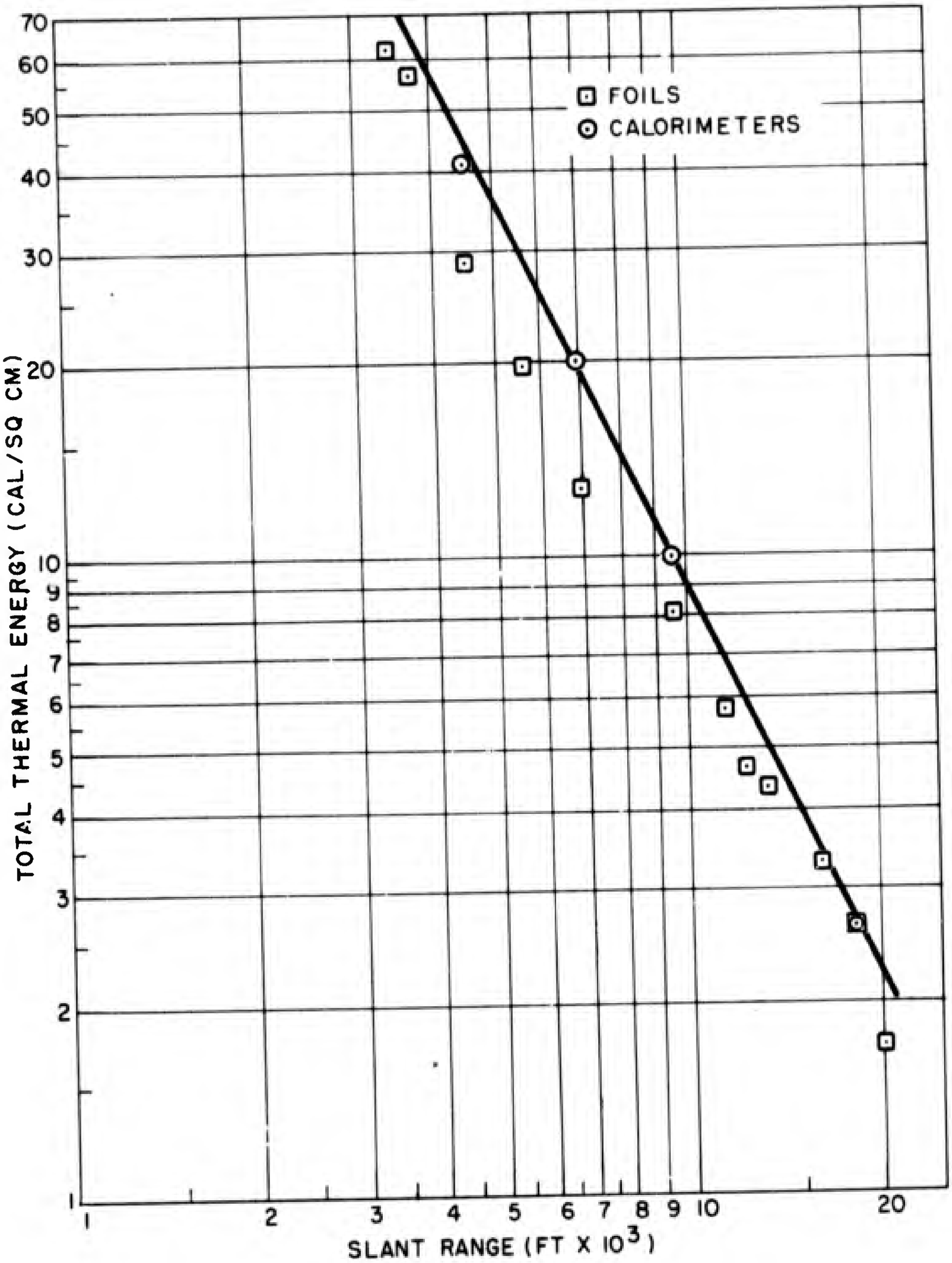

Fig. 5.3 Energy (Corrected for Atmospheric Attenuation) vs Slant Range, Shot 3. Calorimeters and Foils

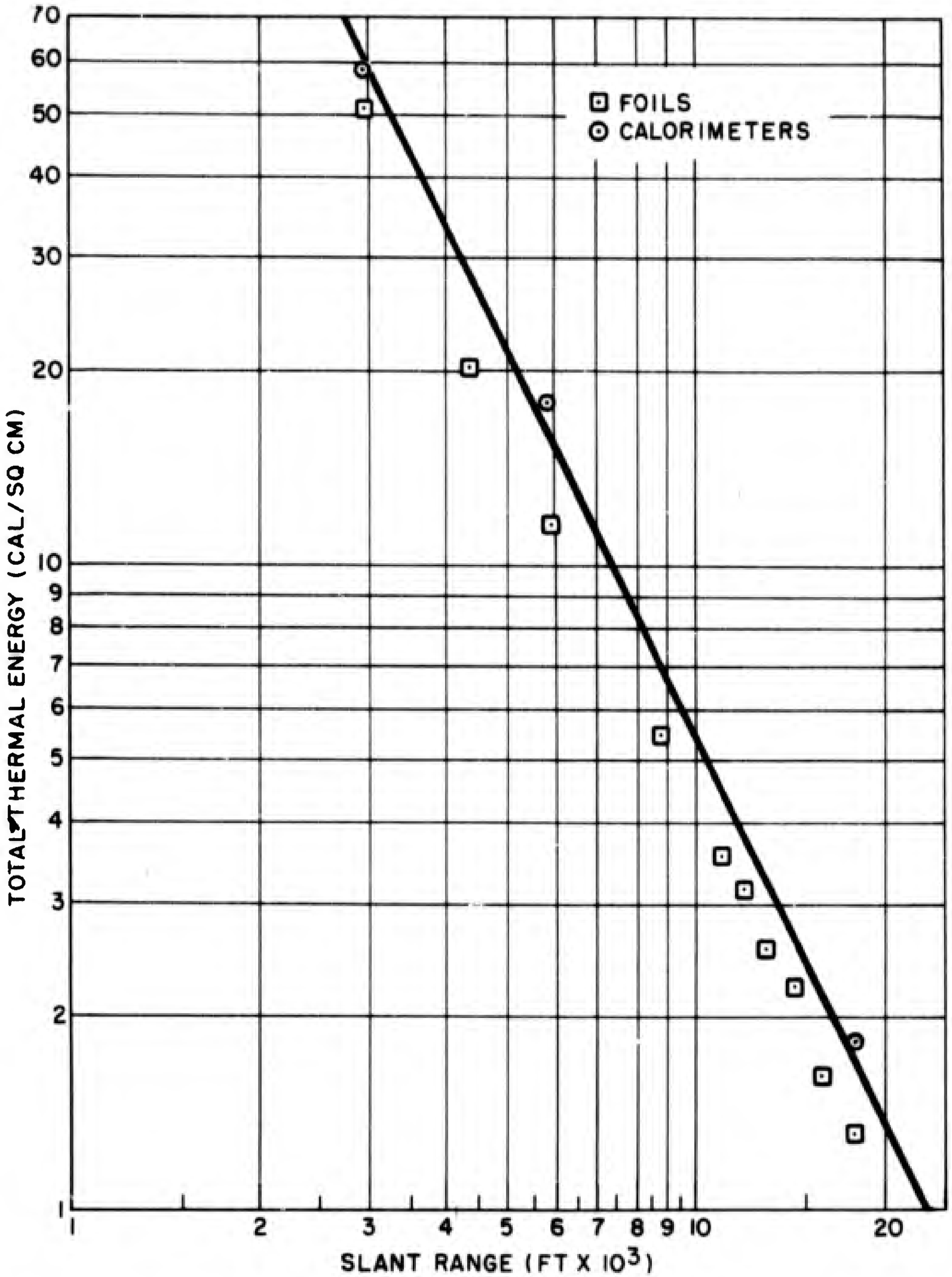

Fig. 5.4 Energy (Corrected for Atmospheric Attenuation) vs Slant Range, Shot 4. Calorimeters and Foils

7 per cent and on the average is only a few per cent. Furthermore, as Equation 5.2 has been checked only for half-angles up to 12.5° there is some doubt as to its validity at much greater angles. Because of the small size and uncertainty of this second-order correction, it was not applied, and the narrow beam transmission values quoted above were used for all fields of view.

An average normalized energy-vs-time curve and intensity-vs-time curve for each shot was obtained by averaging the results from the same calorimeters which were used in the energy-vs-distance plots. In each case the data from four or more calorimeters were used in obtaining the average curve. Figures 5.5 through 5.8, which are the set of individual curves used to obtain the average intensity-vs-time curve for Shot 3, indicate the variation in the shape of the curves obtained from the various calorimeters.

The composite "best" total energy-vs-time curve for each shot is shown in Fig. 5.9 and the composite "best" intensity-vs-time curve for each shot is shown in Fig. 5.10. Intensity-vs-time curves from Operation BUSTER are given in Fig. 5.11 for comparison purposes. The intensity-vs-time curves have been normalized by using the ratio (expressed in per cent) of the intensity at any time to the total energy measured. In addition to permitting comparison of the general shape of these curves, this method of plotting gives an indication of the bomb-to-bomb variation of the peak intensity to total energy ratio.

The curves in Fig. 5.10 indicate that the time to reach peak intensity increases with increasing yield while the ratio of peak intensity to total energy decreases. Although not completely shown in this figure, the larger bombs show much longer thermal tails, measurable energy being recorded out to 6 or 7 sec. The curve for Shot 4 seems to differ appreciably in shape from the curves for the other three shots. The peak rises to a higher value than would be expected for a bomb of that size, and the intensity then drops rapidly to a long tail. Comparison with the Operation BUSTER data in Fig. 5.11 indicates good agreement between data for the two operations.

The agreement among the various calorimeter values for each shot was quite good, as can be seen from the total energy-vs-distance curves in Figs. 5.1 through 5.4. An indication of the constancy of thermal yield may be obtained by plotting the log of the total thermal energy (corrected for atmospheric attenuation) per kiloton as a function of distance. This has been done in Fig. 5.12 for Shots 1 through 4, Operation TUMBLER-SNAPPER, and for Shots Baker through Easy, Operation BUSTER. The line drawn through the points has a slope of -2. In general the fit is fairly good, although there is some indication that the bombs of lower yield gave points above the line while those of higher yield gave points on, or slightly below, the line. This variation can be seen more clearly in Fig. 5.13, which is a log-log plot of the thermal yield vs the total yield, and Fig. 5.14 which

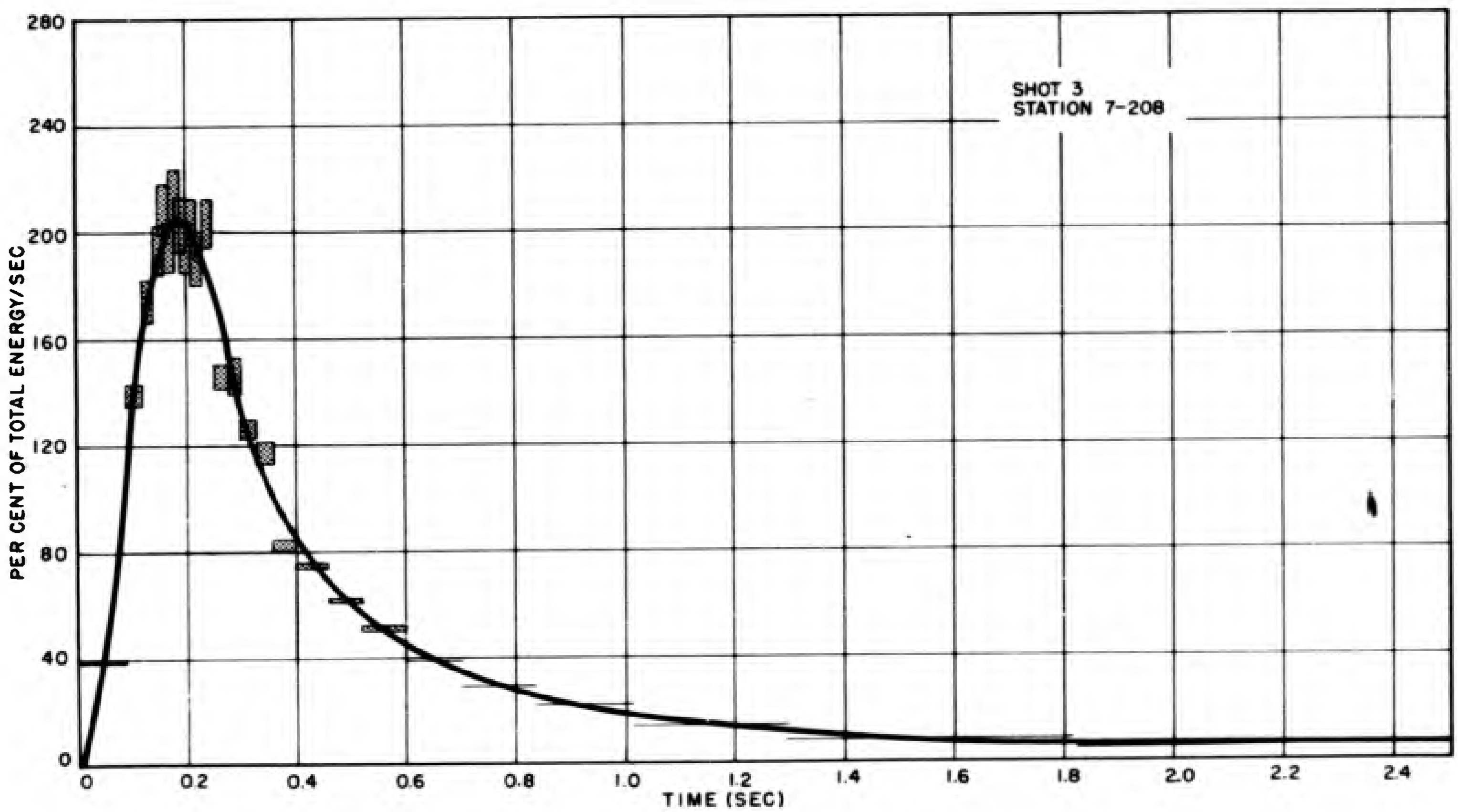

Fig. 5.5 Typical Individual Time Intensity Curves, Shot 3

UNCLASSIFIED

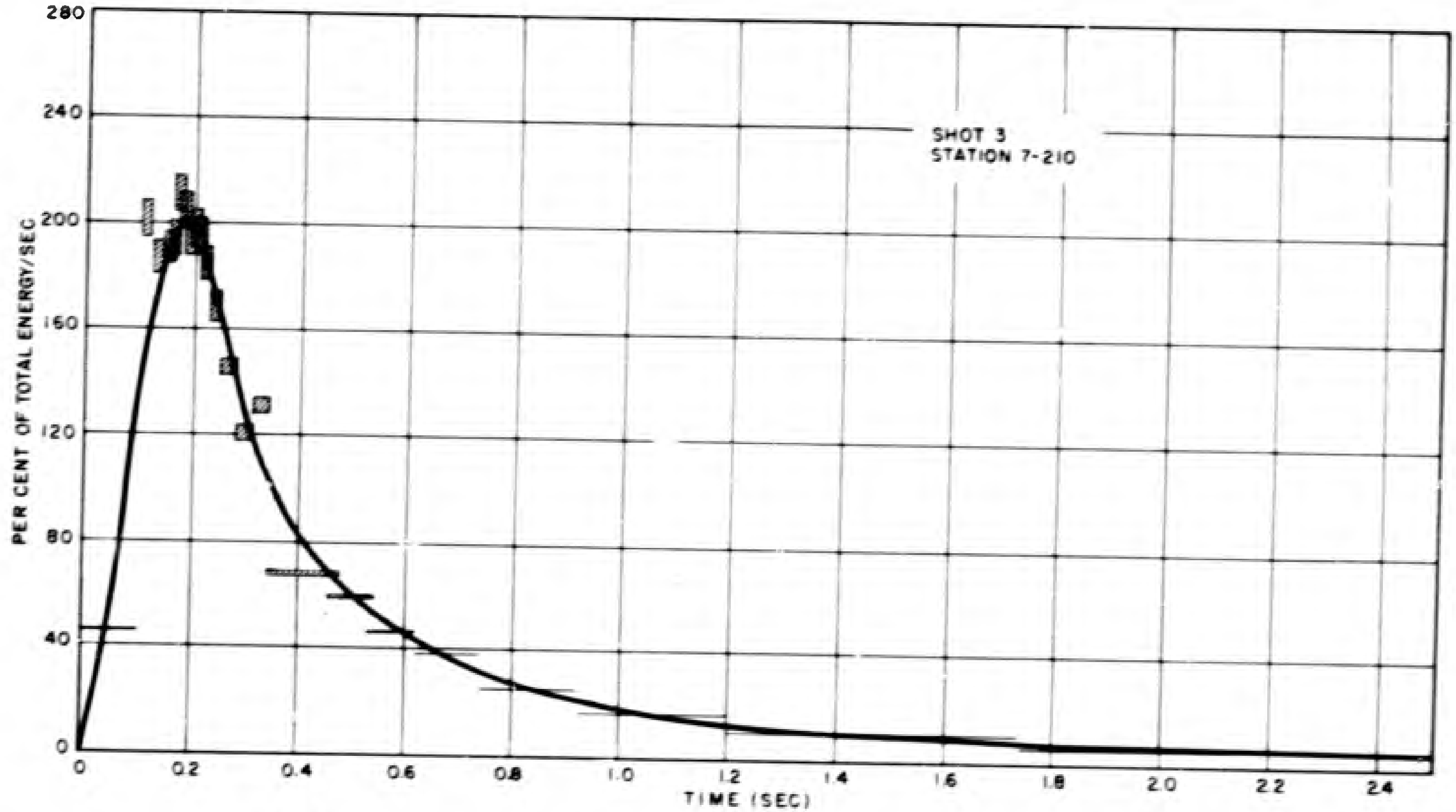

Fig. 5.6 Typical Individual Time Intensity Curves, Shot 3

UNCLASSIFIED

UNCLASSIFIED

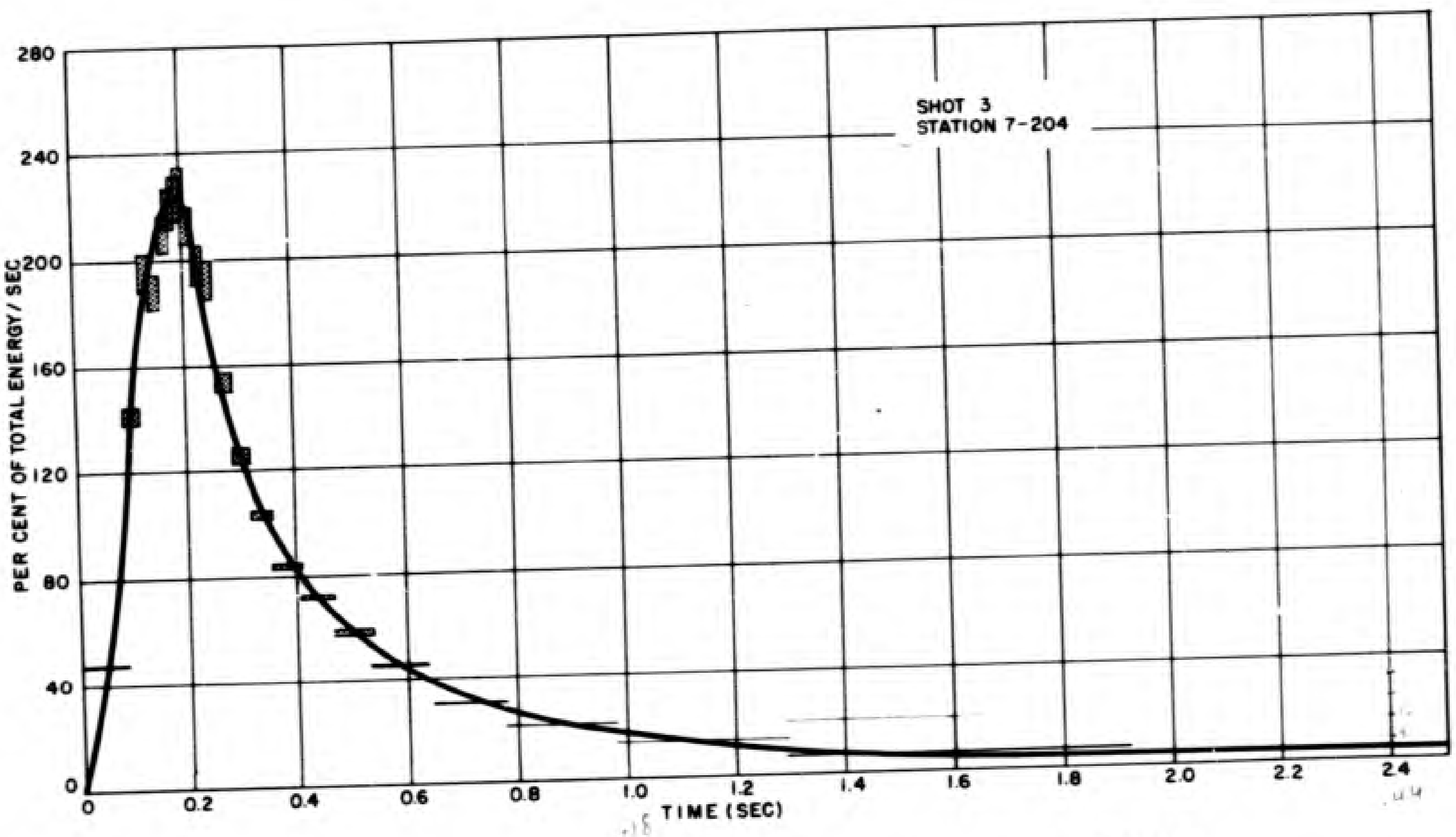

Fig. 5.7 Typical Individual Time Intensity Curves, Shot 3

UNCLASSIFIED

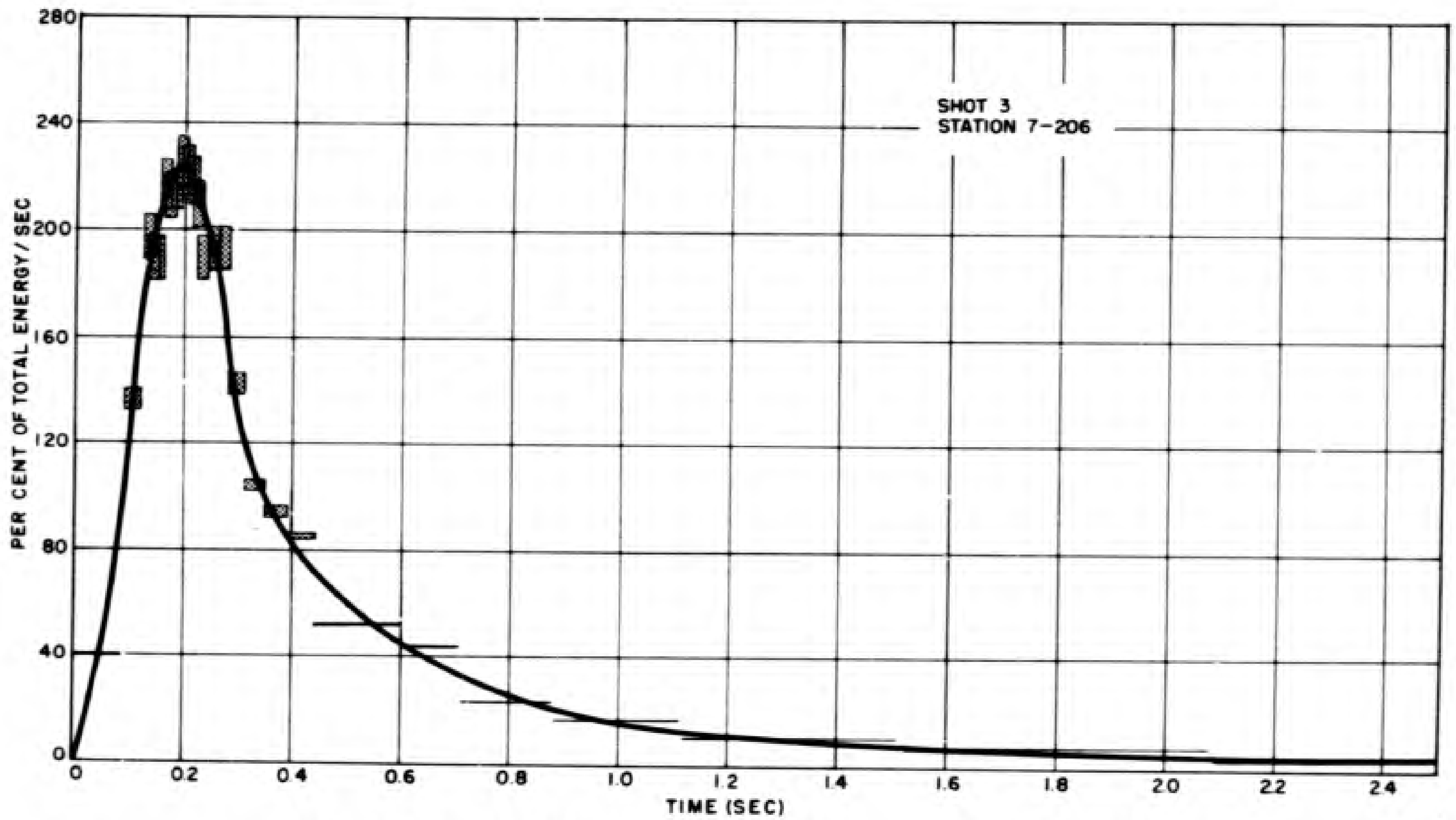

Fig. 5.8 Typical Individual Time Intensity Curves, Shot 3

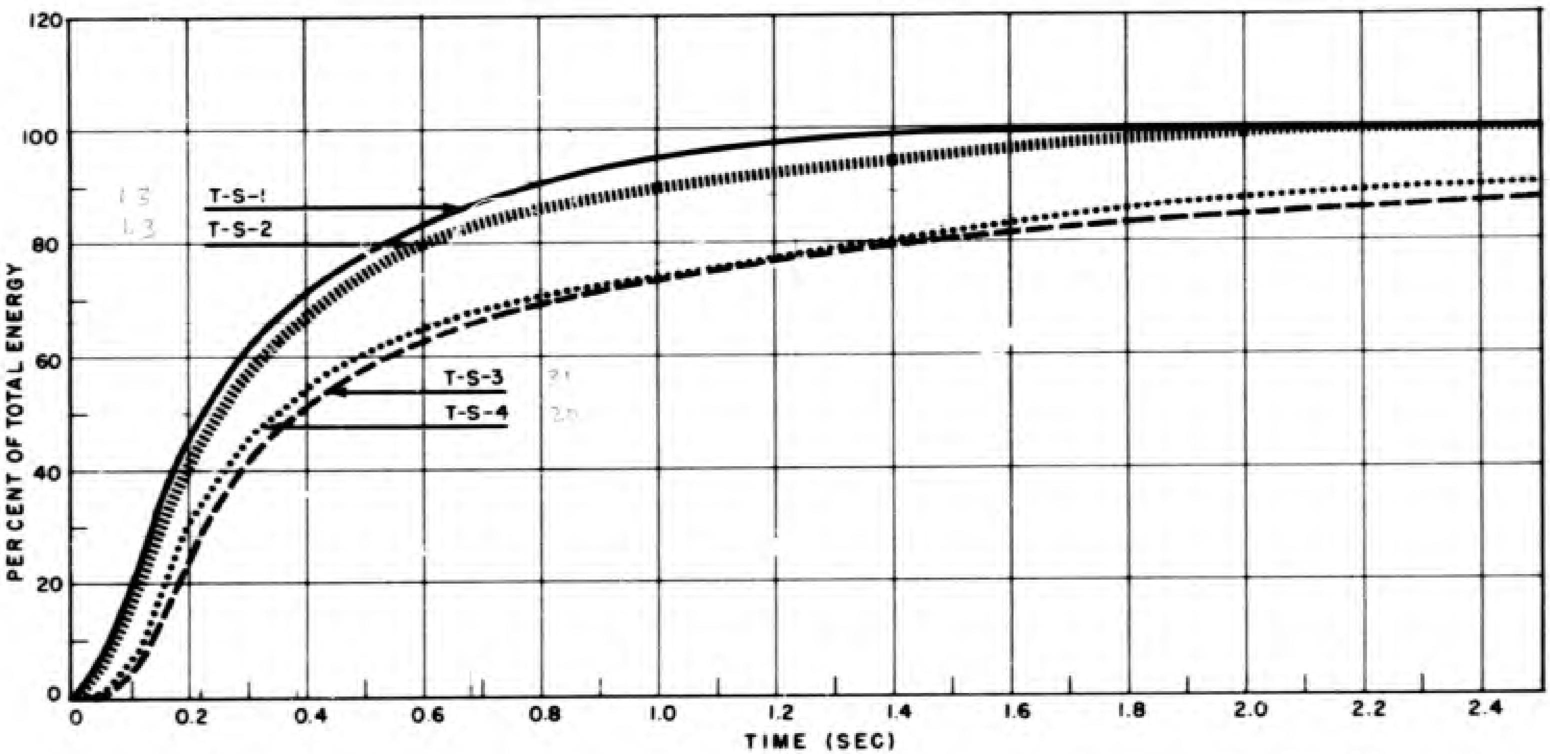

Fig. 5.9 Per Cent of Total Energy vs Time for Shots 1 through 4, Operation TUMBLER-SNAPPER

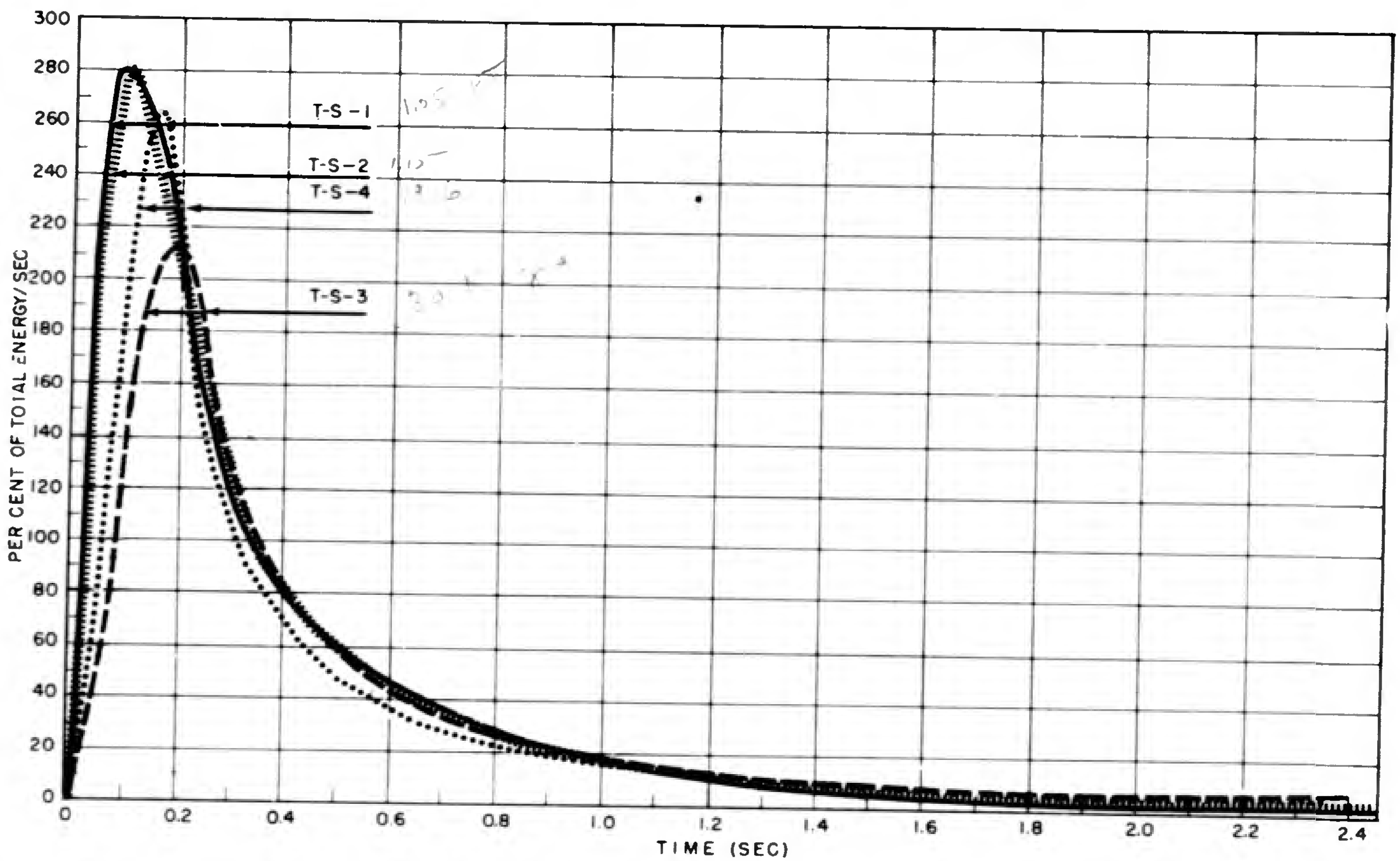

Fig. 5.10 Normalized Intensity vs Time for Shots 1 through 4, Operation TUMBLER-SNAPPER

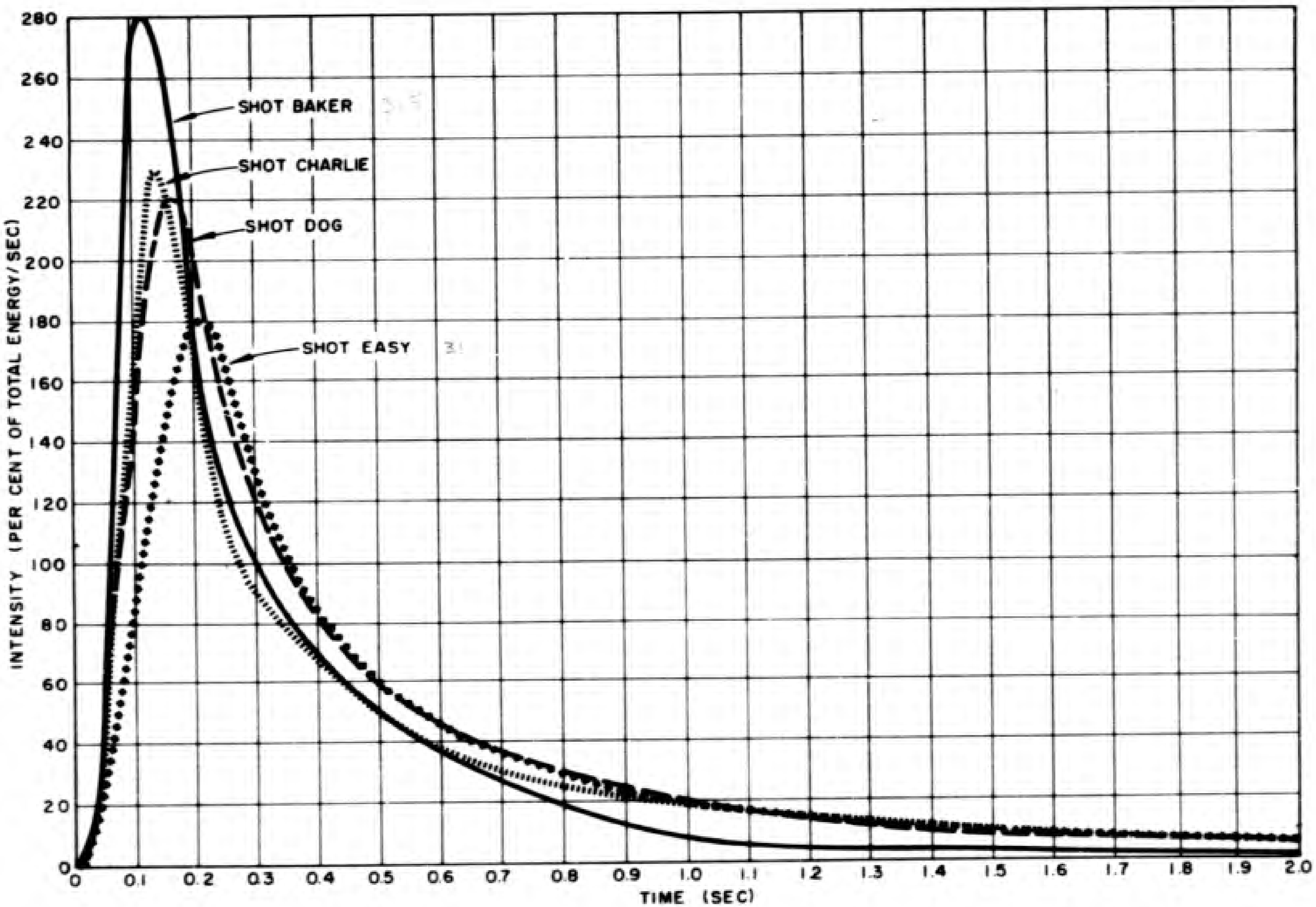

Fig. 5.11 Normalized Intensity vs Time for Shots Baker through Easy, Operation BUSTER

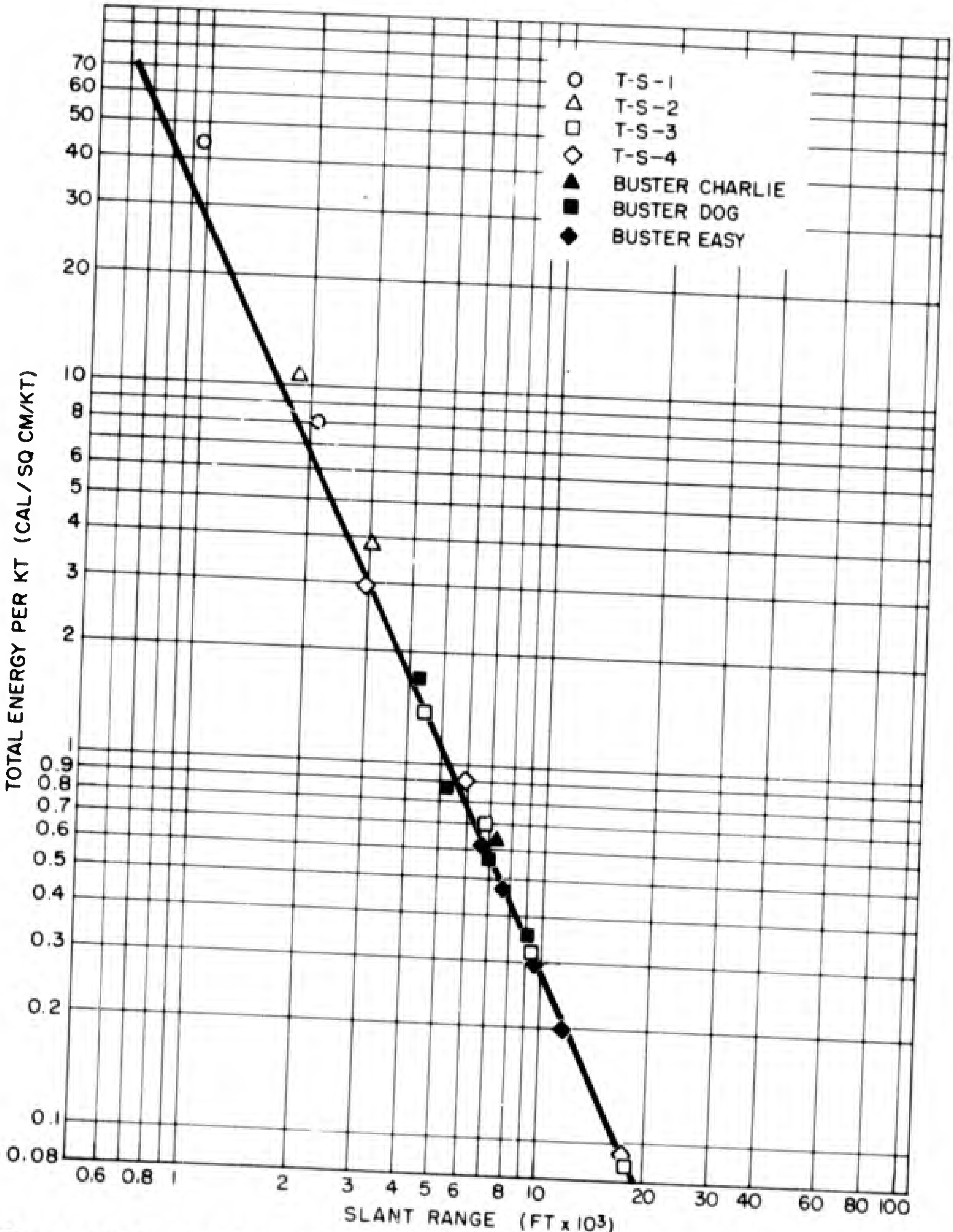

Fig. 5.12 Energy (Corrected for Atmospheric Attenuation) per kt vs Slant Range for Operation TUMBLER-SNAPPER, Shots 1 through 4, and Operation BUSTER, Shots Charlie through Easy

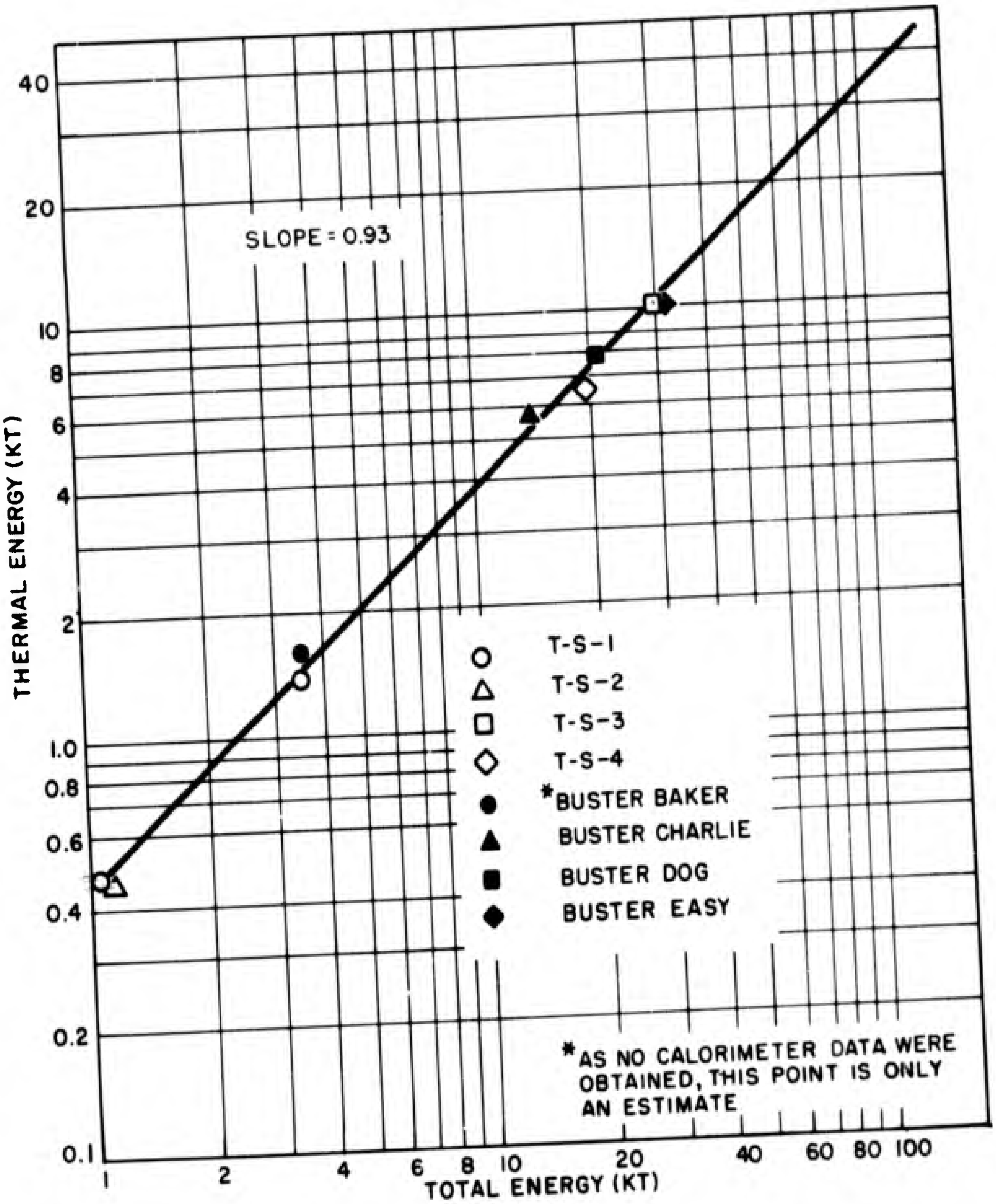

Fig. 5.13 **Thermal Yield vs Total Yield for Operation TUMBLER, Shots 1 through 4 and Operation BUSTER, Shots Baker through Easy**

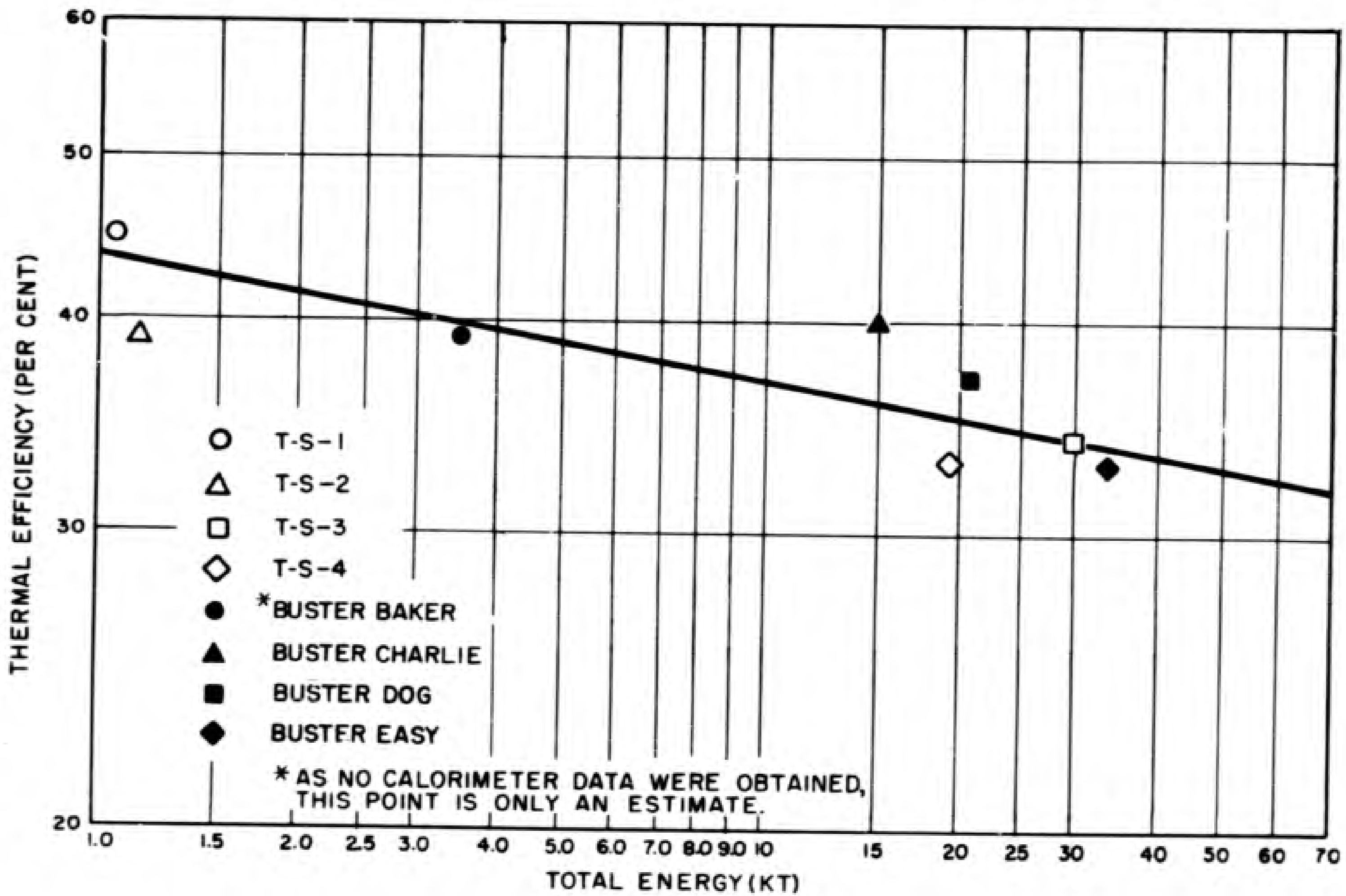

Fig. 5.14 Thermal Efficiency vs Total Yield for Operation TUMBLER, Shots 1 through 4 and Operation BUSTER, Shots Baker through Easy

is a log-log plot of the thermal efficiency vs the total yield. The best straight line through the points in Fig. 5.13 has a slope of 0.93, and correspondingly the line in Fig. 5.14 has a slope of -0.07. The slope of these lines and the individual points are subject to change from time to time as new values of total yields are quoted. The slope of the line in Fig. 5.14 is particularly sensitive to small changes in this parameter. The total yields used in plotting these curves are shown in Table 5.1.

TABLE 5.1

Total Yields for Operations BUSTER and TUMBLER-SNAPPER

Operation	Shot	Yield (kt)
BUSTER[a]	B	3.48
BUSTER	C	14.0
BUSTER	D	20.98
BUSTER	E	31.4
TUMBLER-SNAPPER[b]	1	1.05
TUMBLER-SNAPPER	2	1.15
TUMBLER-SNAPPER	3	30.0
TUMBLER-SNAPPER	4	19.6

(a) BUSTER yield data are final radiochemical yields and were obtained from letter dated 14 August 1952 from Lt. Col. G. B. Page, Chief, Reports Branch, AFSWP (File No. SWPWT/1).

(b) TUMBLER-SNAPPER yield data are preliminary radiochemical yields and were obtained from letter dated 5 August 1952 from Lt. Col. G. B. Page, Chief, Reports Branch, AFSWP (File No. SWPWT/1).

5.2 RADIOMETERS

Comparison of the thermal pulse shapes of the bombs, as measured with the various calorimeters and radiometers, are shown in Figs. 5.15, 5.16, and 5.17 for Shots 1, 2, and 4, respectively. No comparison was made on Shot 3, because of the dust obscuration at Station 7-202 and failure of the timing mechanism at the 18,000-ft station, which caused the time scale to be uncertain. All curves have been normalized so that the peak intensity is 100 per cent. It can be seen that, although the general shape of the curve is similar for all instruments, the USNRDL disk radiometer and the fine-wire radiometer curves appear to lag behind the differentiated calorimeter and MIT radiometer curves. This result is reasonable, as the measured time constant of all but the thickest calorimeters is less than 15 msec, that of the MIT radiometer, 12 msec, and that of the USNRDL disk radiometers, 25 to 30 msec. While no laboratory

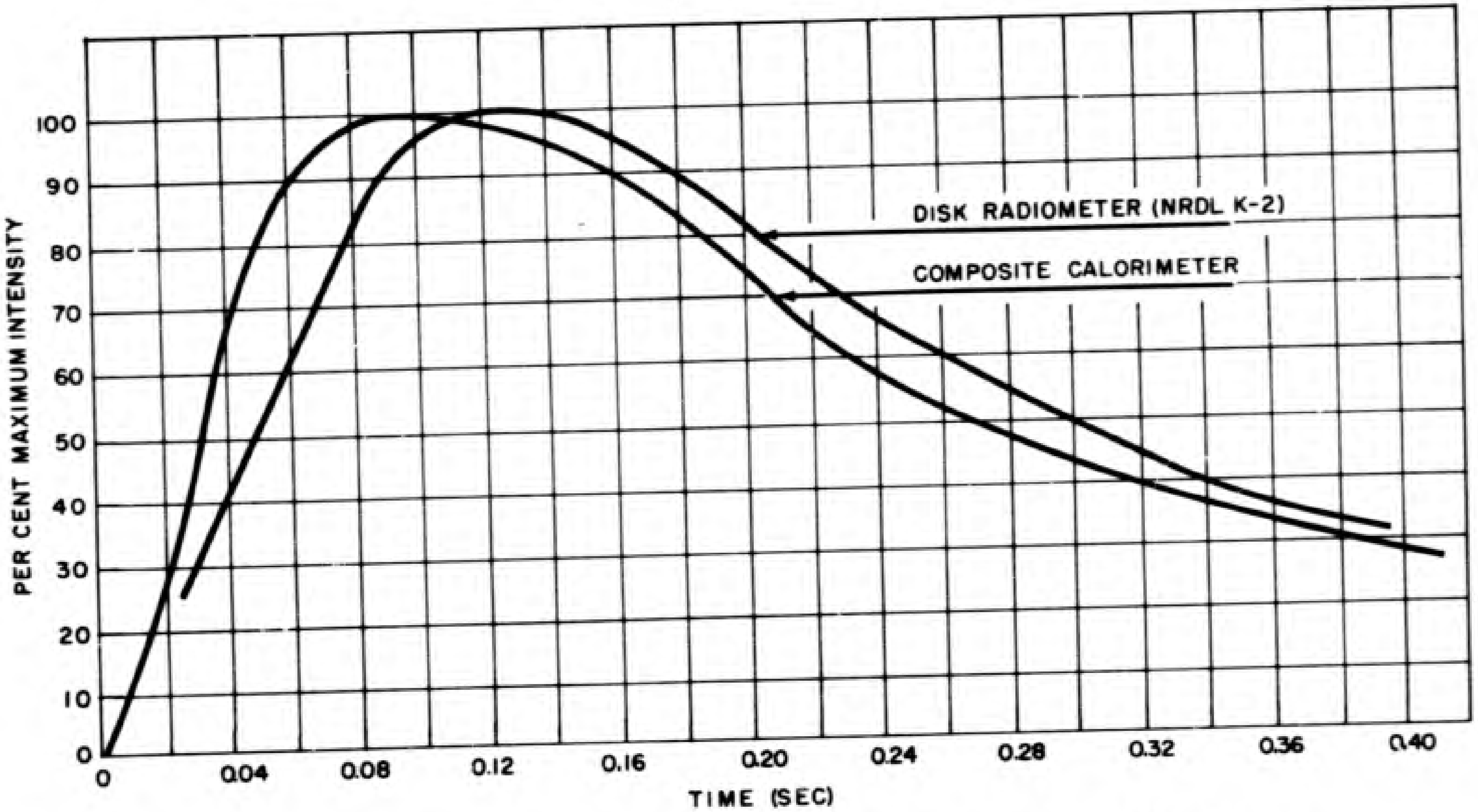

Fig. 5.15 Intensity-vs-time Curves from Various Instruments, Shot 1

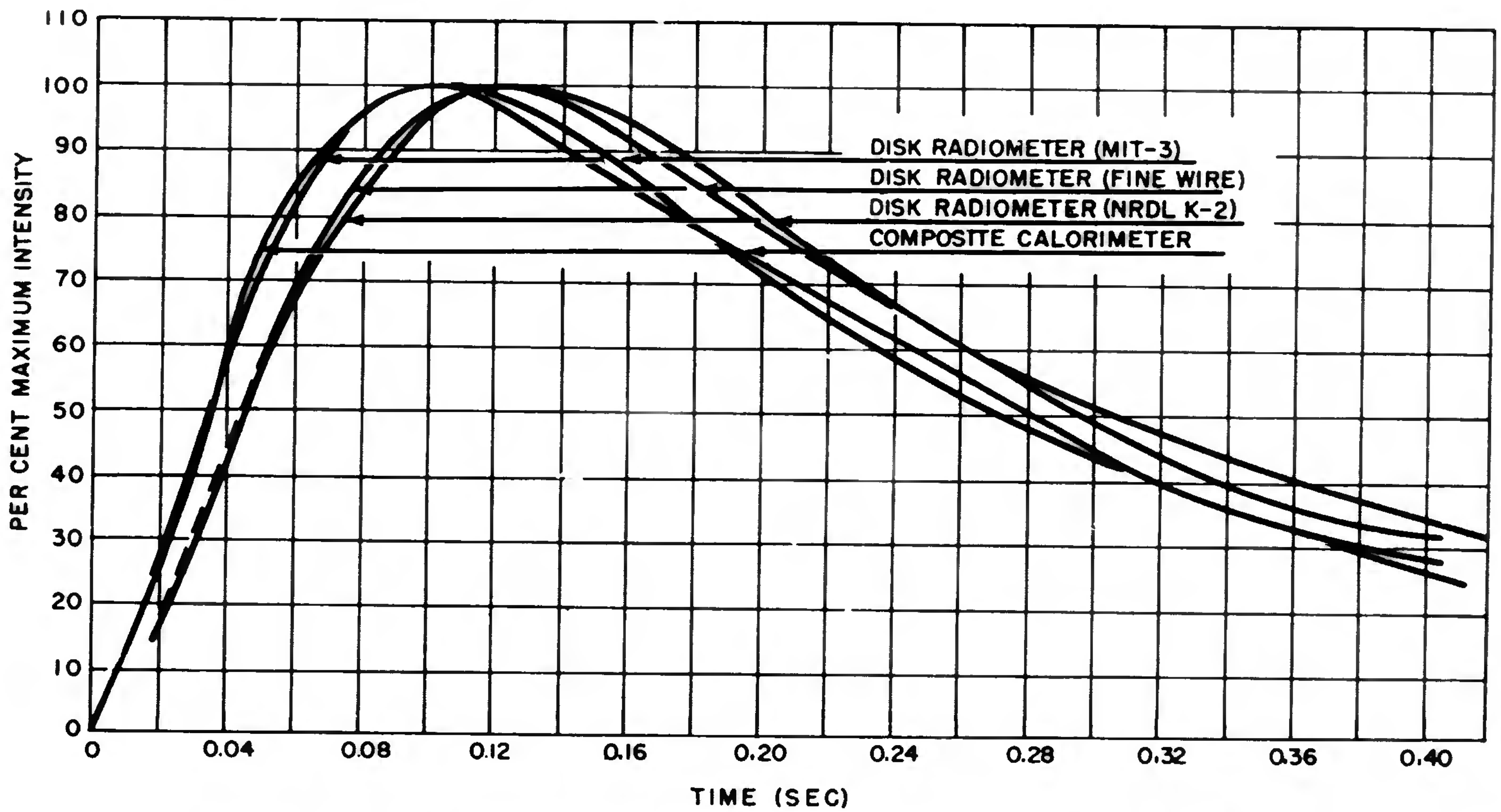

Fig. 5.16 Intensity-vs-time Curves from Various Instruments, Shot 2

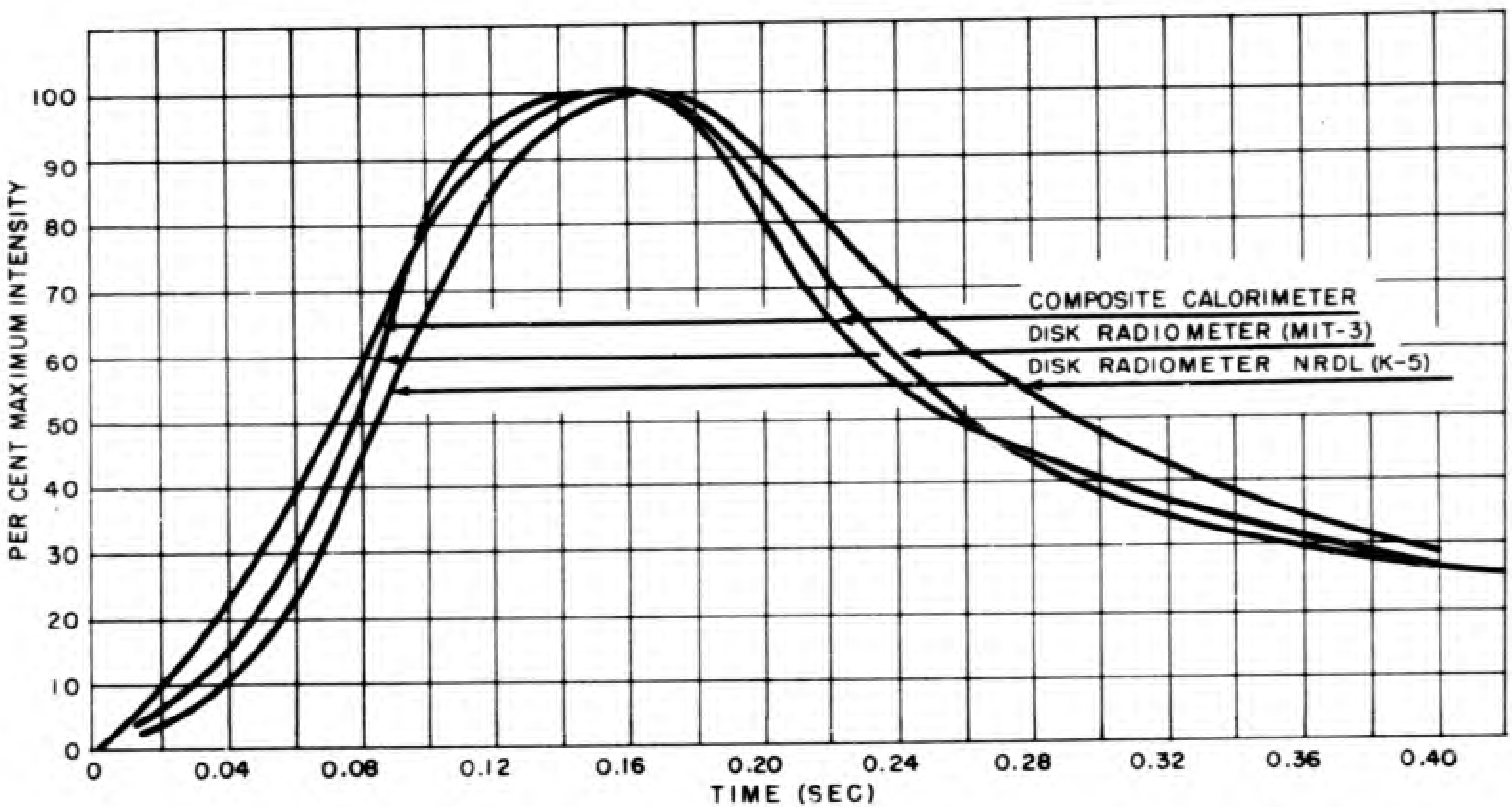

Fig. 5.17 Intensity-vs-time Curves from Various Instruments, Shot 4

determination of time constant of the fine-wire radiometer was obtained, the comparison curves for Shot 2 show that its response is very similar to that of the USNRDL disk radiometer.

5.3 SPECTRAL ENERGY DISTRIBUTION

The results of the spectral investigation are shown in Table 5.2 where the energy received under each filter is given as the percentage of the energy received under quartz. Also shown in the table are similar results from Operations GREENHOUSE and BUSTER, along with the percentages expected from a black body at 6,000°K. The spectral data obtained at Operation GREENHOUSE, indicate appreciably less energy at wave lengths beyond 9500 Å than do the Operation TUMBLER results. Since the GREENHOUSE detonation was a tower burst, in which the resulting dust clouds obscured the tail of the thermal pulse, and since the thermal tail is rich in the longer wave lengths, a net decrease in the contribution of the infrared would be expected for such a burst.

Figures 5.18 and 5.19 show the normalized intensity-vs-time curves for each of the calorimeters under the various filters. Normalization consisted in dividing the measured intensity by the total energy received under the particular filter. The expected gradual shift of the spectral distribution with time can readily be seen.

TABLE 5.2

Per Cent of Total Energy in the Transmission Range of the Filters Used in Operation TUMBLER-SNAPPER

Filter Type	Spectral Range of Transmission Å	Per Cent of Energy Received under Quartz					6,000°K Black Body
		GREENHOUSE EASY	BUSTER DOG	BUSTER EASY	T-S 3	T-S 4	
Quartz	2200-45000	100	100	100	100	100	99
0-52	3600-25000	100	--	--	91	91	88
3-69	5300-25000	75	72	79	70	70	66
2-58	6400-25000	50	43	53	54	55	52
7-56	9500-25000	10	--	--	25	25	26

2 x 6

Table

5.4 LOCAL OBSCURATION: THE EFFECT OF ELEVATION OF MEASURING INSTRUMENT

Examination of the energy received at each station (Tables 4.1 through 4.4) as a function of elevation shows that at the close stations, for the larger bombs, there is a noticeable decrease in energy at the ground level and even at some of the 10-ft levels. Comparison of this parameter for all shots was accomplished by plotting the percentages of energy lost at the grade and 10-ft elevations as functions of the incident total energy (Fig. 5.20). For this purpose the total energy was taken from calorimeters at the 50-ft elevations. Figures 5.21, 5.22, and 5.23, which

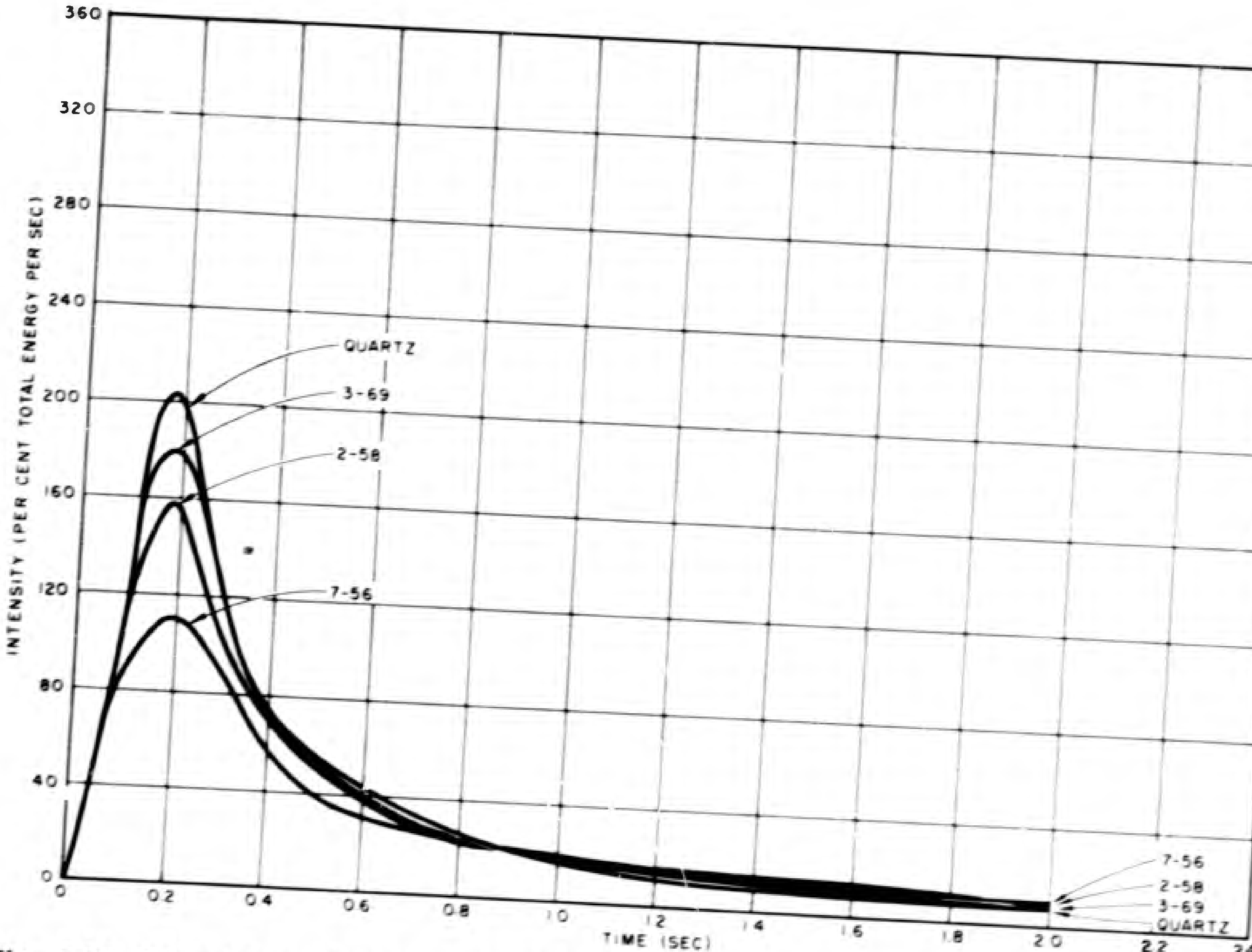

Fig. 5.18 Intensity-vs-time Curves for Calorimeters Used in Spectral Investigation, Shot 3

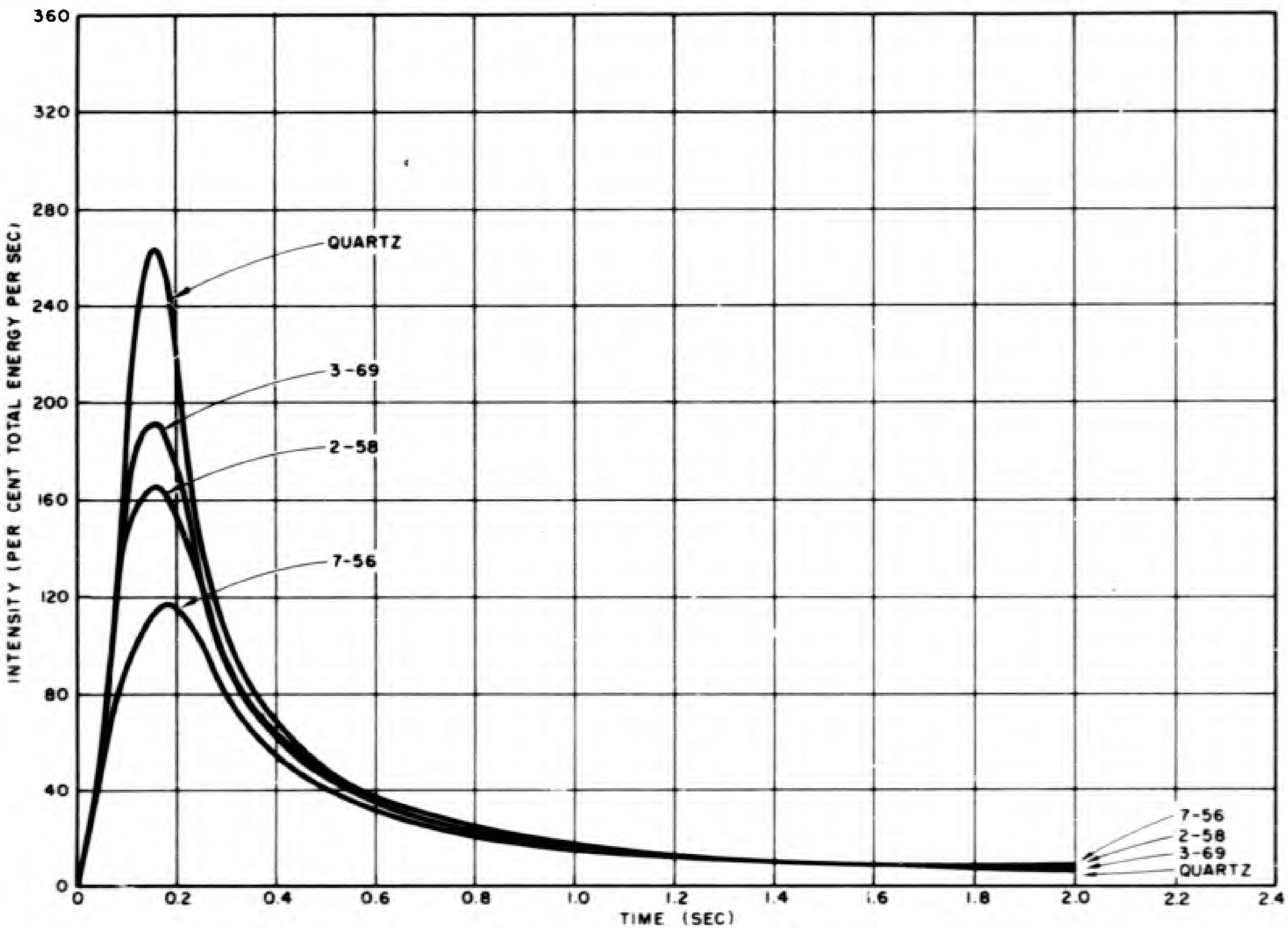

Fig. 5.19 Intensity-vs-time Curves for Calorimeters Used in Spectral Investigation, Shot 4

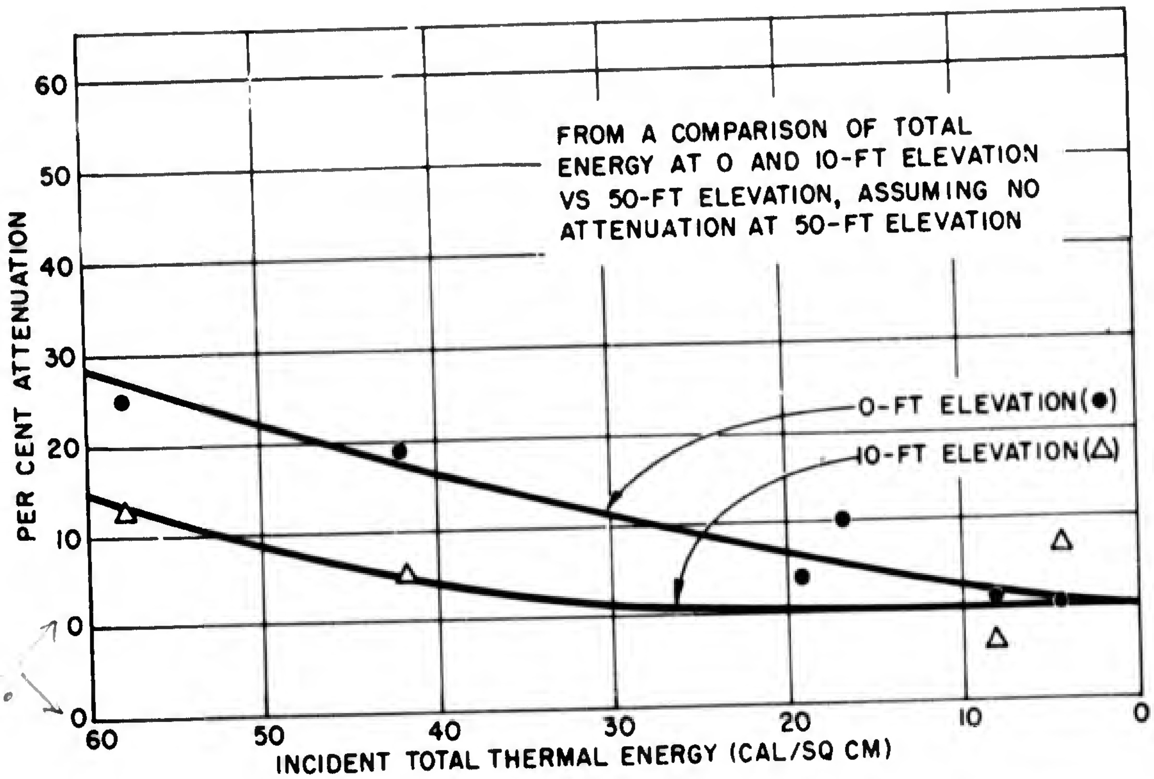

Fig. 5.20 Attenuation Due to Local Obscuration for Air Bursts

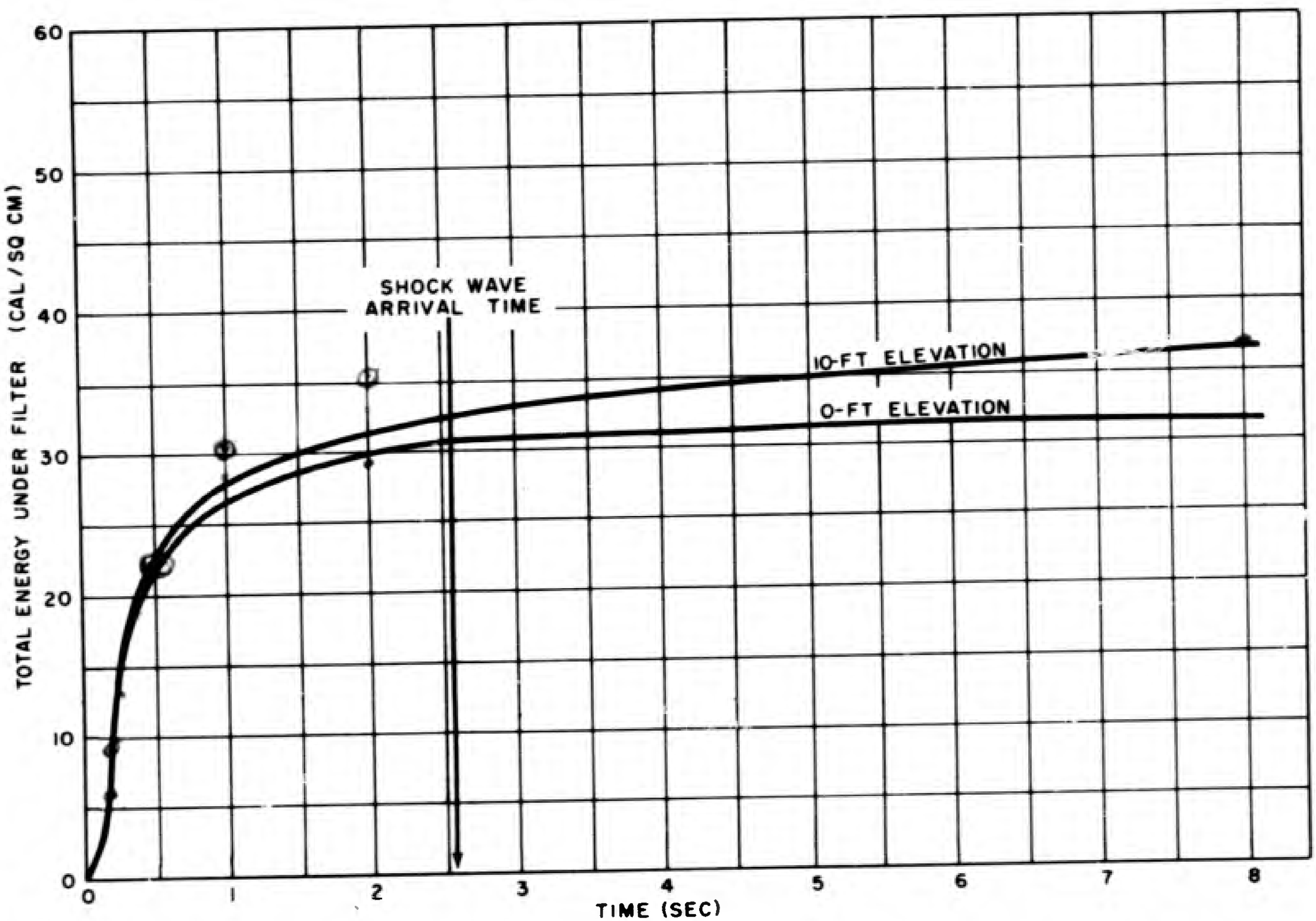

Fig. 5.21 Energy vs Time for 0 and 10-ft Elevations, Station 7-204, Shot 3

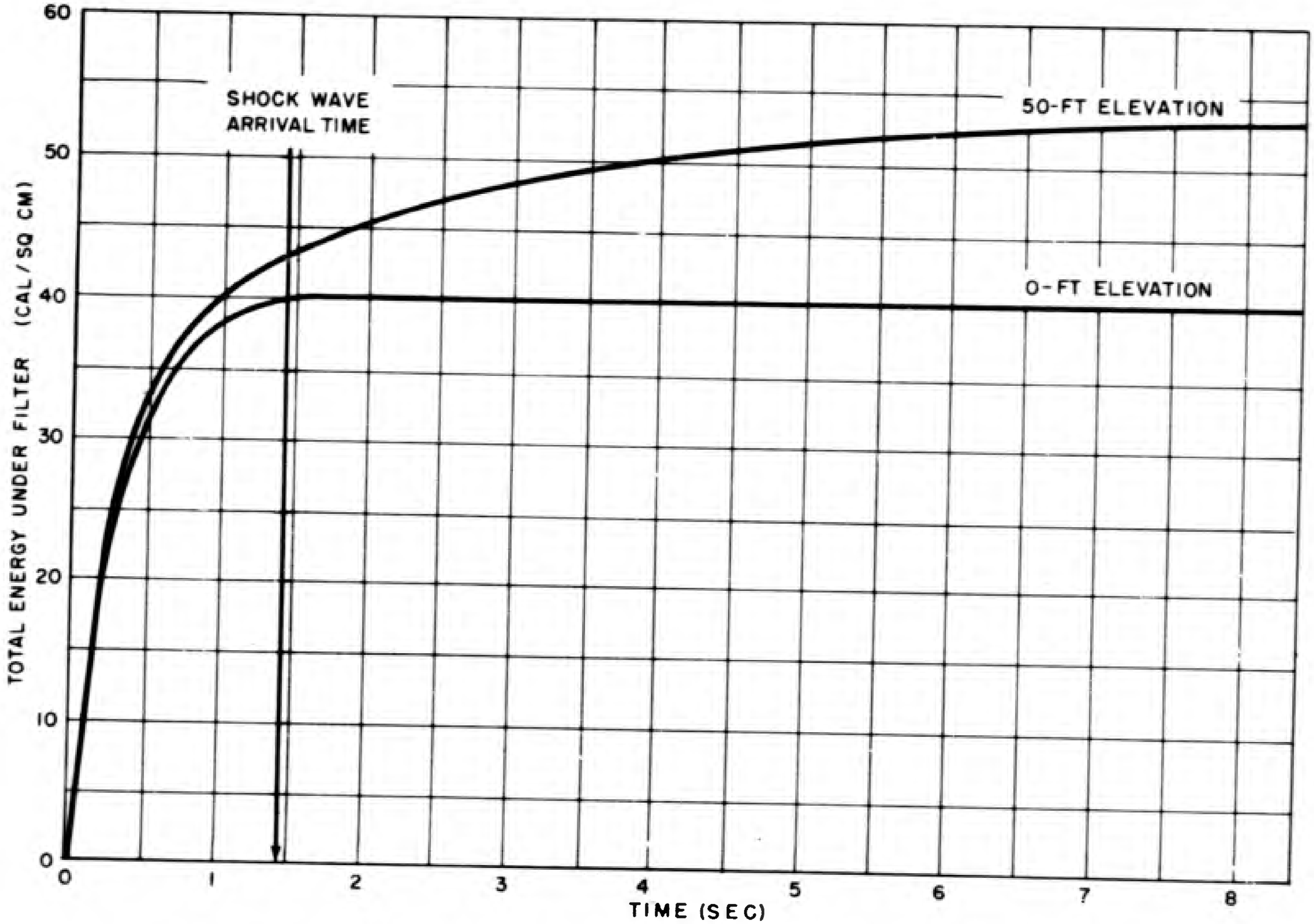

Fig. 5.22 Energy vs Time for 0 and 50-ft Elevations, Station 7-204, Shot 4

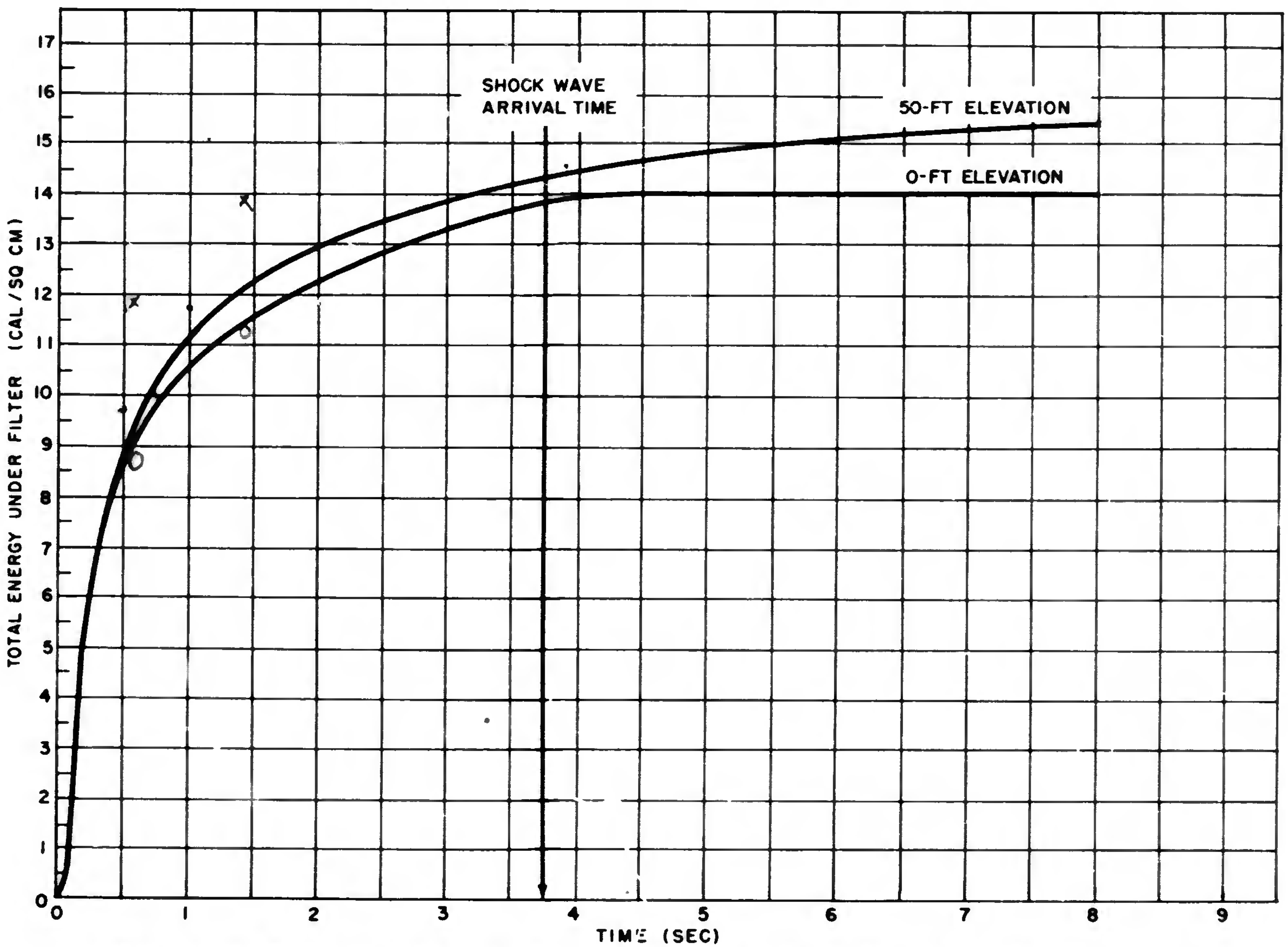

Fig. 5.23 Energy vs Time for 0 and 50-ft Elevations, Station 7-208, Shot 4

are curves of total energy vs time for various elevations at the three most severely obscured stations, indicate the time sequence of the obscuration. As would be expected, very little energy was received at grade level after arrival of the shock wave. The obscuration before the arrival of the shock wave can be attributed to "popcorning" of the sand and to smoke produced by the burning of ground litter.

5.5 FIELD OF VIEW

The results of the field-of-view investigations are shown in Table 5.3. The radius of the fire ball, column 6, was obtained by scaling the value for a nominal (20-kt) bomb, as given in the Effects of Atomic Weapons, assuming that the radius is proportional to the 1/3 power of the yield. The radial error in alignment, column 7, is the distance between the axis of the calorimeter and the expected point of detonation in a plane perpendicular to the axis of the calorimeter, due to an angular error of 2°, which is the estimated maximum error in alignment. The error in the point of detonation, column 8, is the projected distance between the expected and actual points of detonation in the plane perpendicular to the axis of the calorimeter and was obtained from the Operation TUMBLER Preliminary Report[1/]. The estimated maximum displacement of the center of the field of view from the center of the detonation, column 9, is the sum of the two errors given above.

TABLE 5.3

Effect of Field of View

Shot No.	Station	Slant Range (ft)	Elevation (ft)	Field-of-view Radius at Detonation Point (ft)	Radius of Fire Ball (ft)	Radial Error in Alignment (ft)	Error in Detonation Point (ft)	Estimated Maximum Displacement (ft)	Per Cent Total Energy Received by Calorimeter for Half Angle 6°	12°
1	F-208	2,220	0	470	170	77	122	199	--	0[a]
1	F-208	2,210	10	470	170	77	122	199	--	83
3	7-204	4,510	0	960	520	154	124	276	--	41
3	7-204	4,500	10	960	520	154	124	276	--	86
3[b]	7-208	6,830	0	720	520	240	124	364	46	--
4[b]	7-204	3,020	0	640	450	106	153	259	--	61
4[b]	7-208	5,920	0	620	450	208	153	361	40	--

(a) It is believed that this value is due to a faulty circuit.

(b) Fire ball could have been partly outside the field of view.

Examination of this table shows that the field of view should have included the entire fire ball in all but three cases. Even in those three cases it appears that not more than about 20 or 30 per cent of the fire ball could have been outside of the field of view of the calorimeter. The data, however, do not agree with this conclusion, as some of the calorimeters gave values as low as 40 per cent of those measured with maximum field of view. It is apparent that important factors other than the errors in alignment and in point of detonation are influencing the results. One trend that can be noted from the table is that the values obtained at the ground level seemed to show much lower percentages than those obtained above grade. For example, for Shot 3, Station 7-204, the calorimeter at 10 ft with 12° half-angle gave 86 per cent of the energy measured by the standard calorimeter (half-angle 45°) at that elevation, and the one at grade gave 41 per cent of the energy measured by the standard calorimeter at grade. This indicates that dust obscuration might have some influence on the results. However, additional data must be obtained before the reason for the low results with restricted field of view can be confirmed.

As mentioned previously, the effect of field of view of the measuring device has little effect on the energy received for highly transmitting atmospheres and moderate distances. However, this is not necessarily true when instruments are obscured by smoke or dust, as in this case the collimated transmission could be very low. Using Equation 5.2 and assuming as a limiting case that the collimated transmission approaches zero, the calculated ratios of the energy received by the 6 and 12° half-angle field-of-view calorimeters to that received by the 45° half-angle field-of-view calorimeter would be 0.24 and 0.43 respectively. Examination of the data in Table 5.3 indicates that the "field-of-view" results fall within the limits set by Equation 5.2 for zero and 100 per cent transmission, and, qualitatively, that the greatest effects occur whenever the greatest obscuration is to be expected.

The values given in Table 5.3 are lower than expected, even considering the effects of dust. This fact leads to the conclusion that any instrument designed to measure the thermal efficiency of a nuclear weapon should have a field of view such that the radius at the point of detonation will be no less than about two times the sum of the fire ball radius, estimated as above, and the maximum displacement of the center of the field of view from the point of detonation.

As one proceeds to more distant stations and correspondingly smaller fields of view, the instruments would measure less and less of the total energy arriving at the station (more of this energy arrives as scattered radiation). However, since transmission values are determined as narrow-beam results, accuracy of direct correction of the measured values to true thermal efficiency would improve as the measuring angle was decreased. Of course, if the measurements are being made to determine the total thermal energy, direct and scattered, received by an adjacent plane surface, a maximum field of view at all stations would be desirable.

Although additional data must be obtained before the reason for the low results with restricted field of view can be ascertained, one result of practical importance can be obtained from Table 5.3. It appears that any instrument designed to measure the total radiant energy should have a field of view such that the radius at the point of detonation will be greater than about three times the sum of the fire ball radius, calculated as above, and the estimated maximum displacement of the center of the field of view from the point of detonation.

5.6 PASSIVE RECEIVERS

The passive-receiver panels gave reasonably satisfactory results. In most cases the chosen effect was bracketed as expected and in some cases, where the energy was greater or less than anticipated, estimates of total energy could be made from the degree of effect on the last foil in the series of thicknesses. For the ground reflectance measurements, the energy ranges selected in designing the panels were usually too high and gave poor results, including one panel which produced no results. In addition, four panels from Shot 4 (those nearest ground zero) were not recoverable.

The agreement among panels at the same distance was better than 10 per cent at all but one station (at 18,000 ft on Shot 3). However, agreement between different metals in the same panel was not as good. From Table 5.4 it can be seen that for the group-1 panels the lead and tin agree with each other but differ from cadmium by about 14 per cent. Again, with the group-2 panels, silver and lead agree, while cadmium differs by about 28 per cent. The metals used in the group-3 panels show good agreement. Columns 3, 6, and 9 of Table 5.4, which give the standard deviations of the ratios of the energies from the different metals to the mean energy of the panel, indicate that the reproducibility of each metal is good. For this reason it appears that the disagreement between cadmium and the other metals is probably real and not due to random errors. No explanation can be given at the present time for this result.

The total energy values given in Tables 4.6 through 4.9 were corrected for atmospheric attenuation and plotted in Figs. 5.1 through 5.4 for comparison with the calorimeter results. Comparison of the foil and calorimeter data in these figures shows one effect of the size of the tail in the thermal pulse. For Shots 1 and 2, which had short tails, the agreement between foil and calorimeter results is good. For Shots 3 and 4, which had long tails relatively ineffective in producing damage to the foils, the calorimeter values were considerably higher than the foil values.

TABLE 5.4

Mean Ratios of Energy Values of Each Indicator to Energy Value of Panel

Group 1			Group 2			Group 3		
Metal	Mean Ratio	Standard Deviation	Metal	Mean Ratio	Standard Deviation	Metal	Mean Ratio	Standard Deviation
Cd	0.91	0.12	Cd	0.81	0.11	Cu	0.96	0.01
Sn	1.04	0.14	Ag	1.09	0.11	Ag	1.02	0.05
Pb	1.05	0.12	Pb	1.10	0.16	Ag Strip	1.03	0.04

5.7 SHIELDING OF RECORDER CABLES

Because of lack of time and opportunity, no extensive or exhaustive investigation has been made to date to find the cause of the unwanted electrical signals in recorder cables that were so evident during Operation BUSTER.

Operation TUMBLER-SNAPPER afforded a limited opportunity to conduct a preliminary experiment. Four calorimeter circuits were installed with the electrical circuits identical, except for the type of cable connecting the instrument to the recorder. The four cables were Ordnance cable,* also used by USNRDL for all other recording circuits, Romex** in metallic armor, Romex without armor, and telephone wire.***

The results, which may well be complicated by the cross-feeding of the signal from one circuit to another, show that there was no pickup in the circuit using the Ordnance cable, but that the signal in the circuit using the telephone wire was of such magnitude that it caused the galvanometer to burn out. The circuits using Romex showed appreciable signals, although not enough to burn out the galvanometers. The signal in Romex circuits may have been at least partially due to the adjacent telephone wire circuit.

---

* Navy type DHFTA-9 Ordnance cable consists of a twisted pair of insulated wires inside a water-tight rubber cover and a metallic, braided armor.

** Romex, Federal Spec. J-C-103, general purpose wire, consists of two No. 12 solid copper conductors insulated with plastic and a fibrous nonmetallic braid.

*** Telephone wire, Navy type MRI, consists of two stranded and twisted copper wires insulated with synthetic resin.

It is possible, with present knowledge, to eliminate the electrical pickup in nearly all cases by the use of extensive electrical shielding such as was used at Operation TUMBLER-SNAPPER. However, the data on hand are not sufficient to warrant any specific conclusions concerning the nature of the phenomenon.

5.8 CONCLUSIONS

While some small loss of data resulted from instrument failure, all objectives of this operation were fulfilled. Sufficient data were obtained to give confidence in the thermal energy-vs-distance and intensity-vs-time curves obtained for the various weapons. The spectral distribution of the thermal energy probably was obtained to as great an accuracy as is possible through the use of the simple filter method employed. The data on energy vs elevation of measuring instrument gave a fair idea of the amount of local obscuration caused by thermal radiation. Although only preliminary models of the various radiometers were available for use in the field, these instruments gave good data concerning the intensity-vs-time relationship of the thermal output of the weapons. The passive receivers gave quite consistent data in most cases, and proved valuable for measurements where recorders were not available.

The major conclusions are summarized below:

1. Although the range of weapon yields (1 - 30 KT) is not sufficiently great (because of uncertainties both in thermal and total yield) to completely rule out the possibility of constant thermal yield, the data reported here indicate a decrease in thermal efficiency with increasing weapon yield - ranging from about 44 per cent at 1 KT to about 34 per cent at 30 KT.

2. As expected, the thermal pulse lengthens with increasing yield. The time to second maximum ranges from about 100 msec for a 1 KT weapon to about 200 msec for a 30 KT weapon. The range of weapon yields reported here is still not sufficiently great to allow accurate assessment of scaling laws.

3. The spectral measurements obtained during this operation indicate appreciably more energy at wave lengths beyond 9500 Å (25 per cent) than was found at Operation GREENHOUSE (10 per cent). Since the dust clouds produced by the surface detonation at GREENHOUSE obscured the later (cooler) phases of the fire ball this result is not surprising.

4. Care must be taken in interpreting data obtained near the ground, because measurements may be influenced by obscuration produced both by the shock wave and by effects of the thermal pulse itself. Obscuration resulting from the thermal radiation precedes that produced by the shock wave, and is exemplified by "popcorning" of sand and by smoke produced by burning of ground litter.

5. Because of uncertainties involved, it appears that any instrument designed to measure the thermal efficiency of a weapon should have a field of view such that the radius at the point of detonation will be no less than about two times the sum of the fire-ball radius, calculated by scaling from values given in the Effects of Atomic Weapons, and the estimated maximum displacement of the center of the field of view from the point of detonation. On the other hand, instrumentation designed to measure the total thermal energy, direct and scattered, received by an adjacent plane sample should have a field of view approaching 180°.

6. If properly interpreted, passive receiver panels can give reasonably satisfactory, self-consistent, results. For the 1 KT weapons, with short thermal tails, the agreement between foil and calorimeter results is excellent. For the weapons of larger yield which have long thermal tails, relatively ineffective in producing damage to the foils, the calorimeter results are considerably higher than the foil values.

7. As can be seen from Appendix B, the thermal energy received by aircraft above the point of detonation may be considerably higher than that at the equivalent distances along the ground (about 50 per cent higher for the drop plane on TUMBLER Shot 4). This result is partially due to the higher atmospheric transmission in a vertical path, but mostly due to reflection of thermal energy by the ground.

However, it is to be emphasized that the results and conclusions are very limited in their scope, and that great care must be taken when applying them to other cases. The data presented pertain to air bursts over the Nevada desert, for certain particular altitudes of detonation, for a limited range of weapon sizes, and for particular types of weapons. Extrapolation to other conditions, particularly to weapons of much larger yields, may be extremely misleading.

5.9 RECOMMENDATIONS

On the basis of measurements made at the TUMBLER-SNAPPER Operation and at previous operations the following recommendations are made with regard to measurements which should be carried out at future tests of nuclear weapons:

1. If the data obtained at previous tests are confirmed at Operation UPSHOT-KNOTHOLE, basic thermal measurements should be made only at future tests in which the conditions are considerably different.

2. In order to determine the danger to aircraft from the thermal radiation, further above-ground measurements are necessary. Also, a theoretical and experimental program should be prosecuted in order to evaluate the contribution of radiation reflected from the surface of the earth and from clouds and to establish atmospheric attenuation along a non-horizontal path.

3. Further work should be done on the effect of field of view of the measuring instruments on the measurements, particularly at the larger fields of view.

4. For further rough estimates of the effectiveness of the thermal energy, passive receivers should be exposed at detonations which deviate appreciably in yield from those already measured.

5. Although the results are not compared in this report, certain discrepancies appear in comparing USNRDL data with data obtained by the Naval Research Laboratory. An attempt should be made to resolve these differences and to determine whether or not they are real. Assuming no obvious errors in either set of data, a further study of variation of the thermal pulse with distance from the detonation may be in order.

APPENDIX A

MEASUREMENT OF THERMAL RADIATION INCIDENT UPON PARKED AIRCRAFT

USNRDL was asked to assist Project 3.1 personnel in the measurement of the thermal flux incident upon certain parked aircraft which were to be exposed to the effects of nuclear weapons for the purpose of determining damage repair criteria for the aircraft. Nine calorimeters were constructed and thermally calibrated at USNRDL. They were then delivered to the test site where they were installed and electrically calibrated by Project 3.1 personnel. A check electrical calibration was also made by USNRDL in the field.

Measurements were made at three locations during Shots 2, 3, and 4. Details concerning the location and mounting of the instruments may be found in the Project 3.1 report.

Copies of the records were supplied to USNRDL so that the data could be reduced along with similar data taken at Project 8.3 installations. The data presented in Table A.1 were obtained by methods of analysis similar in all respects to those described for calorimeter data elsewhere in this report.

The total thermal energy-vs-distance data agree very well with USNRDL thermal line data under similar circumstances, with the exception of the closest station on Shots 3 and 4, and the 8,000-ft station on Shot 4. The disagreement at the close stations is most probably due to local dust and smoke obscuration.

Both Project 3.1 and Project 8.3 personnel analysed the data; and while the results obtained by the two groups agree fairly well, not all differences have been explained because time and distance considerations have prevented more than preliminary consultation to date. Care should be taken in application of these data, as the values are subject to change.

TABLE A.1

TUMBLER-SNAPPER Calorimeter Data:[a] WADC Airplanes on Ground

Station	Slant Range (ft)	Half-angle of Field of View (deg)	Orientation[b]	Elevation (ft)	Cal. No.	Filter	Total Energy under Filter (cal/sq cm)	Total Energy Incident (cal/sq cm)
Shot 2								
A	2,490	45	AZ	5	Red 8	Quartz	No record available	
A	2,490	45	AZ	5	Red 10	Quartz	No record available	
B	8,060	45	AZ	5	Black 8	Quartz	0.51	0.55
B	8,060	45	AZ	(c)	Black 9	(d)	0.14	0.15
B	8,060	45	AZ	5	Black 10	Quartz	0.57	0.62
C	10,538	45	AZ	5	Gray 9	Quartz	0.26	0.28
C	10,538	45	AZ	5	Gray 10	Quartz	0.30	0.33
Shot 3								
A	4,087	45	AZ	5	Red 8	Quartz	27.3	29.7
A	4,087	45	AZ	5	Red 10	Quartz	27.2	29.6
B	8,622	45	AZ	5	Black 8	Quartz	10.3	11.2
B	8,622	45	AZ	(c)	Black 9	(d)	3.2	3.5
B	8,622	45	AZ	5	Black 10	Quartz	7.8	8.5
C	10,988	45	AZ	5	Gray 9	Quartz	5.9	6.4
C	10,988	45	AZ	5	Gray 10	Quartz	5.5	6.0
Shot 4								
A	2,508	45	AZ	5	Red 8	Quartz	---	---
A	2,508	45	AZ	5	Red 10	Quartz	33.4	36.3
A4	3,960	45	AZ	5	Black 8	Quartz	24.8	27.0
A4	3,960	45	AZ	(e)	Black 9	(d)	19.7	21.4
A4	3,960	45	AZ	5	Black 10	Quartz	24.9	27.1
B	7,890	45	AZ	5	Gray 9	Quartz	6.1	6.6
B	7,890	45	AZ	5	Gray 10	Quartz	7.1	7.7

(a) Not corrected for atmospheric attenuation.

(b) AZ = Calorimeter aligned toward air zero.

(c) Inside B-17.

(d) Quartz and windshield.

(e) Inside F-47.

APPENDIX B

MEASUREMENT OF THERMAL RADIATION INCIDENT ON DROP AIRCRAFT

The 4925th Air Bombardment Group asked USNRDL to assist in an attempt to measure the thermal radiation incident upon the drop aircraft.

Three standard disk calorimeters, of the type described elsewhere in this report, were delivered to Capt. O. R. Hill, USAF, Project Officer for the drop aircraft, at the test site. The calorimeters and the recorders were then mounted in the aircraft under his direction.

Calibration was carried out by USNRDL personnel at the Indian Springs Air Force Base on two occasions, and also when, at the conclusion of the operation, the complete circuits were returned to USNRDL. Data were reduced and analyzed by the same procedure described in the body of this report.

Table B.1 shows the results of the measurements taken on the B-50 aircraft in flight.

TABLE B.1

TUMBLER-SNAPPER Calorimeter Data:[a] B-50 in Flight over Detonation

Shot	Slant Range (ft)	Half-angle of Field of View (deg)	Orientation[b]	Elevation (ft)	Cal. No.	Filter	Total Energy under Filter (cal/sq cm)	Total Energy Incident (cal/sq cm)
1	18,700	45	AZ	19,000	Brass 2	Quartz	No energy detected	
	18,700	45	AZ	19,000	Brass 5	Quartz	No energy detected	
	18,700	45	AZ	19,000	Brass 7	Quartz	No energy detected	
2	18,020	45	AZ	19,000	Brass 2	Quartz	No energy detected	
	18,020	45	AZ	19,000	Brass 5	Quartz	No energy detected	
	18,020	45	AZ	19,000	Brass 7	Quartz	No energy detected	
3	Not Available	45	AZ	Not Available	Brass 2	Quartz	Timing failure	
		45	AZ		Brass 5	Quartz	Timing failure	
		45	AZ		Brass 7	Quartz	Timing failure	
4	18,885	45	AZ	19,800	Brass 2	Quartz	2.2	2.3
	18,885	45	AZ	19,800	Brass 5	Quartz	2.0	2.1
	18,885	45	AZ	19,800	Brass 7	Quartz	No energy detected	

(a) Not corrected for atmospheric attenuation.

(b) AZ = Calorimeter aligned toward air zero.

Though a small amount of energy was expected on Shots 1 and 2, no detectable energy was received. This could be due to errors in alignment of the calorimeters or to condensation on the quartz filter, but no certain explanation has yet been found. No readings were obtained on Shot 3, owing to a failure in the starting sequence for the recorder. On Shot 4 two of the three calorimeters operated properly and gave values in good agreement with each other. These values have been raised 5 per cent to correct for the changes in the properties of the measuring system at the lower temperatures encountered at high altitudes.

In order to compare the values measured from the B-50 with those measured at the ground installations, it is necessary to correct for the atmospheric attenuation. Since no measurements were made of the transmission in a vertical direction, an estimate of this value was obtained from the measured 95-per-cent-per-mile transmission for a horizontal path by assuming that the attenuation coefficient is proportional to the atmospheric density and that the change of density with altitude was that of a standard atmosphere7/. This results in an estimated average atmospheric transmission of 96.3 per cent per mile for the nearly vertical path between the point of detonation and the B-50. As the total correction for the atmospheric attenuation is less than 15 per cent, uncertainties in the value of the absorption coefficient should cause less than 5 per cent error in the energy values.

Using the value of atmospheric transmission given above, the energy value at the plane is about 50 per cent higher than the value on the surface at the same distance. This is most probably due to the reflection of energy from the ground. Preliminary calculations on the amount of energy reflected from the ground, using a value of 45 per cent for the reflectivity of the soil (Appendix C), indicate that a value of 50 per cent is not unreasonable.

APPENDIX C

REFLECTIVITY OF NEVADA PROVING GROUNDS SOILS

Due to the interest in the amount of thermal radiation absorbed by the ground during the detonation of a nuclear weapon, it seemed advisable to measure the reflectivity of the soil in the areas where thermal radiation and air temperatures were being measured.

Measurements of the reflectivity of the soil, using the sun as a source, were made on 5 May 1952 between hours 1130 and 1230, PDT, in the T-7 Area of Yucca Flat, and between hours 1300 and 1400, PDT, on Frenchman Lake. The reflectometer used was made at USNRDL and has a field of view of half-angle 3°. The receiver consists of a Weston Photronic cell, Type 856 RR. The instrument makes use of a test plate smoked with magnesium oxide as a reflection standard, and thus all reflection measurements are expressed as percentages of the reflectivity of the magnesium oxide.

Measurements were made, while the sun was near apparent noon, with the receiver viewing the ground vertically, and at 10° intervals up to 70°E and 70°W from the vertical. The axis of the receiver was at all times in the vertical east-west plane. The angle between the zenith and the sun's rays was approximately 20°. The measurements were made for areas in front of towers upon which Project 8.2 and 8.3 instruments were mounted. The area on the ground seen by the instrument was approximately 10 sq in. when the instrument was normal to the ground. The results of these measurements are tabulated in Table C.1. The 70° measurements have questionable validity because the area viewed by the receiver approached the area of the standard plate.

These data are of value in correlating the amount of energy absorbed by the ground with the amount of energy incident, and in determining the increase in thermal energy received by objects due to ground reflection of the thermal pulse.

TABLE C.1

Reflectivity of Soils

Angle of Observation(a)	Reflectivity Relative to Magnesium Oxide (%)					
	7-210	7-208	7-206	F-202	F-208	F-210
70E	53	50	53	70	76	75
60E	47	48	50	66	67	69
50E	45	46	46	62	62	65
40E	44	46	45	60	61	64
30E	44	45	44	58	60	63
20E	44	45	43	58	59	62
10E	44	45	43	59	58	62
0	44	45	43	58	58	62
10W	44	45	42	58	58	62
20W	42	44	42	58	59	62
30W	41	45	42	56	59	63
40W	41	45	42	57	59	63
50W	41	46	42	58	62	64
60W	43	48	45	62	66	67
70W	47	51	49	66	71	71

(a) Measured from vertical.

BIBLIOGRAPHY

1/. Armed Forces Special Weapons Project, Summary Report, Weapon Effects Test, Operation TUMBLER Report.

2/. Broido, A., et al., "The Effect of Thermal Radiation on Material", Operation GREENHOUSE, Annex 6.2, Final Report.

3/. Broido, A., Butler, C. P., and Hillendahl, R. W., "Basic Thermal Radiation Measurements", Operation BUSTER, Project 2.4-1, Final Report, WT-409.

4/. Broida, T. R., Broido, A., and Willoughby, A. B., "Air Temperatures in the Vicinity of a Nuclear Detonation", Operation TUMBLER, Project 8.2, WT-542.

5/. Broido, A., Butler, C. P., and Hillendahl, R. W., "Basic Thermal Radiation Measurements", Operation BUSTER, Project 2.4-1, Final Report, p 42, WT-409

6/. Day, R. P., Hopton, R. L., and Schmidt, A. C., "A Fully Automatic, High-speed Shutter for Use in a Convergent Beam of High-intensity Thermal Radiation", USNRDL Report, to be published.

7/. Fowle, F. E., Smithsonian Physical Tables, Smithsonian Institute, Washington, D. C., 1934.

8/. Hulbert, E. O., "Atmospheric Transmission", report communicated by AFSWP, 30 October 1952.

9/. Martin, S. B., "Preparation and Evaluation of Blackened Surfaces on Various Metals", USNRDL Report, to be published.

10/. McAdams, W. H., "Heat Transmission", McGraw-Hill Book Co., New York, 1942; p 220.

11/. Willoughby, A. B., "A Simple High-speed Calorimeter for the Measurement of Intense Beams of Thermal Radiation", USNRDL Report, to be published.

12/. Willoughby, A. B., "A Water-flow Calorimeter for the Measurement of Intense Beams of Thermal Radiation", USNRDL Report, to be published.

DISTRIBUTION

ARMY ACTIVITIES

	Copy No.
Asst. Chief of Staff, G-2, D/A, Washington 25, D. C.	1
Asst. Chief of Staff, G-3, D/A, Washington 25, D. C. ATTN: DACofS, G-3, (RR&SW)	2
Asst. Chief of Staff, G-4, D/A, Washington 25, D. C.	3
Chief of Ordnance, D/A, Washington 25, D. C. ATTN: ORDTX-AR	4
Chief Signal Officer, D/A, P&O Div., Washington 25, D. C. ATTN: SIGOP	5- 7
The Surgeon General, D/A, Washington 25, D. C. ATTN: Chairman, Medical R&D Board	8- 10
Chief Chemical Officer, D/A, Washington 25, D. C.	11- 12
Chief of Engineers, D/A, Military Construction Division, Protective Construction Branch, Washington 25, D. C. ATTN: ENGEB	13
Chief of Engineers, D/A, Civil Works Division, Washington, 25, D. C. ATTN: Engineering Division, Structural Branch	14
The Quartermaster General, CBR, Liaison Office, Research and Development Division, Washington 25, D. C.	15- 16
Chief of Transportation, D/A, Washington 25, D. C. ATTN: Military Planning and Intelligence	17
Chief, Army Field Forces, Ft. Monroe, Va.	18- 21
Army Field Forces Board #1, Ft. Bragg, N. C.	22
Army Field Forces Board #2, Ft. Knox, Ky.	23
Army Field Forces Board #4, Ft. Bliss, Tex.	24
Commanding General, First Army, Governor's Island, New York 4, N. Y. ATTN: ACofS, G-4	25- 26
Commanding General, Second Army, Ft. George G. Meade, Md. ATTN: AIAME	27
Commanding General, Second Army, Ft. George G. Meade, Md. ATTN: AIACM	28
Commanding General, Third Army, Ft. McPherson, Ga. ATTN: ACofS, G-3	29- 30
Commanding General, Fourth Army, Ft. Sam Houston, Tex. ATTN: G-3 Section	31- 32
Commanding General, Fifth Army, 1660 E. Hyde Park Blvd., Chicago 15, Ill. ATTN: ALFEN	33
Commanding General, Fifth Army, 1660 E. Hyde Park Blvd., Chicago 15, Ill. ATTN: ALFOR	34
Surplus in TISOR	35- 39
Commanding General, Sixth Army, Presidio of San Francisco, Calif. ATTN: AMGCT-4	40
Commander-in-Chief, European Command, APO 403, c/o PM, New York, N. Y.	41

DISTRIBUTION (Continued)

	Copy No.
Commander-in-Chief, U. S. Army Europe, APO 403, c/o PM, New York, N. Y. ATTN: OPOT Division Combat Dev. Branch	42- 43
Commander-in-Chief, Far East Command, APO 500, c/o PM, San Francisco, Calif. ATTN: ACofS, G-3	44- 48
Commanding General, U. S. Army Alaska, APO 942, c/o PM, Seattle, Wash.	49
Commanding General, U. S. Army Caribbean, APO 834, c/o PM, New Orleans, La. ATTN: CG, USARCARIB	50
Commanding General, U. S. Army Carbbbean, APO 834, c/o PM, New Orleans, La. ATTN: CG, USARFANT	51
Commanding General, U. S. Army Caribbean, APO 834, c/c PM, New Orleans, La. ATTN: Cml Off, USARCARIB	52
Commanding General, U. S. Army Caribbean, APO 834, c/c PM, New Orleans, La. ATTN: Surgeon, USARCARIB	53
Commanding General, U. S. Army Pacific, APO 958, c/o PM, San Francisco, Calif. ATTN: Cml Off	54- 55
Commanding General, Trieste U. S. Troops, APO 209, c/o PM, New York, N. Y. ATTN: ACofS, G-3	56
Commandant, Command and General Staff College, Ft. Leavenworth, Kan. ATTN: ALLIS(AS)	57- 58
Commandant, The Infantry School, Ft. Benning, Ga. ATTN: C.D.S.	59- 60
Commandant, The Artillery School, Ft. Sill, Okla.	61
Commandant, The AA&GM Branch, The Artillery School, Ft. Bliss, Tex.	62
Commandant, The Armored School, Ft. Knox, Ky. ATTN: Classified Document Section, Evaluation and Research Division	63- 64
Commanding General, Medical Field Service School, Brooke Army Medical Center, Ft. Sam Houston, Tex.	65
Commandant, Army Medical Service Graduate School, Walter Reed Army Medical Center, Washington 25, D. C. ATTN: Dept. of Biophysics	66
The Superintendent, U. S. Military Academy, West Point, N. Y. ATTN: Professor of Ordnance	67- 68
Commanding General, The Transportation Center and Ft. Eustis, Ft. Eustis, Va. ATTN: Asst. Commandant, Military Science and Tactics	69
Commandant, Chemical Corps School, Chemical Corps Training Center, Ft. McClellan, Ala.	70
Commanding General, Research and Engineering Command, Army Chemical Center, Md. ATTN: Special Projects Officer	71
RD Control Officer, Aberdeen Proving Ground, Md. ATTN: Director, Ballistic Research Laboratories	72- 73
Commanding General, The Engineer Center, Ft. Belvoir, Va. ATTN: Asst. Commandant, The Engineer School	74- 76

DISTRIBUTION (Continued)

	Copy No.
Chief of Research and Development, D/A, Washington 25, D. C.	77
Commanding Officer, Engineer Research and Development Laboratory, Ft. Belvoir, Va. ATTN: Chief, Technical Intelligence Branch	78
Commanding Officer, Picatinny Arsenal. Dover, N. J. ATTN: ORDBB-TK	79
Commanding Officer, Frankford Arsenal, Philadelphia, Pa. ATTN: RD Control Officer	80
Commanding Officer, Army Medical Research Laboratory, Ft. Knox, Ky.	81
Commanding Officer, Chemical Corps Chemical and Radiological Laboratory, Army Chemical Center, Md. ATTN: Technical Library	82- 83
Commanding Officer, Transportation R&D Station, Ft. Eustis, Va.	84
Commanding Officer, Psychological Warfare Center, Ft. Bragg, N. C.	85
Asst. Chief, Military Plans Division, Rm 516, Bldg 7, Army Map Service, 6500 Brooks Lane, Washington 25, D. C. ATTN: Operations Plans Branch	86
Director, Technical Documents Center, Evans Signal Lab., Belmar, N. J.	87
Director, Waterways Experiment Station, PO Box 631, Vicksburg, Miss. ATTN: Library	88
Director, Operations Research Office, Johns Hopkins University, 6410 Connecticut Ave., Chevy Chase, Md. ATTN: Library	89

NAVY ACTIVITIES

Chief of Nav Operations, D/N, Washington 25, D. C. ATTN: C[illegible]-36	90- 91
Chief of Naval Operations, D/N, Washington 25, D. C. ATTN: OP-51	92
Surplus in TISOR	93
Chief of Naval Operations, D/N, Washington 25, D. C. ATTN: OP-374 (OEG)	94
Chief, Bureau of Medicine and Surgery, D/N, Washington 25, D. C. ATTN: Special Weapons Defense Division	95- 96
Chief, Bureau of Ordnance, D/N, Washington 25, D. C.	97
Chief, Bureau of Ships, D/N, Washington 25, D. C. ATTN: Code 348	98- 99
Chief, Bureau of Supplies and Accounts, D/N, Washington 25, D. C.	100

DISTRIBUTION (Continued) Copy No.

Chief, Bureau of Personnel, D/N, Washington 25, D. C. ATTN: Pers C	101
Chief, Bureau of Yards and Docks, D/N, Washington 25, D. C. ATTN: P-312	102
Chief, Bureau of Aeronautics, D/N, Washington 25, D. C.	103-104
Office of Naval Research, Code 219, Rm 1807, Bldg. T-3, Washington 25, D. C. ATTN: RD Control Officer	105
Commander-in-Chief, U. S. Atlantic Fleet, Fleet Post Office, New York, N. Y.	106-107
Commander-in-Chief, U. S. Pacific Fleet, Fleet Post Office, San Francisco, Calif.	108-109
Commandant, U. S. Marine Corps, Headquarters, USMC, Washington 25, D. C. ATTN: (Code AO3H)	110-113
President, U. S. Naval War College, Newport, Rhode Island	114
Superintendent, USN Postgraduate School, Monterey, Calif.	115-116
Commanding Officer, USN Schools Command, Naval Station, Treasure Island, San Francisco, Calif.	117-118
Director, USMC Development Center, USMC Schools, Quantico, Va. ATTN: MC Tactics Board	119
Director, USMC Development Center, USMC Schools, Quantico, Va. ATTN: MC Equipment Board	120
Commanding Officer, Fleet Training Center, Naval Base, Norfolk 11, Va. ATTN: Special Weapons School	121-122
Commanding Officer, Fleet Training Center (SPWP School), Naval Station, San Diego 36, Calif.	123-124
Commanding Officer, Air Development Squadron 5, USN Air Station, Moffett Field, Calif.	125
Commander, Operational Development Force, U. S. Fleet, Naval Base, Norfolk 11, Va. ATTN: Tact Dev Gp	126
Commander, Operational Development Force, U. S. Fleet, Naval Base, Norfolk 11, Va. ATTN: Air Dept.	127
Commander, Air Force, U. S. Pacific Fleet, Naval Air Station, San Diego, Calif.	128
Commander, Training Command, U. S. Pacific Fleet, c/o Fleet Sonar School, San Diego 47, Calif.	129
Commanding Officer, Naval Damage Control Training Center, U. S. Naval Base, Philadelphia 12, Pa. ATTN: ABC Defense Course	130
Commanding Officer, Naval Unit, Chemical Corps School, Ft. McClellan, Ala.	131
Joint Landing Force Board, Marine Barracks, Camp Lejeune, N. C.	132
Commander, USN Ordnance Laboratory, Silver Spring 19, Md. ATTN: EE	133
Commander, USN Ordnance Laboratory, Silver Spring 19, Md. ATTN: Alias	134

DISTRIBUTION (Continued)	Copy No.
Commander, USN Ordnance Laboratory, Silver Spring 19, Md. ATTN: Aliex	135
Commander, USN Ordnance Test Station, Inyokern, China Lake, Calif.	136
Officer-in-Charge, USN Civil Engineering Research & Evaluation Laboratory, Construction Batallion Center, Port Hueneme, Calif. ATTN: Code 753	137-138
Commanding Officer, USN Medical Research Institute, National Medical Center, Bethesda 14, Md.	139
Director, USN Research Laboratory, Washington 25, D. C.	140
Director, The Materiel Laboratory, N. Y. Naval Shipyard, New York, N. Y.	141
Commanding Officer and Director, USN Electronics Laboratory, San Diego 52, Calif. ATTN: Code 210	142
Commanding Officer, USN Radiological Defense Laboratory, San Francisco, Calif. ATTN: Technical Information Division	143-146
Commanding Officer and Director, David W. Taylor Model Basin, Washington 7, D. C. ATTN: Library	147
Commander, Naval Air Development Center, Johnsville, Pa.	148
Commanding Officer, Office of Naval Research Branch Office, 1000 Geary St., San Francisco, Calif.	149-150
Clothing Supply Office, USN Supply Activities, New York, 3d Ave. & 29th St., Brooklyn 32, N. Y. ATTN: R&D Div.	151

AIR FORCE ACTIVITIES

Surplus in TISOR	152
Asst. for Atomic Energy, Headquarters, USAF, Washington 25, D. C. ATTN: DCS/O	153
Asst. for Development Planning, Headquarters, USAF, Washington 25, D. C.	154-155
Director of Operations, Headquarters, USAF, Washington 25, D. C.	156-157
Director of Plans, Headquarters, USAF, Washington 25, D. C. ATTN: War Plans Division	158
Directorate of Requirements, Headquarters, USAF, Washington 25, D. C. ATTN: AFDRQ-SA/M	159
Directorate of Research and Development, Armament Division, DCS/D, Headquarters, USAF, Washington 25, D. C.	160
Directorate of Intelligence, Headquarters, USAF, Washington 25, D. C.	161-162
The Surgeon General, Headquarters, USAF, Washington 25, D. C.	163-164

DISTRIBUTION (Continued)	Copy No.
Commanding General, U. S. Air Forces in Europe, APO 633, c/o PM, New York, N. Y.	165
Commanding General, Far East Air Forces, APO 925, c/o PM, San Francisco, Calif.	166
Commanding General, Alaskan Air Command, APO 942, c/o PM, Seattle, Wash. ATTN: AAOTN	167-168
Commanding General, Northeast Air Command, APO 862, c/o PM, New York, N. Y.	169
Commanding General, Strategic Air Command, Offutt AFB, Omaha, Neb. ATTN: Chief, Operations Analysis	170
Commanding General, Tactical Air Command, Langley AFB. Va. ATTN: Document Security Branch	171-173
Commanding General, Air Defense Command, Ent AFB, Colo.	174-175
Commanding General, Air Materiel Command, Wright-Patterson AFB, Dayton, Ohio	176-178
Commanding General, Air Training Command, Scott AFB, Belleville, Ill.	179-180
Commanding General, Air Research and Development Command, PO Box 1395, Baltimore 3, Md. ATTN: RDDN	181-183
Commanding General, Air Proving Ground, Eglin AFB, Fla. ATTN: AG/TRB	184
Commanding General, Air University, Maxwell AFB, Ala.	185-189
Commandant, Air Command and Staff School, Maxwell AFB, Ala.	190-191
Commandant, Air Force School of Aviation Medicine, Randolph AFB, Tex.	192-193
Commanding General, Wright Air Development Center, Wright-Patterson AFB, Dayton, Ohio. ATTN: WCOESP	194-199
Commanding General, AF Cambridge Research Center, 230 Albany St., Cambridge 39, Mass. ATTN: Atomic Warfare Directorate	200
Commanding General, AF Cambridge Research Center, 230 Albany St., Cambridge 39, Mass. ATTN: CRTSL	201
Commanding General, AF Special Weapons Center, Kirtland AFB, N. Mex. ATTN: Chief, Technical Library Branch	202-204
Commandant, USAF Institute of Technology, Wright-Patterson AFB, Dayton, Ohio. ATTN: Resident College	205
Commanding General, Lowry AFB, Denver, Colo. ATTN: Dept. of Armament Training	206-207
Commanding General, 1009th Special Weapons Squadron, Tempo "T", 14th & Constitution Sts., N.W., Washington, D. C.	208-210
The RAND Corporation, 1700 Main St., Santa Monica, Calif. ATTN: Nuclear Energy Division	211-212

OTHER DEFENSE DEPT. ACTIVITIES

Executive Secretary, JCS, Washington 25, D. C.	213

DISTRIBUTION (Continued) Copy No.

Director, Weapons Systems Evaluation Group, OSD, Rm 2E1006, Pentagon, Washington 25, D. C.	214
Asst. for Civil Defense, OSD, Washington 25, D. C.	215
Chairman, Armed Services Explosives Safety Board, D/D, Rm 2403, Barton Hall, Washington 25, D. C.	216
Chairman, Research and Development Board, D/D, Washington 25, D. C. ATTN: Technical Library	217
Executive Secretary, Committee on Atomic Energy, Research and Development Board, Rm 3E1075, Pentagon, Washington 25, D. C.	218-219
Executive Secretary, Military Liaison Committee, PO Box 1814, Washington 25, D. C.	220
Commandant, Armed Forces Staff College, Norfolk 11, Va. ATTN: Secretary	221
Commanding General, Field Command, AFSWP, PO Box 5100, Albuquerque. N. Mex.	222-227
Chief, AFSWP, PO Box 2610, Washington 13, D. C.	228-236

ATOMIC ENERGY COMMISSION ACTIVITIES

University of California Radiation Laboratory, PO Box 808, Livermore, Calif. ATTN: Margaret Folden	237
U. S. Atomic Energy Commission, Classified Document Room, 1901 Constitution Ave., Washington 25, D. C. ATTN: Mrs. J. M. O'Leary (for DMA)	238-240
Los Alamos Scientific Laboratory, Report Library, PO Box 1663, Los Alamos, N. Mex. ATTN: Helen Redman	241-243
Sandia Corporation, Classified Document Division, Sandia Base, Albuquerque, N. Mex. ATTN: Wynne K. Cox	244-263
Weapon Test Reports Group, TIS	264
Surplus in TISOR for DMA	265-314
Surplus in TISOR for AFSWP	315-339

ADDITIONAL DISTRIBUTION

Director of Special Weapons Developments, OCAFF, Fort Bliss, Texas. ATTN: Major Hale Mason, Jr.	340

AEC, Oak Ridge, Tenn., A33320